

The regulation of cell motility by tropomyosin

Author:

Brayford, Simon

Publication Date:

2016

DOI:

<https://doi.org/10.26190/unsworks/19088>

License:

<https://creativecommons.org/licenses/by-nc-nd/3.0/au/>

Link to license to see what you are allowed to do with this resource.

Downloaded from <http://hdl.handle.net/1959.4/56483> in <https://unsworks.unsw.edu.au> on 2024-04-30

The Regulation of Cell Motility by Tropomyosin

An investigation into the role of the cytoskeletal tropomyosins Tpm1.8/1.9 in the regulation of actin dynamics at the leading edge of migrating cells



UNSW
AUSTRALIA

Simon Brayford

School of Medical Sciences
Faculty of Medicine
UNSW Australia
Sydney, Australia

A Thesis submitted in fulfilment of the requirements for the degree of
Doctor of Philosophy (Medicine)
(August 2016)

COPYRIGHT STATEMENT

'I hereby grant the University of New South Wales or its agents the right to archive and to make available my thesis or dissertation in whole or part in the University libraries in all forms of media, now or here after known, subject to the provisions of the Copyright Act 1968. I retain all proprietary rights, such as patent rights. I also retain the right to use in future works (such as articles or books) all or part of this thesis or dissertation.

I also authorise University Microfilms to use the 350 word abstract of my thesis in Dissertation Abstract International (this is applicable to doctoral theses only).

I have either used no substantial portions of copyright material in my thesis or I have obtained permission to use copyright material; where permission has not been granted I have applied/will apply for a partial restriction of the digital copy of my thesis or dissertation.'

Signed

Date

AUTHENTICITY STATEMENT

'I certify that the Library deposit digital copy is a direct equivalent of the final officially approved version of my thesis. No emendation of content has occurred and if there are any minor variations in formatting, they are the result of the conversion to digital format.'

Signed

Date

Originality Statement

‘I hereby declare that this submission is my own work and to the best of my knowledge it contains no materials previously published or written by another person, or substantial proportions of material which have been accepted for the award of any other degree or diploma at UNSW or any other educational institution, except where due acknowledgement is made in the thesis. Any contribution made to the research by others, with whom I have worked at UNSW or elsewhere, is explicitly acknowledged in the thesis. I also declare that the intellectual content of this thesis is the product of my own work, except to the extent that assistance from others in the project's design and conception or in style, presentation and linguistic expression is acknowledged.’

Signed:



Simon Brayford

Date: 23 / 08 / 2016

Abstract

Metastasis accounts for over 90% of cancer related mortality, it is therefore of interest to further develop an understanding of the way in which cells migrate. At the leading edge of migrating cells, protrusion of the lamellipodium is driven by Arp2/3-mediated polymerisation of actin filaments. This dense, branched actin network is promoted and stabilised by cortactin. In order to drive filament turnover, Arp2/3 networks are remodelled by proteins such as GMF which blocks the actin-Arp2/3 interaction, and coronin 1B which acts by directing SSH1L to the lamellipodium where it activates the actin severing protein cofilin. It has been shown in vitro that cofilin-mediated severing of Arp2/3 actin networks results in the generation of new pointed ends to which the actin-stabilising protein tropomyosin (Tpm) can bind. The presence of Tpm in lamellipodia however has been controversial with studies reporting the absence of Tpm from lamellipodia, and others reporting their presence at or near lamellipodia. These opposing observations are partly due to the lack of appropriate reagents to detect the Tpm. This thesis reports that the Tpm isoforms 1.8/1.9 are enriched in the lamellipodium of mouse fibroblasts as detected with a novel, isoform-specific monoclonal antibody. RNAi-mediated silencing of Tpm1.8/1.9 led to an increase in Arp2/3 accumulation at the cell periphery paralleled by a reduction in cell speed and the persistence of lamellipodia, a phenotype consistent with coronin 1B-deficient cells. In the absence of coronin 1B or cofilin, Tpm1.8/1.9 protein levels are reduced while conversely, inhibition of Arp2/3 with CK666 led to an increase in Tpm1.8/1.9 protein. The findings presented in this thesis establish a novel regulatory mechanism within the lamellipodium whereby Tpm collaborates with Arp2/3 to promote lamellipodial persistence and cell motility. This study also provides a solution to the controversy found in the literature and serves as a broader paradigm by which to understand how cells can create and utilise multiple actin filament populations to achieve a singular biological outcome.

Acknowledgements

My PhD journey would not have been possible without the support from those around me. With far too many to mention, I would like offer my sincere thanks to a handful of those closest to me here.

First and foremost, I'd like to thank my supervisor, Peter. Peter, you gave me the fantastic opportunity to enter the exciting world of basic science, and kick-start my research career. Your enthusiasm for science and seemingly endless knowledge has made my PhD journey an absolute joy. Thank-you for your constant encouragement. Thank-you for your guidance, your time, your advice, your patience and your inspiration over the years.

To my honours-year and initial PhD co-supervisor Galina, you were there from day one to nurture my burgeoning interest in cell biology and over the years have provided incalculable knowledge and advice. Thank-you for always being willing and more than able to help out whenever I had a question about anything at all.

To my PhD co-supervisor for the last two years, Nicole. Thanks for all your help both with my PhD work and also for all your advice about what follows. Most of all, thank-you for all your help and encouragement which ultimately led to obtaining my first publication. I could not have done it without you.

Thanks to Edna. Your remarkable leadership of the research unit has made for a smooth and enjoyable journey. Thank-you for sharing your wisdom at lab meetings and for all your help in steering the direction of this project. Staff and students of the CGMU are lucky to have you at the helm.

Many thanks to the lab support staff over the years; Rachael, Carol, Paul and Andrea. Every success of the lab is a testament to your hard work and dedication.

I would like to thank each and every member of the Oncology Research Unit; Thanks to Jeff for all your valuable help and technical assistance over the years. Thanks to Mel, Ashleigh, Joyce, Iman, Bin and Hossai as well as the other CGMU members; Florence, Cesar, Paulina, Nadia, Andrius, Mark, Christine and Lingyan and anyone else I've forgotten to mention. Whether in the lab or the pub, thank-you all for the laughs and support and for making a sometimes mundane lab-life infinitely better.

Thanks to the supervisors from the other groups; Anthony, Annemiek, Lars, Thomas, Justine and Steve, for always being available to help out with your advice whenever it was needed.

Special thanks to our collaborators on this project, Jim and Liz from UNC for experiment recommendations or data analysis and guidance over Skype meetings. Getting this project to publication would not have been possible without your help.

Finally, thanks for the love and constant support of my wonderful family. Thank you to Mum, Dad, Nanna and Stacey for always being there, for believing in me, for motivation and encouragement when I needed it most. Finally, thank-you to my beautiful girlfriend, Allison. You were there from the very beginning of my PhD journey and your unwavering support through it all has been an immeasurable source of inspiration.

Publications

Brayford, S., Bryce, N.S., Schevzov, G., Bear, J.E., Haynes, E.M., Hardeman, E.H., and Gunning, P.W. (2016). Tropomyosin Promotes Lamellipodial Persistence by collaborating with Arp2/3 at the Leading Edge. *Current Biology* 26 (10) pp. 1312-1318.

Brayford, S., Schevzov, G., Vos, J., and Gunning, P. W. (2015). The Role of the Actin Cytoskeleton in Cancer and Its Potential Use as a Therapeutic Target. *The Cytoskeleton in Health and Disease*, H. Schatten, ed. (Springer New York), pp. 373-391.

Meeting Abstracts

Brayford S.,Bryce N. S., Schevzov G., , Hardeman E.C., Bear J.E., Haynes E. M.and Gunning P.W. Tropomyosin promotes lamellipodial persistence by facilitating the transition from protrusive to adhesive actin networks.ComBio2015 Scientific Meeting. Melbourne Convention and Exhibition Centre, Melbourne, Australia. October 2015.

Brayford S.,Schevzov G., Bryce N. S., Hardeman E. C., Bear J. E. and Gunning P. W. Tropomyosin 5a/b actin filaments collaborate with Arp2/3 actin filaments to regulate cell motility. American Society for Cell Biology (ASCB) Annual Meeting. Pennsylvania Convention Centre, Philadelphia, PA, USA. December 2014. (Recipient of ASCB International student travel grant).

Brayford S.,Schevzov G., Hardeman E. C. and Gunning P. W. Tropomyosin based regulation of actin dynamics at the leading edge of migrating cells. ComBio2014 Scientific Meeting. National Convention Centre, Canberra, Australia. October 2014. (Recipient of ASBMB student travel grant).

Brayford S,Schevzov G, Hardeman E. C. and Gunning P. W. The role of Tm5a/5b in the regulation of lamellipodial dynamics and cell migration. Australian Society for Medical Research (ASMR) Annual Meeting. Powerhouse Museum, Sydney, Australia. June 2014.

Brayford S,Schevzov G, Hardeman E. C and Gunning P. W. Tropomyosin Based Regulation of Actin Dynamics at the Leading Edge. ComBio2013 Scientific Meeting. Perth Convention and Exhibition Centre, Perth, Australia. October 2013. (Recipient of ANZSCDB student travel grant).

Prizes Awarded

Australian Society for Biochemistry and Molecular Biology (ASBMB) Best Student Poster Prize, ComBio2013 Scientific Meeting. Perth Convention and Exhibition Centre, Perth, Australia. October 2013

Australian and New Zealand Society for Cell and Developmental Biology (ANZSCDB) Best Student Poster Prize, ComBio2013 Scientific Meeting. Perth Convention and Exhibition Centre, Perth, Australia. October 2013

PhD Top Up Scholarship 2014 & 2015, Translational Cancer Research Network (TCRN)

List of Abbreviations

ABPs	Actin binding proteins
ADF	Actin depolymerising factor
ADP	Adenosine-diphosphate
AF	Alexafluor
AIP1	Actin Interactin Protein 1
Amp	Ampicillin
APS	Ammonium persulphate
Arp2/3	actin-related proteins 2 and 3 complex
ATP	Adenosine-triphosphate
BSA	Bovine serum albumin
CAR	cytokinetic actomyosin ring
Cdc42	Cell division control protein 42 homolog
cDNA	complementary deoxyribonucleic acid
CFTR	cystic fibrosis transmembrane conductance regulator
c-Src	Proto-oncogene tyrosine-protein kinase
DAD	Diaphanous Activating Domain
DAPI	4',6-Diamidino-2-Phenylindole, Dihydrochloride
DID	Diaphanous Inhibitory Domain
DMEM	Dulbecco's modified eagle's medium
DMSO	Dimethyl sulphoxide
DNA	Deoxyribonucleic acid
EDTA	Ethylenediaminetetraacetic acid

EGF	Epidermal growth factor
EM	Electron Microscopy
ERK	extracellular-signal-regulated kinase
F-actin	Filamentous actin
FAK	Focal adhesion kinase
FBS	Foetal Bovine Serum
G-actin	Globular actin
GAPDH	Glyceraldehyde 3-phosphate dehydrogenase
GDP	guanosine diphosphate
GRB2	Growth Factor receptor-bound protein 2
GTP	guanosine triphosphate
GTPase	guanosine triphosphate hydrolase
HMW	High molecular weight
HRP	Horseradish peroxidase
Hsp70	Heat shock protein 70
kb	Kilo base pair
kDa	Kilo Dalton
KO	Knockout
LB	Lysogeny broth
LIM Kinase	LIM (Lin11, Isl-1 & Mec-3) domain containing Kinase
LMW	Low molecular weight
MEFs	Mouse embryonic fibroblasts
MLCK	Myosin light chain kinase
mRNA	Messenger ribonucleic acid
MW	Molecular weight

n	Number of replicate experiments
NCK	non-catalytic region of tyrosine kinase adaptor protein
NIH	National Institute of Health
NP40	nonyl-phenoxypolyethoxylethanol
N-WASP	neuronal Wiskott-Aldrich Syndrome protein
PAK	p21 activated kinase
PBS	Phosphate buffered saline
PCR	polymerase chain reaction
PDGF	Platelet-derived growth factor
PFA	Paraformaldehyde
Pi	Inorganic phosphate
PIP2	Phosphatidylinositol 4,5-bisphosphate
PKC	Protein Kinase C
PM	Plasma membrane
PMEF	Primary Mouse Embryonic Fibroblast
PVDF	Polyvinylidene fluoride
qPCR	quantitative polymerase chain reaction
Rac	Ras-related C3 botulinum toxin substrate
Rho	Rho family of GTPases
RIPA	Radio-immunoprecipitation assay buffer
RNA	Ribonucleic acid
ROCK	Rho-associated protein kinase
ROI	Region of Interest
RT-qPCR	Reverse transcription qPCR
RT	Room temperature

WAVE/Scar	WASP family Verprolin-homologous protein
SDS	Sodium dodecyl sulphate
SDS-PAGE	Sodium dodecyl sulphate-PAGE
SEM	Standard error of the mean
SH2	Src Homology 2 domain
SiRNA	Small interfering ribonucleic acid
SOC	Super Optimal broth with Catabolite repression
SSH	Slingshot homolog
SSH1L	slingshot homolog 1 (long isoform)
SV40	Simian vacuolating virus 40
TAE	Tris-acetate-EDTA
TBS	Tris buffered saline
TBST	Tris buffered saline and Tween 20
TEMED	N, N, N',N'-tetraethylmethylenediamine
<i>TPM</i>	Tropomyosin (human gene)
<i>Tpm</i>	Tropomyosin (mouse gene)
Tpm	Tropomyosin (protein)
UV	Ultraviolet
v/v	volume/volume
w/v	weight/volume
WASP	Wiskott-Aldrich Syndrome protein
WIP	WASP interacting protein
WT, wt	Wild Type

List of Figures

Figure 1.1. Major cellular processes regulated by the actin cytoskeleton in eukaryotic cells.....	3
Figure 1.2. Regulation of actin dynamics by actin binding proteins.....	6
Figure 1.3. Actin Filament Elongation, ATP Hydrolysis, and Phosphate Dissociation...7	
Figure 1.4. Model of tropomyosin on the actin filament.....	10
Figure 1.5. The four Mammalian Tpm genes and their major protein products.....	12
Figure 1.6. Tpm isoforms regulate the interactions of actin filaments with actin binding proteins.....	15
Figure 1.7. Schematic illustration of the actin cytoskeleton in a migrating cell.....	21
Figure 1.8. Dendritic Nucleation/Array Treadmilling Model for Protrusion of the Leading Edge.....	24
Figure 1.9. Focal adhesion initiation events.....	27
Figure 3.1. Difference in clarity between the sheep polyclonal and rat monoclonal $\alpha/1b$ antibodies.....	59
Figure 3.2. Characterisation of the $\alpha/1b$ rat monoclonal antibody.....	61
Figure 3.3. Tpm1.8/9 display a unique lamellipodial localisation compared to other Tpm isoforms.....	64
Figure 3.4. Tpm2.1 knockdown does not result in loss of lamellipodial staining.....	66
Figure 3.5. Tpm2.1 is not detected in the lamellipodium of MEF cells.....	68

Figure 3.6. Tpm1.8/9 and Arp2/3 co-occupy the lamellipodium.....	70
Figure 3.7. Incorrect sorting of tagged Tpms.....	75
Figure 3.8. Failure of the $\alpha/1b$ to bind to exogenous Tpm1.8 or Tpm1.9.....	76
Figure 3.9. Vector map of PG538 showing the orientation of Tpm1.8 and m- NeonGreen relative to the mammalian CMV promoter.....	78
Figure 3.10. Western blot of MEF lysates and MEF lysates transfected with PG538 as probed with the $\alpha/1b$ antibody.....	80
Figure 3.11. Cellular localisation and detection of Tpm1.8-mNG.....	82
Figure 4.1. siRNA directed silencing of Tpm1.8/9 expression.....	88
Figure 4.2. Knockdown of Tpm1.8/9 results in no compensatory expression of other Tpm isoforms.....	90
Figure 4.3. Knockdown of Tpm1.8/9 leads to its depletion from the lamellipodium...	92
Figure 4.4. Tpm1.8/9 knockdown results in an increase in peripheral Arp2/3.....	94
Figure 4.5. Tpm1.8/9 knockdown results an increased lamellipodial thickness.....	96
Figure 4.6. Arp2/3 inhibition leads to an increase in Tpm1.8/9 protein.....	98
Figure 4.7. Representative confocal image of a MEF cell following 6 h CK666 treatment.....	100
Figure 5.1. Tpm1.8/9 knockdown affects random cell migration.....	109
Figure 5.2. Tpm1.8/9 knockdown does not impact 3D random cell migration.....	111
Figure 5.3. Impaired protrusion persistence in Tpm1.8/9 knockdown cells.....	113

Figure 5.4. Knockdown of Tpm1.8/9 disrupts the formation of focal adhesions.....	115
Figure 5.5. Knockdown of Tpm1.8/9 disrupts the maturation of focal adhesions.....	118
Figure 6.1. Sequence of appearance of other actin binding proteins following activation of the Arp2/3 complex.....	131
Figure 6.2. Cortactin knockdown has no significant impact on the localisation or expression levels of Tpm1.8/9.....	134
Figure 6.3. Confirmation of gene silencing by Coronin 1B and cofilin siRNA.....	137
Figure 6.4. Coronin and cofilin knockdown removes Tpm1.8/9 from the leading edge.....	139
Figure 6.5. Coronin and cofilin knockdown results in a decrease in Tpm1.8/9 protein.....	141
Figure 6.6. mRNA levels remain constant.....	143
Figure 6.7. Tpm1.8/9 is not degraded by the 26S Proteasome.....	145
Figure 7.1. Working model for the regulation of lamellipodial persistence by tropomyosin.....	158

List of Tables

Table 2.1. Commercially available reagents and kits.....	37
Table 2.2. List of equipment and manufacturers.....	39
Table 2.3. Composition of buffers and solutions.....	40
Table 2.4. Primary antibodies used for Western blotting and immunofluorescence.....	41
Table 2.5. Secondary antibodies for Western blotting and immunofluorescence.....	42
Table 2.6. siRNA sequences used in this thesis.....	43

Table of Contents

Originality Statement	i
Abstract	ii
Acknowledgements	iii
Publications	v
Meeting Abstracts	vi
Prizes Awarded	vii
List of Abbreviations.....	viii
List of Figures	xii
List of Tables.....	xv
Table of Contents	xvi
Chapter 1: Introduction	2
Actin; the building block of a functionally diverse cytoskeleton.....	2
Actin Nucleating Factors	4
Actin disassembly.....	8
Actin bundling and cross-linking	8
Tropomyosins; master regulators of actin filament form and function.....	9
Alterations to the actin cytoskeleton in cancer.....	16
The problem with targeting the actin cytoskeleton for chemotherapy	17
Tropomyosin as a regulator of cancer cell transformation.....	17
Down-regulation of HMW tropomyosins; a crucial step in oncogenic transformation	18
Novel strategies for anticancer compounds to target the actin cytoskeleton.....	19
The actin cytoskeleton in cell migration	19
Cellular motility is initiated by the rapid assembly of actin filaments.....	21
Leading edge protrusion is coupled to cell-matrix adhesions	25

Tropomyosin regulates the interaction of non-muscle myosins with actin to generate contractile force	27
Controversy surrounding the organisation of actin filaments at the leading edge	28
Tropomyosin at the leading edge	30
Aims and significance	31
Chapter 2: Materials and Methods	35
Reagents, Equipment and Chemicals used in this Thesis	35
Commercial Reagents used in this Thesis	36
Equipment used in this Thesis	38
Buffers used in this Thesis.....	39
Antibodies used in this Thesis	40
siRNAs used in this Thesis	42
Cell Culture	43
General maintenance of cells.....	43
Passaging of cells.....	43
Cryopreservation of cells	43
Antibody Production	44
Western Blot Analysis.....	44
Extraction of protein	44
SDS-polyacrylamide gel electrophoresis (SDS-PAGE).....	45
Protein transfer and western blotting.....	45
Gene Silencing by Small Interfering RNA (siRNA).....	46
Transient transfection of siRNA	46
Cell Imaging	46
Immunofluorescent staining	46
Microscopy and fluorescence quantification	47
Live-cell imaging.....	48

Random migration assay.....	48
Preparation of collagen gels.....	48
Imaging of cells in collagen gels	49
Kymography	49
Cell Morphometry.....	49
Focal adhesion morphometry.....	50
Measurement of protein recruitment into lamellipodia	50
Molecular Biology.....	51
Restriction endonuclease digestion.....	51
Gel purification of DNA fragments	51
Ligation of DNA fragments and bacterial transformation.....	51
Purification of plasmid DNA.....	52
Extraction of RNA	52
Preparation of cDNA	53
qPCR.....	53
Standard PCR.....	54
Statistical Analysis	54
Chapter 3: Characterisation of the $\alpha/1b$ rat monoclonal antibody and the lamellipodial localisation of Tpm1.8/9.....	56
Introduction	56
Results	59
Characterisation of the $\alpha/1b$ rat monoclonal antibody.....	59
Tpm1.8/9 display a unique cellular localisation compared to other Tpm isoforms	61
Cross-reactivity of the $\alpha/1b$ rat monoclonal antibody with Tpm2.1.....	64
Confirmation of the lamellipodial localisation of Tpm1.8/9	68
Discussion	70
Tropomyosin in the lamellipodium.....	70

Summary of findings	71
Problems associated with fluorescently-labelled Tpm1.8/9	72
Concluding Remarks.....	80
Chapter 4: siRNA knockdown of Tpm1.8/9 and its effect on cell morphology and Arp2/3 activity	83
Introduction	83
Results	85
Design of Tpm1.8/9 specific siRNA.....	85
Tpm1.8/9 knockdown results in increased peripheral Arp2/3	92
Tpm1.8/9 knockdown results an increased lamellipodial thickness.....	94
Arp2/3 inhibition results in an increase in Tpm1.8/9 protein levels.....	96
Discussion	100
Regulating the dynamics of two distinct actin networks	100
Summary of Findings.....	100
A higher level of actin filament regulation.....	101
Chapter 5: The effects of Tpm1.8/9 knockdown on cell motility, lamellipodial persistence and focal adhesions.....	104
Introduction	104
Results	107
Tpm1.8/9 knockdown affects random, 2D cell migration	107
Tpm1.8/9 knockdown does not affect 3D random cell migration	109
Tpm1.8/9 knockdown results in more dynamic, less persistent lamellipodia	111
Knockdown of Tpm1.8/9 results in the formation of fewer focal adhesions	113
Knockdown of Tpm1.8/9 disrupts the maturation of focal adhesions.....	115
Discussion	119
Summary of findings	119
Relationship between lamellipodial persistence and whole-cell motility.....	120

Relationship between efficiency of focal adhesion production and lamellipodial persistence.....	120
Relationship between Tpm1.8/9 and focal adhesion maturation	121
Chapter 6: Mechanistic insight into the generation of Tpm1.8/9 actin filaments in the lamellipodium.....	124
Introduction	124
Cortactin.....	125
Coronin 1B and cofilin	126
Results	128
Arp2/3 and cortactin occupy newly formed lamellipodia, whereas coronin 1B and Tpm1.8/9 recruitment is delayed	128
Cortactin knockdown does not affect Tpm1.8/9 localisation or protein levels	132
Tpm1.8/9 is depleted from the leading edge following knockdown of coronin 1B or cofilin	135
Tpm1.8/9 protein levels are reduced following knockdown of coronin 1B or cofilin	139
mRNA levels remain constant following coronin 1B or cofilin knockdown	141
Figure 6.6. mRNA levels remain constant following coronin 1B or cofilin knockdown.....	142
Tpm1.8/9 is not degraded by the 26S Proteasome.....	143
Discussion	145
Collaboration of distinct actin networks.....	145
Summary of findings	146
Proposed mechanism of generation of Tpm1.8/9-containing actin filaments at the leading edge	147
Chapter 7: General Discussion	151
Outcomes and significance of the study	151
Tropomyosin at the leading edge	152

The relationship between tropomyosin and the Arp2/3 complex.....	153
Coupling the dynamics of two actin networks	154
Tropomyosin allows the collaboration of distinct actin networks.....	155
Working model for tropomyosin-mediated regulation of lamellipodial persistence.	155
Concluding Remarks	158
References	161

Chapter One

Introduction

Chapter 1: Introduction

Actin; the building block of a functionally diverse cytoskeleton

Actin is the most abundant protein found in eukaryotic cells and represents the basic subunit of the microfilament system (Dominguez & Holmes, 2011). As well as the role of actin filaments in muscle cells as part of the contractile apparatus, non-muscle actin plays a role in almost all cellular functions including cell division, polarity, maintenance of cell shape and cell motility (Dominguez & Holmes, 2011) (Figure 1.1). This 42 kDa globular protein undergoes cycles of polymerisation and disassembly between its globular (G-actin) and filamentous (F-actin) forms. The filaments formed are helical polymers with an overall molecular polarity and exist in a constant state of flux with new monomers being added to the barbed end, and removed at the pointed end to produce free monomers in an ATP dependent process (Pollard, 1986). This cyclical process, known as tread-milling, gives rise to the dynamic nature of actin filaments, allowing precise cytoskeletal structures to be quickly and efficiently assembled as needed. Actin filaments are found as organised assemblies localised in discrete areas of the cytoplasm where they perform their functions in response to different stimuli. As well as individual filaments, actin is often found bundled into thick cables which traverse the cell, known as stress fibres. The biochemistry of actin alone cannot explain the complexity of function observed under physiological conditions. Actin achieves its vast array of functions via its interaction with a rich variety of actin binding proteins, of which more than 60 classes have been described (Pollard, Blanchoin & Mullins, 2000) (Figure 1.2). A handful of these relevant to this study will be discussed here.

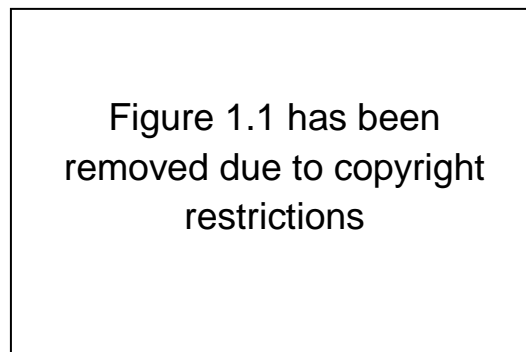


Figure 1.1. Major cellular processes regulated by the actin cytoskeleton in eukaryotic cells.

(A) The activation of cell membrane receptors leads to a cascade of intracellular signalling events, which often converge on the actin cytoskeleton to mediate cellular responses. Motility: cells develop a polarised morphology, characterised by the development of actin-based protrusions of the leading edge. Adhesion: the actin cytoskeleton regulates integrin-mediated adhesion between the cell and extracellular matrix; these adhesions facilitate cellular movement by forming at the leading edge and disassembling at the trailing edge. The cytoskeleton also regulates cell-cell adherens junctions necessary to maintain the integrity of epithelia. Trafficking: at the plasma membrane, actin polymerisation is associated with the invagination and formation of clatherin-coated pits (endocytosis) and the fusion of secretory vesicles (exocytosis). Actin is also required during the budding, fission and transport of proteins through the Golgi apparatus. Apoptosis: the actin cytoskeleton regulates mitochondrial events involved the apoptotic cascade. Cell division: actin is the core constituent of the contractile ring necessary for cytokinesis. (B) Contraction: the sarcomere is the smallest contractile unit of striated muscle, consisting of highly organised actin and myosin filaments that interdigitate to produce contractile force (Bonello, Stehn & Gunning, 2009).

Actin Nucleating Factors

Spontaneous assembly of pure actin monomers is energetically unfavourable due to the instability of actin dimers and trimers, but once polymerisation has initiated, filaments grow rapidly. Subunit addition at the barbed end is diffusion limited, meaning that the rate of growth is determined by the probability of subunits colliding with the end (Drenckhahn & Pollard, 1986). Although ADP-actin subunits dissociate faster from the barbed end than ATP-actin subunits, the resulting tread-milling would still be very slow (Carlier & Pantaloni, 1986) (Figure 1.3). Under physiological conditions, actin assembly proteins or ‘nucleating factors’ mediate filament assembly by bringing monomers within close proximity to one another, promoting rapid polymerisation. The actin-related proteins 2 and 3 complex (Arp2/3) was the first actin nucleating factor to be described (Goley & Welch, 2006). Upon activation, Arp2/3 binds to the side of a pre-existing actin filament, generating a stable trimer for the growth of a daughter filament, forming a branch at a 70° angle from the mother filament (Mullins, Heuser & Pollard, 1998). Subsequent branching creates a dendritic actin network. The promotion and stabilisation of the branched actin network is co-ordinated by cortactin, which has been shown to promote cell motility by acting synergistically with N-WASp to enhance activation of Arp2/3 while simultaneously stabilising newly generated filament branch points (Bryce et al., 2005; Weaver et al., 2001). Another family of actin filament nucleating factors are the formins which can mediate both actin assembly and disassembly to produce a vast array of cytoskeletal structures. Formins have been demonstrated to be capable of nucleating, polymerising, bundling and severing actin filaments in vitro (Pruyne et al., 2002). To date, there are 15 known mammalian formins, grouped into 7 families (Higgs & Peterson, 2005). Unlike the Arp2/3 complex, formins nucleate actin filaments and remain bound to the barbed end, generating

unbranched actin filaments through a processive capping mechanism (Otomo et al., 2005). Generally, formins exist in an auto-inhibited state between their N-terminal Diaphanous Inhibitory Domain (DID) and C-terminal Diaphanous Activating Domain (DAD). Activation occurs when an active Rho-GTPase disrupts the interaction between the DID and DAD domains (Seth, Otomo & Rosen, 2006).

Figure 1.2 has been
removed due to copyright
restrictions

Figure 1.2. Regulation of actin dynamics by actin binding proteins (Winder & Ayscough, 2005).

Figure 1.3 has been removed due to copyright restrictions

Figure 1.3. Actin Filament Elongation, ATP Hydrolysis, and Phosphate Dissociation.

The EM shows an actin filament seed decorated with myosin heads and elongated with ATP-actin. The association rate constants have units of $\mu\text{M}^{-1} \text{s}^{-1}$. Dissociation rate constants have units of s^{-1} . The ratio of the dissociation rate constant to the association rate constant gives K , the dissociation equilibrium constant with units of μM . Note that the equilibrium constants for ATP-actin differ at the two ends, giving rise to slow steady state treadmilling. Hydrolysis of ATP bound to each subunit is fast, but dissociation of the γ phosphate is very slow (Pollard & Borisy, 2003).

Actin disassembly

In order to drive filament turnover, actin networks are also required to be disassembled. ADF/Cofilin (hereafter referred to as cofilin) severs and potentially enhances depolymerisation of filaments by cooperatively binding along the sides of actin filaments and inducing conformational changes in filament structure (Bamburg, 1999). The activity of Cofilin is regulated in a variety of ways including phosphorylation, PIP2 binding, intracellular pH changes and interactions with binding partners such as AIP1 (Bamburg, 1999). Coronin 1B disassembles Arp2/3-containing actin filament branches to drive the turnover of branched networks (Cai et al., 2008) by interacting with the Arp2/3 complex to inhibit filament nucleation and also by directing protein phosphatase slingshot homolog 1 (SSH1L) to the lamellipodium where it activates Cofilin via dephosphorylation (Cai et al., 2007). In addition, Arp2/3 networks are remodelled by proteins such as GMF which blocks the actin-Arp2/3 interaction (Haynes et al., 2015; Poukkula et al., 2014).

Actin bundling and cross-linking

Filaments are assembled into superstructures by actin-filament-bundling proteins. Some bundling proteins (e.g. fascin) form parallel bundles, whereas others (e.g. α -actinin) can form both parallel and mixed polarity bundles (Bartles, 2000). In general, crosslinking proteins have two actin-binding sites, often because they dimerise, and the location of actin-binding sites determines the filament arrangement and type of crosslinked structure formed. Bundling proteins can be selective about the orientation with which they bind to the filament, allowing the specific formation of bundles of either mixed or uniform polarity. Bundling proteins are often modular and contain repeated actin-filament-binding domains (Stevenson, Veltman & Machesky, 2012).

Tropomyosins; master regulators of actin filament form and function

It is important to note that, while plants express many isoforms of actin (McDowell et al., 1996) suggesting an evolutionary need to diversify function, only two cytoskeletal isoforms of actin exist in mammalian cells. Given the functional diversity of actin observed in higher organisms, it begs the question of how a putatively more complex system can achieve this with a seemingly simpler array of building blocks at its disposal. The answer lies in the fact that, unlike plants, actin filaments in animal and yeast cells are not a homogeneous system but rather consist of compositionally distinct filaments arising from the inclusion of various isoforms of tropomyosin (Gunning, O'Neill & Hardeman, 2008).

Tropomyosin (Tpm) is an alpha-helical, coiled-coil protein, dimers of which associate head-to-tail to form a continuous polymer which lies along the major groove of actin filaments (Li et al., 2011) (Figure 1.4). The role of tropomyosin in muscle is very well understood where it is responsible for regulating the interaction between actin and myosin (Holmes & Lehman, 2008). Non-muscle cells also contain tropomyosin where its proposed role is to stabilise actin filaments by modulating their interactions with actin binding proteins (Schevzov et al., 2005). Recent studies in a variety of systems have shown that the diversity of actin cytoskeletal function is paralleled by a diversity of tropomyosin isoforms (Gunning et al., 2005).

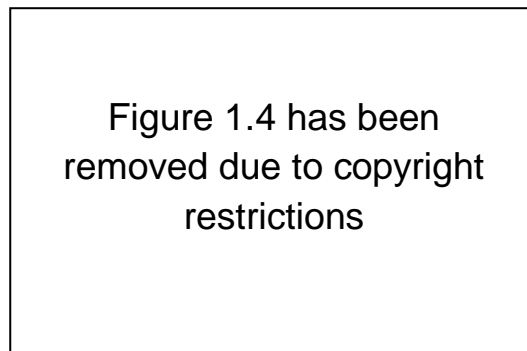


Figure 1.4. Model of tropomyosin on the actin filament as proposed by (Li et al., 2011).

Tropomyosin winds symmetrically along the two long-pitch helices of the actin filament, making similar contacts with each actin subunit (numbered) along its 385-Å-long path (Dominguez, 2011).

Isoforms of tropomyosin are generated by the alternative splicing of four mammalian genes resulting in over 40 isoforms, the majority of which are cytoskeletal. The use of alternative promoters at the amino terminus gives rise to either high molecular weight (HMW) isoforms or low molecular weight (LMW) isoforms (Gunning et al., 2005) (Figure 1.5). Different tropomyosin isoforms can differentially regulate actin filament function. Actin filaments decorated by different isoforms of tropomyosin have been shown to recruit different actin binding proteins and myosin motors, leading to a difference in filament stability (Bryce, Schevzov, Ferguson, Percival, Lin, Matsumura, Bamberg, Jeffrey, Hardeman, Gunning, et al., 2003; Creed et al., 2011). Functionally distinct sub-populations of actin filaments can therefore be defined on the basis of their tropomyosin isoform composition.

Figure 1.5 has been removed due to copyright restrictions

Figure 1.5. The four Mammalian Tpm genes and their major protein products.

Schematic representation of the organisation of the mammalian Tpm genes. Coloured boxes represent the protein coding exons numbered 1 to 9 and lines the introns. Unshaded boxes signify untranslated sequences and black boxes are exons common to all the genes which share a high degree of homology. The various isoforms generated via alternative exon splicing are listed under each gene and only the major products verified by northern or protein gel blots are shown. (Gunning et al., 2005).

It should be noted that recently the nomenclature of the mammalian tropomyosin isoforms has changed. Geeves et al., (2014) provide a detailed outline of this new nomenclature with reference to some common, now superseded isoform names (Geeves, Hitchcock-DeGregori & Gunning, 2014).

Tropomyosin isoforms also display extensive intracellular sorting, resulting in spatially distinct actin filament populations. Sorting of Tpm isoforms has been observed in a number of cell types, including fibroblasts, epithelial cells, osteoclasts, neurons and muscle cells (Martin & Gunning, 2008). The exact mechanism underlying the way in which different isoforms of tropomyosin are targeted to specific actin structures within the cell remains unknown but a few independent experiments have provided some insights. On one hand, a molecular sink model has been proposed whereby isoforms accumulate in actin-based structures where they have the highest affinity, rather than the presence of an intrinsic sorting signal that directs particular isoforms to a single geographical location (Martin, Schevzov & Gunning, 2010). Other groups' work in yeast has revealed the importance of the N-terminal acetylation of tropomyosin in effecting its cellular localisation and function.

Acetylated tropomyosin (Cdc8) is found predominantly in the contractile cytokinetic actomyosin ring (CAR) whereas the un-acetylated form is seen exclusively on interphase actin filaments (Coulton et al., 2010; Skoumpla et al., 2007). In addition, the acetylated state of yeast tropomyosin can regulate the motility of myosin, with the motility of class II myosin being affected but not that of class I and V myosin (Clayton et al., 2010; Skau & Kovar, 2010). Johnson et al (2014) have recently demonstrated that the formin isoform used to build an actin filament in yeast determines which tropomyosin is incorporated into the filament and that in turn dictates the functional

characteristics of the filament including binding of specific myosin motors (Johnson, East & Mulvihill, 2014).

Data so far provides us with a working model for tropomyosin-directed regulation of actin filament function (Figure 1.6). Cell culture studies have shown that actin filaments decorated with different Tpm isoforms recruit different actin binding proteins ultimately regulating the organisational and functional properties of the filaments (Bryce, Schevzov & Gunning, 2003; Creed et al., 2011). Finally, there is the issue of whether a single actin filament is restricted to being decorated by only one isoform of tropomyosin or if hetero-polymers can lie along the same filament. With the advancement of super-resolution microscopy techniques, answers to these questions are likely on the horizon.

Figure 1.6 has been removed due to copyright restrictions

Figure 1.6. Tpm isoforms regulate the interactions of actin filaments with actin binding proteins.

Tpm 3.1, Tpm 1.12 and Tpm1.7 have different impacts on the association of myosin II, ADF/cofilin and fascin with actin filaments. For example, actin filaments coated with Tpm3.1 recruit non-muscle myosin II resulting in stable microfilaments under tension (left). Conversely, filaments coated with Tpm1.12 allow binding of ADF/cofilin which results in higher filament turnover and shorter actin filaments (middle). Finally, filaments coated with Tpm1.7 can incorporate fascin, resulting in short cross-linked filaments (right) (Bryce, Schevzov & Gunning, 2003; Creed et al., 2011).

Alterations to the actin cytoskeleton in cancer

Most of the alterations that lead to tumour formation and metastasis can be described as being associated with several hallmarks of cancer cells, which represent the properties that are necessary for cancer cell survival and tumour spreading. These genomic or epigenetic changes target pathways that lead to uncontrolled proliferation, disruption of apoptotic mechanisms, initiation of angiogenesis, evasion of immune surveillance and the ability to invade into surrounding tissues to form metastases (Hanahan & Weinberg, 2011). Owing to the critical role of invasion and migration in metastasis, there has been considerable interest in targeting cancer cells' migration machinery as a novel therapeutic approach. However, it has become clear that cancer cells use a range of motility phenotypes to migrate and invade (Friedl, 2004). Transitions between epithelial and mesenchymal phenotypes of cells are required for normal morphogenetic processes and tissue remodelling during embryogenesis. However, sustained signalling by oncogenic Ras may result in morphological transformation to a mesenchymal phenotype, which is associated with changes in gene expression, loss of cell-cell adhesions and increased invasiveness of tumour cells (Behrens et al., 1989). Alterations to the actin based cytoskeleton are also an established characteristic of transformed cells. Oncogenic signalling pathways directly target the actin cytoskeleton leading to disruption of stress fibres (Pollack, Osborn & Weber, 1975) and associated adhesive structures which in turn leads to enhanced motility and invasiveness of tumour cells along with anchorage-independent growth and cellular tumorigenicity (Shin et al., 1975). These findings are supported by studies in which oncogenic-mediated changes to the actin cytoskeleton were able to be reversed by ectopic expression of specific actin filament stabilising proteins such as tropomyosin (Braverman et al., 1996; Gimona, Kazzaz & Helfman, 1996; Janssen & Mier, 1997; Prasad, Fuldner & Cooper, 1993;

Takenaga & Masuda, 1994; Yager et al., 2003). The precise mechanisms by which these changes to the actin cytoskeleton contribute to signalling events that provide a tumour cell with a selective growth advantage remain to be fully understood. Consequently, the observed aberrant organisation of the actin cytoskeleton in transformed cells has made it an attractive target for early chemotherapeutic strategies (Bonello, Stehn & Gunning, 2009).

The problem with targeting the actin cytoskeleton for chemotherapy

To date little progress has been made with compounds that disrupt the organisation of actin filaments, mainly due to the essential role of actin in the composition of the functional unit of muscle contraction, the sarcomere, universal disruption of which results in intolerable toxicity to cardiac and respiratory muscle. Furthermore, selective drug targeting has been hampered by the plasticity of the actin cytoskeleton (Bonello, Stehn & Gunning, 2009). As mentioned earlier, the actin cytoskeleton is not a single, uniform system but rather a series of unique filament populations with distinct functions arising from their inclusion of various isoforms of tropomyosin. This opens up the exciting possibility that certain filament populations may be indispensable for tumour cell function, yet molecularly distinct from those found in the contractile apparatus of heart and skeletal muscle.

Tropomyosin as a regulator of cancer cell transformation

The changes in rearrangement of microfilament bundles seen in transformed cells appear to correlate with alterations in tropomyosin expression. Decreased expression of non-muscle tropomyosins is commonly associated with the transformed phenotype. In addition, these changes in Tpm expression occur in cells of all species examined including chicken, rodents and human, indicating that alterations of Tpm expression is a

common feature of the transformed phenotype (Helfman et al., 2008). In particular, the expression of HMW Tpm isoforms (Tpm2.1, 1.6 & 1.7) is decreased during oncogenic transformation (Franzen et al., 1996; Jung et al., 2000; Wang et al., 1996). The drive behind this shift in tropomyosin expression in transformed cells is not well understood but may reflect a requirement for the cell to eliminate certain functions associated with HMW Tpm containing actin filaments (O'Neill, Stehn & Gunning, 2008).

Down-regulation of HMW tropomyosins; a crucial step in oncogenic transformation

It has been demonstrated that Tpm1.6 is reduced in malignant ovarian carcinomas compared to benign ovarian tumours (Alaiya et al., 1997) and that Tpm2.1 and Tpm1.6 are reduced in prostate carcinoma compared to prostate hyperplasia (Alaiya et al., 2001). Although it remains unclear whether suppression of HMW Tpm contributes directly to the disruption in cyto-architecture, or the loss of Tpm is simply associated with the formation of aberrant filaments, decreased expression of HMW Tpm correlates with the disruption of stress fibres seen in transformed cells and is supported by studies which also showed that forced expression of HMW Tpm2.1 reverses transformation-associated changes by restoring the structural components of the cell and abolishing anchorage independent growth (Prasad, Fuldner & Cooper, 1993; Yager et al., 2003). Comparison between low- and highly-metastatic lung carcinoma cells showed that a decrease in Tpm1.6 is associated with a higher level of metastasis (Takenaga, Nakamura & Sakiyama, 1988; Takenaga et al., 1988).

While further studies will be required to determine how changes in Tpm expression contribute to tumour growth and if Tpm expression can be utilised as a diagnostic tool (Stehn et al., 2006), these observations have sparked interest in tropomyosins as a

potential new target for chemotherapy. While traditionally, the approach has been to try and restore the expression of HMW Tpm's in transformed cells in the hope of reversing tumourigenicity, another more exciting possibility is that an increased reliance on LMW Tpm's may in fact make tumour cells more vulnerable and therefore a better target for cancer chemotherapy.

Novel strategies for anticancer compounds to target the actin cytoskeleton

Recently, Stehn and colleagues described a novel class of anti-tropomyosin compounds which preferentially target Tpm3.1 containing actin filaments in cancer cells. The lead compound, TR100, has been shown to be effective against a panel of neural crest-derived tumour cell lines in both 2D and 3D cultures, with minimal impact on the contractile properties of isolated rat adult cardiomyocytes. Furthermore, using xenograft models, Stehn and colleagues showed that TR100 is effective in reducing tumour cell growth in vivo without compromising cardiac function (Stehn et al., 2013), showing that it is indeed possible to selectively target actin filaments fundamental to tumour cell viability based on their tropomyosin isoform composition. This improvement in specificity provides a pathway for the development of a novel class of anti-actin compounds for the potential treatment of a wide variety of cancers.

The actin cytoskeleton in cell migration

Directional motility is a fundamental cellular process essential for embryonic morphogenesis, wound healing, immune surveillance and tissue repair. Dysregulation of this process resulting in aberrant cell movement is a hallmark feature of metastatic cancer cells. The development of metastases accounts for more than 90% of cancer related mortality (Sporn, 1996), highlighting the need for an understanding in the

regulatory mechanisms underlying cell motility. Almost universally, eukaryotic cell migration involves a series of four highly orchestrated steps including protrusion of the leading plasma membrane, formation of cell-substrate adhesions, generation of actomyosin contractile force and release of substrate adhesions at the trailing cell rear (Lauffenburger & Horwitz, 1996) (Figure 1.7). Dynamic remodelling of the actin cytoskeleton underlies cell migration, with many essential cytoskeletal proteins conserved across eukaryotes. This may explain why similar motility phenotypes are observed across a broad range of cells such as fibroblasts, neuronal and epithelial cells.

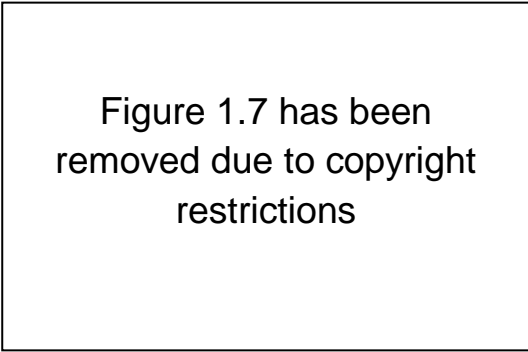


Figure 1.7 has been removed due to copyright restrictions

Figure 1.7. Schematic illustration of the actin cytoskeleton in a migrating cell.

This schematic cell contains the major structures found in migrating cells but does not correspond to a precise cell type. **(A)** In lamellipodia, branched actin filaments are generated at the plasma membrane by the signal responsive WASP-Arp2/3 machinery and maintained in fast treadmilling by a set of regulatory proteins. **(B)** During cell migration, cells extend finger like protrusions called filopodia beyond the leading edge of protruding lamellipodia to sense the environment. At the tip of filopodia, formins catalyse the processive assembly of actin. The resulting non-branched actin filaments are tightly bundled by several proteins including fascin. **(C)** Slow moving cells form focal adhesions in response to RhoA signalling. Focal adhesions connect the extracellular matrix to contractile bundles made of actin filaments, myosin II, and bundling proteins including α -actinin. **(D)** The lamella is characterized by a slow actin turnover and contains the signature proteins tropomyosin and myosin II. Lp, lamellipodium; Fp, filopodium; Lm, lamella; SF, stress fibre; FA, focal adhesion; FC, focal complex (Le Clainche & Carlier, 2008).

Cellular motility is initiated by the rapid assembly of actin filaments

As mentioned earlier, rapid assembly of actin filaments by addition of monomers at the barbed end and disassembly at the pointed end results in a tread-milling effect. This retrograde flow of the actin filament in a particular direction underlies the principal step in cell migration. Although this process has been widely studied, a detailed mechanism underlying how this process is regulated and coupled to the rest of the cell migration cycle to translate a persistent protrusive force into whole cell translocation remains to be fully understood. Cells extend four different plasma membrane protrusions at the leading edge; lamellipodia which can extend long distances through the extracellular matrix to pull cells through tissues (Friedl & Gilmour, 2009), filopodia which explore the cell's surroundings, blebs which have been described to drive directional migration during development (Charras & Paluch, 2008) and invadopodia are protrusions which allow invasion through tissues via metalloprotease mediated degradation of the extracellular matrix (Buccione, Caldieri & Ayala, 2009). Each of these structures uniquely contributes to migration and, depending on the specific circumstances can also co-exist at the leading edge as has been previously observed in migrating zebrafish cells during gastrulation (Diz-Munoz et al., 2010). Perhaps the most well-studied of these structures is the lamellipodium. These thin, sheet-like projections were first described and named by Abercrombie in 1970 who observed them at the leading edge of fibroblasts in culture (Abercrombie, Heaysman & Pegrum, 1970b). In 1971, it was shown by Wessels and colleagues that the dominant structural component of lamellipodia was actin, whereby it was demonstrated that lamellipodia were sensitive to cytocholasin (Yamada, Spooner & Wessells, 1971). Later, it was demonstrated that lamellipodial actin networks were branched, that Arp2/3 complex localised to branch junctions in these networks and that the branches adhered very closely to the 70° angle

observed *in vitro* (Svitkina & Borisy, 1999; Svitkina et al., 1997). Unsurprisingly, the Arp2/3 complex is abundant at the leading edge of migrating cells where it functions downstream of WAVE and N-WASp activators, respectively, in response to Rac signalling (Pollitt & Insall, 2009). The major driving force behind leading edge protrusion is therefore Arp2/3 mediated polymerisation of actin filaments, which results in the generation of a dense network of short, branched actin filaments with a rapid turnover of filament assembly (Pollard & Borisy, 2003) (Figure 1.8) and it has been demonstrated that cells lacking Arp2/3 expression are unable to produce lamellipodia. Interestingly however, Arp2/3-depleted cells respond normally to shallow gradients of PDGF, indicating that lamellipodia are not required for chemotaxis (Wu et al., 2012). The stabilisation and disassembly of the branched actin network of the lamellipodium is co-ordinated by a defined network of proteins. These include cortactin, which has been shown to promote cell motility by acting synergistically with N-WASp to enhance activation of Arp2/3 while simultaneously stabilising newly generated filament branch points (Bryce et al., 2005; Weaver et al., 2001). Conversely, coronin 1B disassembles Arp2/3-containing actin filament branches to drive the turnover of branched networks (Cai et al., 2008) by interacting with the Arp2/3 complex to inhibit filament nucleation and also by directing protein phosphatase slingshot homolog 1 (SSH1L) to the lamellipodium where it activates the actin filament severing protein cofilin via dephosphorylation (Cai et al., 2007).

Figure 1.8 has been removed due to copyright restrictions

Figure 1.8. Dendritic Nucleation/Array Treadmilling Model for Protrusion of the Leading Edge.

(1) Extracellular signals activate receptors. (2) The associated signal transduction pathways produce active Rho-family GTPases and PIP2 that (3) activate WASp/Scar proteins. (4) WASp/Scar proteins bring together Arp2/3 complex and an actin monomer on the side of a pre-existing filament to form a branch. (5) Rapid growth at the barbed end of the new branch (6) pushes the membrane forward. (7) Capping protein terminates growth within a second or two. (8) Filaments age by hydrolysis of ATP bound to each actin subunit (white subunits turn yellow) followed by dissociation of the γ phosphate (subunits turn red). (9) ADF/cofilin promotes phosphate dissociation, severs ADP-actin filaments and promotes dissociation of ADP-actin from filament ends. (10) Profilin catalyses the exchange of ADP for ATP (turning the subunits white), returning subunits to (11) the pool of ATP-actin bound to profilin, ready to elongate barbed ends as they become available. (12) Rho-family GTPases also activate PAK and LIM kinase, which phosphorylates ADF/cofilin. This tends to slow down the turnover of the filaments (Pollard & Borisy, 2003)

Leading edge protrusion is coupled to cell-matrix adhesions

Also essential for migration of mammalian cells is the formation of adhesions to the substratum. These sites are typically composed of integrins as transmembrane proteins connecting the extracellular matrix with intracellular adhesion molecules. Up to now more than 100 different molecules have been identified in adhesion structures (Zaidel-Bar et al., 2007). Although their roles are diverse, their main function is the formation of a stable but still dynamic connection between integrins and the actin cytoskeleton enabling the transmission of cytoskeletal forces to the cell environment (Schäfer et al., 2010) (Figure 1.9). In motile cells, new adhesions are formed at the cell front and disassembled at the cell's rear. This is regulated by cell polarity which guides cell movement. The intracellular domain of integrin-mediated adhesions contains a large number of proteins, some of which directly mediate or strengthen the mechanical linkage between the ECM and the cytoskeleton, while others participate in adhesion-mediated signalling (Critchley, 2000; Geiger et al., 2001; Petit & Thiery, 2000). Recent studies have shown that integrin-mediated adhesions are not all alike and different molecular and cellular variants may be distinguished (Zamir & Geiger, 2001). For many cell types the lamellipodium is described as the origin of adhesion site formation. (Zaidel-Bar et al., 2003). At the cell periphery of motile cells, small matrix adhesions, denoted 'focal complexes' are formed (Nobes & Hall, 1995). Focal complexes are short-lived structures, containing β_3 -integrin (Ballestrem et al., 2001), vinculin (Rottner, Hall & Small, 1999), paxillin and α -actinin (Laukaitis et al., 2001). Focal complexes are early adhesions, which transform into Focal Adhesions following the activation of Rho-A (Ballestrem et al., 2001; Rottner, Hall & Small, 1999). Adhesions are thought to mature by a sequential mechanism coupled to tension or myosin II activity (Bershadsky, Kozlov & Geiger, 2006; Giannone et al., 2007), and inhibition of several signalling

components, including FAK, Src and ERK kinases, stops adhesion turnover and promotes maturation, suggesting a role for phosphorylation-mediated affinity changes of adhesion components (Webb et al., 2004).

Figure 1.9 has been removed due to copyright restrictions

Figure 1.9. Focal adhesion initiation events.

Initial integrin clusters (top left), after activation by talin binding, provide avenue for initial actin polymerisation (top middle) by recruiting focal adhesion components FAK and paxillin. New actin filaments tether to talin, the clusters get pushed away and then pulled closer by myosin contractions (top right). This causes cycles of transient talin stretching and vinculin binding until the talin- actin bond stabilises. Upon stable vinculin binding (bottom), further integrin clustering and signalling promote Rac1 activation. Rac1, in turn, further activates actin polymerisation modules, Arp2/3 and formins (Choi et al., 2008).

Tropomyosin regulates the interaction of non-muscle myosins with actin to generate contractile force

Much like the contractile apparatus of the sarcomere in muscle, contraction of the cell body to generate force is achieved in non-muscle cells via the interaction between actin and myosin motor proteins. The non-muscle myosin II is a ubiquitous molecular motor which, upon phosphorylation by Rho Kinase, binds and contracts actin bundles in an ATP dependent manner (Bresnick, 1999). The tension induced by myosin II depends upon the tethering of actin stress fibres to the substratum via focal adhesions. Through fluorescence microscopy studies it has been established that the HMW tropomyosins; Tpm2.1, 1.6 & 1.7 as well as the LMW tropomyosins; Tpm3.1 & 3.2 clearly localise to actin stress fibres in a variety of cell types. Studies show that the Tpm3.1 isoform is able to promote isoform-specific recruitment of a myosin II motor to stress fibres containing this Tpm. By contrast, a Tpm that induces lamellipodia, Tpm1.12, leads to a reduction in active myosin II levels (Bryce, Schevzov & Gunning, 2003) This is compatible with the observation that Tpm isoforms can differentially regulate myosin mechano-chemistry in a cell-free system and suggests a possible mechanism to explain the effects of Tpm3.1 and Tpm1.12 on myosin location and activity (Fanning et al., 1994).

Controversy surrounding the organisation of actin filaments at the leading edge

The precise spatial organisation of actin filaments at the leading edge has been disputed in the literature primarily due to different methods employed to visualise these filaments. The development of electron tomography, which allows the visualisation of the three-dimensional organisation of lamellipodia, shows that unbranched actin

filaments are present throughout the lamellipodium and link filaments of variable lengths (Small, 2015; Urban et al., 2010). Studies conducted by Vinzenz et al. (2012) also postulated that cross-linkers must be recruited to stabilise and stiffen the actin filament network in order to push the lamellipodium forward (Vinzenz et al., 2012).

For many years, the Arp2/3 complex was thought to be the sole mediator of actin filament assembly in lamellipodia. More recently however, other actin nucleators have been found to contribute to lamellipodium extension, including several members of the formin family. As mentioned earlier, formins promote filament elongation without branching through a processive capping mechanism and the formin mDia1, a RhoA target, has been shown to localise to the leading edge (Chesarone, DuPage & Goode, 2010).

It has been proposed that two structurally distinct populations of actin filaments may actually overlap at the leading edge to occupy the same space (Ponti et al., 2004). In other words, the actin cytoskeleton is organised into two molecularly distinct yet collaborating filament networks wherein the narrow lamellipodium undergoing fast, Arp2/3 mediated treadmilling is superimposed by a more stable, linear array of actin filaments that reach all the way to the leading edge (Danuser, 2005). A critique of this model has raised the question of how these two structures, both composed of actin and occupying the same cellular region, are differentially regulated and coordinated in time and space to maintain a state of persistent protrusion coupled to cell translocation (Vallotton & Small, 2009).

A major hypothesis of this thesis is that a potential candidate molecule that could maintain stable actin filaments at the leading edge is the actin associated protein, tropomyosin.

Tropomyosin at the leading edge

The precise localisation of Tpm at the leading edge of cells has also been controversial with studies reporting the absence of Tpm from lamellipodia (Blanchoin, Pollard & Hitchcock-DeGregori, 2001; Bugyi, Didry & Carlier, 2010; DesMarais et al., 2002; Gupton et al., 2005; Iwasa & Mullins, 2007; Koestler et al., 2013; Lazarides, 1976; Ponti et al., 2004; Skau et al., 2015), and others reporting their presence at or near lamellipodia (Bryce, Schevzov & Gunning, 2003; Hillberg et al., 2006; Lin, Hegmann & Lin, 1988; Schevzov et al., 2011). These opposing observations are partly due to the lack of appropriate reagents to detect the Tpm.

It has previously been demonstrated in vitro that tropomyosin competes with Arp2/3 for binding sites on actin filaments (Blanchoin, Pollard & Hitchcock-DeGregori, 2001). Due to the enrichment of Arp2/3 and the branched organisation of actin filaments observed in lamellipodia it was proposed that tropomyosin must be absent from this region. This model was supported by DesMarais, et al., (2002) who examined cells stained with anti-tropomyosin antibodies and found that none stained the lamellipodia (DesMarais et al., 2002). However, more recent work in neuroblastoma cells has shown that, in contrast to Tpm3.1, Tpm1.12 (previously shown to induce lamellipodia formation in non-neuronal cells (Bryce, Schevzov & Gunning, 2003)) actually supported the activity of the Arp2/3 complex rather than inhibiting it, indicating that Tpm1.12 may work simultaneously with the Arp2/3 complex in neuronal cells (Kis-Bicskei et al., 2013a). Finally, through the use of antibodies and fluorescently-tagged isoforms it has been demonstrated that tropomyosins are indeed present in significant amounts in the lamellipodia and filopodia of spreading normal and transformed cells (Hillberg et al., 2006). These observations indicate that the view of the role of

tropomyosin in regulating actin filaments within the lamellipodium needs to be significantly revised.

Recent experiments indicate the importance of building multiple actin filament types in the same location to generate functional outcomes (Kee et al., 2015; Tojkander et al., 2011). Studies in a variety of systems support that Tpm isoforms are used to specify the functional and molecular properties of actin filaments to allow the collaboration of different filament populations within the cell (Gunning et al., 2015).

It has recently been shown in vitro that severing of Arp2/3-generated networks by cofilin results in the generation of new pointed ends, to which the *Drosophila*-derived Tpm, Tm1A preferentially binds and that two sets of actin filaments, a Tpm-coated set and a Tpm-free set, that is competent to bind Arp2/3, can be stably maintained in vitro because they are insulated from one another (Hsiao et al., 2015b). These findings point toward a potential mechanism of how branched actin filaments may in fact be remodelled in cells to include Tpm.

Aims and significance

Actin microfilaments are core constituents of the cytoskeletal network fundamental to all eukaryotic cells. The actin cytoskeleton is essential for many biological processes including cell motility, intracellular organisation, cytokinesis and endocytosis. Structural alterations to the actin cytoskeleton are an established characteristic of transformed cancer cells. Despite the disruption of their internal architecture, transformed cells retain, or even increase many actin-based functional properties such as enhanced motility, invasiveness and metastasis. The actin cytoskeleton therefore represents a point for chemotherapeutic intervention. To date, little progress has been made with compounds that universally disrupt actin filaments due to their essential role

in the function of cardiac and skeletal muscle. Tropomyosins are actin-associated polymers which form an integral component of the actin filament. Mammals have over 40 isoforms of tropomyosin which sort to spatially distinct actin filament populations and differentially regulate the interaction of various actin binding proteins. A new class of anti-tropomyosin compounds have been developed which selectively target the low molecular weight Tpm3.1 (Stehn et al., 2013). This tropomyosin is sufficiently different from those found in muscle cells and therefore represents a novel way to target the actin cytoskeleton of cancer cells without damaging the contractile apparatus of the heart or diaphragm. This shows that it is possible to target specific actin filament populations fundamental to tumour cell viability based on their tropomyosin isoform composition and represents a novel approach to potentially treat a wide variety of cancers. The development of metastases accounts for more than 90 % of cancer related mortality (Sporn, 1996). It is therefore of interest to develop a greater understanding of the mechanisms underlying cellular migration. Dynamic remodelling of the actin cytoskeleton underlies cell migration, with protrusion of the leading edge in the direction of movement being the principal step in motility across many different cell types. Cells moving across a two-dimensional substratum often produce large, flat, actin-rich structures known as lamellipodia. Though widely studied, the exact organisation of actin filaments within lamellipodia, and how these filaments are regulated, remains controversial in the scientific literature. Based on earlier observations that the tropomyosin isoforms Tpm1.8/9 appear to occupy the periphery of various cell types (Schevzov et al., 2011; Sung et al., 2000; Temm-Grove, Guo & Helfman, 1996; Temm-Grove et al., 1998), it was hypothesised that these isoforms may play a role in the regulation of cell motility. Furthermore the mere presence of Tpm's within lamellipodia has also been a major point of disagreement between experts in the field.

The specific aims of this study therefore were to confirm and investigate in more detail, the putative lamellipodial localisation of Tpm1.8/9. This was achieved through the characterisation and use of a novel monoclonal antibody which is specific to Tpm1.8/9. The next aim of this project was to determine the functional role of Tpm1.8/9 in lamellipodial and whole-cell dynamics. This was achieved using siRNA knockdown alongside a variety of live-cell imaging techniques, kymography and focal adhesion morphometry. The final aim of this project was to examine the way in which actin filaments within the lamellipodium may come to incorporate Tpm1.8/9. This was done using a combination of siRNA knockdown, small molecule inhibitor, Western blotting and RT-qPCR approaches.

The significance of this study is that, following confirmation of the lamellipodial enrichment of Tpm1.8/9, a functional role for Tpm1.8/9 in regulating cell motility has been established. This raises this interesting possibility that this population of actin filaments may also be targeted for the inhibition of invasion and metastasis exhibited by certain cancer cells. Finally, as mentioned earlier, there has been great controversy in the literature over the organisation of actin filaments within the lamellipodium. This study helps to resolve this controversy by identifying a second population of actin filaments which are required for effective lamellipodial persistence. These actin filaments are created using severed actin branches which are stabilised by recruitment of the tropomyosins Tpm1.8/9, allowing two actin filament populations to co-exist within the same location, which in turn promotes the maturation of focal adhesions, driving cellular motility. These findings also serve as a broader paradigm by which to understand how cells can create and utilise multiple actin filament populations to collaborate and achieve a singular biological outcome.

Chapter Two

Materials & Methods

Chapter 2: Materials and Methods

Reagents, Equipment and Chemicals used in this Thesis

All chemicals and reagents used in these protocols were of analytical reagent grade, molecular biology grade or tissue culture grade. A list of chemical reagents and equipment used showing manufacturers and suppliers is provided in Tables 2.1 and 2.2 respectively. A list of buffer recipes is provided in table 2.3. A list primary and secondary antibodies used is given in tables 2.4 and 2.5 respectively and finally, a list of siRNAs used along with their target sequences is provided in table 2.6.

Commercial Reagents used in this Thesis

A list of reagents used showing manufacturers and suppliers is provided in Table 2.1.

Table 2.1. Commercially available reagents and kits.

Reagent	Manufacturer / Supplier
2-Mercaptoethanol	Sigma-Aldrich
30 % Acrylamide / bis-acrylamide 29:1 Solution	Bio-Rad Laboratories
Ammonium persulfate (APS)	MP Biomedicals
CK666	Sigma-Aldrich
Completemini EDTA-free Protease Inhibitor Cocktail Tablets	Roche
Dimethyl Sulfoxide (DMSO) – Hybrimax cell culture grade	Sigma-Aldrich
Dulbecco’s Modified Essential Medium (DMEM) High Glucose	Sigma-Aldrich
Ethylenediaminetetraacetic acid (EDTA)	Sigma-Aldrich
Fibronectin from Bovine Plasma	Sigma-Aldrich
Foetal Bovine Serum (FBS)	Life Technologies
Formaldehyde (16%)	ProSciTech
Fuji X-ray Film Medical SuperRX	FujiFilm
Lipofectamine 3000	Life Technologies
Lipofectamine RNAiMAX	Life Technologies
Hygromycin B	Life Technologies
N,N,N',N'-Tetramethylethylenediamine (TEMED)	Sigma-Aldrich
Opti-MEM low serum medium	Life Technologies
PBS Tablets	MP Biomedicals
pcDNA3.1+ (Hygro)	Life Technologies
Phalloidin Atto-565	Atto Tec GmbH

Prolong Gold Anti-fade Mounting Reagent with DAPI	Life Technologies
PVDF (Polyvinylidene fluoride) membrane Immobilon P	Millipore Australia
Skim milk powder	Coles
Small interfering RNA targeted against cofilin	Life Technologies
Sodium chloride (NaCl)	Chem Supply
Sodium dodecyl sulfate (SDS) 20 % solution	Bio-Rad Laboratories
Triton X-100	Sigma-Aldrich
Trypsin/EDTA (0.25/0.1 %)	Sigma-Aldrich
Western Lightning Chemiluminescence Reagent	Perkin-Elmer

Equipment used in this Thesis

General Equipment used in this Thesis is listed in Table 2.2.

Table 2.2. List of equipment and manufacturers.

Equipment Name	Manufacturer / Supplier
3K30 refrigerated centrifuge	Sigma-Aldrich
5415R Microcentrifuge	Eppendorf
Block heater	Stuart Equipment
Class II Safety Cabinet, HERAsafe KS12	Thermo Scientific
Countess Automated Cell Counter	Life Technologies
CP1000 film processor	AGFA
Criterion blotter transfer tank	BioRad
Direct Detect Spectrophotometer	Millipore
Eclipse Ti-E DIC microscope	Nikon
GelDoc	BioRad
Heracell 150i CO2 Incubator	Thermo Scientific
Horizontal shaker	Ratek
LSM780 Confocal microscope	Zeiss
Mini-PROTEAN Tetra cell gel running tank	BioRad
NanoDrop ND-1000 Spectrophotometer	Thermo Scientific
Orbital shaker	Ratek
Power Pac 300	BioRad
Sonicator	Branson
Stratagene Mx3000P qPCR machine	Agilent Technologies
Water Bath	Edwards Instruments

Buffers used in this Thesis

Buffers used in this Thesis and their recipes are listed in Table 2.3.

Table 2.3. Composition of buffers and solutions.

Buffer	Components
Blocking Buffer (Western blot)	5 % (w/v) Skim milk powder in 1x TBS
Coomassie Stain	10 % (v/v) acetic acid, 40% (v/v) methanol, 0.1 % (w/v) coomassie Blue
Destain	10 % (v/v) acetic acid, 10% (v/v) methanol
Incubation Buffer (Western blot)	2 % (w/v) Skim milk powder in 1x TBST
LB agar	1% (w/v) bactotryptone, 0.5% (w/v) yeast extract, 0.5% (w/v) NaCl, 1.5% (w/v) agar
Luria broth (LB media)	1% (w/v) bactotryptone, 0.5% (w/v) yeast extract, 0.5% (w/v) NaCl
PBS (1x)	0.1M NaCl, 2.7M KCl, 0.015M NaHPO ₄ , pH 7.2
Protein Sample Buffer Loading Dye (25 mL)	0.5 M Tris pH 6.8, 5 mL glycerol, 2.5 mL 20 % (w/v) SDS, 5 mL, 2-mercaptoethanol
RIPA buffer	50mM Tris, 150mM NaCl, 5mM EDTA, 1% Nonidet P-40, 0.1% SDS,
Running Buffer (1x)	10 % (v/v) 10 x Tris-glycine, 10 mL 20 % SDS
TBS (10x)	0.05M Tris-HCl, 0.15M NaCl, pH 7.5
TBST (1x)	10 % (v/v) 10 x TBS, 0.1 % (v/v) Tween-20
TE	10mM Tris, 1mM EDTA
Transfer Buffer (1x)	10 % (v/v) 10 x Tris-glycine, 40 % (v/v) methanol
Tris Glycine (10 x)	0.25 M Tris, 1.92 M Glycine

Antibodies used in this Thesis

Primary antibodies used in this Thesis are listed in Table 2.4. Secondary antibodies are listed in Table 2.5.

Table 2.4. Primary antibodies used for western blotting and immunofluorescence.

Antibody	Specificity	Species	Dilution	Company	Catalogue# / reference
ADF/Cofilin	Cofilin	Rabbit	1/1000	Sigma	C8736
Arp2	Arp2	Rabbit	1/500	Abcam	ab47654
Arp3	Arp3	Mouse	1/250	Sigma	A5979
CG1	Tpm2.1	Mouse	1/200	Lab reagent	(Schevzov et al., 2011)
Coronin 1B	Coronin 1B	Rabbit	1/500	Sigma	SAB4200096
Cortactin	Cortactin	Rabbit	1/500	Sigma	C6987
GAPDH	GAPDH	Mouse	1/5000	Millipore	AB2302
Paxillin	Paxillin	Rabbit	1/500	Abcam	Ab32084
TM311	Tpm2.1, Tpm1.6, Tpm1.7	Mouse	1/500	Sigma	T2780
$\alpha/1b$	Tpm1.8, Tpm1.9	Sheep	1/200	Lab reagent	(Schevzov et al., 2011)
$\alpha/1b$	Tpm1.8, Tpm1.9	Rat	1/250	Lab Reagent	This Thesis
α -tubulin	α -tubulin	Mouse	1/5000	Sigma	T9026
β -actin	β -actin	Mouse	1/250	Sigma	A5316
$\gamma/9d$	Tpm3.1, Tpm3.2	Sheep	1/500	Lab reagent	(Schevzov et al., 2011)
$\delta/9d$	Tpm4.2	Rabbit	1/500	Lab reagent	(Schevzov et al., 2011)

Table 2.5. Secondary antibodies for western blotting and immunofluorescence.

Antibody Name	Dilution	Company
Alexa Fluor 488 Donkey anti-mouse IgG	1/500	Life Technologies
Alexa Fluor 488 Donkey anti-rabbit IgG	1/500	Life Technologies
Alexa Fluor 488 Donkey anti-rat IgG	1/500	Life Technologies
Alexa Fluor 488 Donkey anti-sheep IgG	1/500	Life Technologies
Alexa Fluor 568 Donkey anti-mouse IgG	1/500	Life Technologies
Alexa Fluor 568 Donkey anti-rabbit IgG	1/500	Life Technologies
Alexa Fluor 568 Donkey anti-rat IgG	1/500	Life Technologies
Alexa Fluor 568 Donkey anti-sheep IgG	1/500	Life Technologies
HRP-linked Goat anti-mouse	1/5000	GE Healthcare
HRP-linked Goat anti-rabbit	1/5000	GE Healthcare
HRP-linked Goat anti-rat	1/5000	GE Healthcare
HRP-linked Goat anti-sheep	1/5000	GE Healthcare

siRNAs used in this Thesis

A list of all small interfering RNAs and their target sequences is provided in table 2.6.

Table 2.6. siRNA sequences used in this Thesis.

Knockdown Target	Target DNA sequence	Company
AllStars non-silencing	proprietary (cat# 1027281)	Qiagen
Cofilin	proprietary (cat# 4390771 s63901)	Ambion
Coronin 1B	5'-GTCATTGCCAGTGGATCAG-3'	Sigma
Cortactin	5'-GCATGAGTCTCAGAAAGAT-3'	Sigma
Tpm1.8/9	5'-GGAGCGGAAGCTGCGGGAAAC-3'	Qiagen
TPM2	proprietary (cat# 4390771 s75392)	Ambion

Cell Culture

General maintenance of cells

Mouse embryonic fibroblasts (MEF) were from wild-type C57-BL/6 mice. Cells had previously been subjected to a well-established retroviral technique for immortalisation by the SV40 Large T antigen (Coombes et al., 2015). MEFs were maintained in complete DMEM medium (supplemented with 10 % FBS) at 37° C and 95 % air / 5 % CO₂. For routine maintenance, cells were cultured in 10 cm diameter plastic culture dishes and split approximately every 3 days or when approaching confluence.

Passaging of cells

Culture medium was aspirated from culture dishes and MEFs were then washed with 37 °C PBS to remove any residual medium or dead cells. 1 mL of 37 °C 0.25 % trypsin /0.1 % EDTA was added to the culture dish, followed by incubation at 37 °C for approximately 3 min to detach cells from the plastic substratum. Once detached, approximately 5 mL of warm complete DMEM medium was added to inactivate the trypsin and cells were re-suspended. An appropriate volume of the cell suspension was then transferred into a new culture dish containing 10 mL of warmed complete medium. Cells were incubated at 37 °C with 5 % CO₂. For plating cells at specific cell densities (e.g. for transfection or immunofluorescence), re-suspended cells were counted and then diluted to the appropriate density. Cells were counted using a Neubauer-Improved 0.1 mm depth haemocytometer or the Countess Automated Cell Counter (Invitrogen).

Cryopreservation of cells

MEFs grown to 90 % confluence in culture dishes were trypsinised and re-suspended in 10 mL complete medium. Cells were then centrifuged at 1500 rpm for 5 min, re-suspended in freezing medium (90 % FBS and 10 % DMSO), and then transferred to

screw-top cryovials. Cells were chilled to -80°C for 48 h before being transferred to liquid nitrogen. To recover cryopreserved cells for subsequent cell culture, cryovials were removed from liquid nitrogen and quickly thawed in a 37°C water bath. The thawed contents were transferred to a 10 cm dish containing 10 mL of warm complete medium. Medium was changed 24 h post-plating to remove DMSO and unattached cells.

Antibody Production

The anti- $\alpha/1b$ rat monoclonal antibody was generated by ProMab Biotechnologies Inc. (Richmond, CA). The entire sequence of exon 1b of the human *TPMI* gene was used as the immunogen with two 28mer peptides comprising of overlapping sequences (Figure 3.1A). The purified rat ascites fluid was used in all experiments reported in this study except where otherwise indicated. The specificity of the $\alpha/1b$ antibody was determined with the use of recombinant Tpm protein as previously described (Schevzov et al., 2011).

Western Blot Analysis

Extraction of protein

MEF cells were washed three times in PBS and all residual PBS removed. Cold RIPA buffer (100 μL /well) containing protease inhibitors (complete, mini EDTA-free) was added to the well, and cells scraped into the lysis buffer using a cell scraper. Lysed solutions were collected and sonicated, pulsing 10 times for 2 seconds each. The protein concentration in samples was quantified using a DirectDetect[®] Spectrometer (Millipore) according to the manufacturer's instructions. Protein lysates were diluted in 2 x Laemmli sample buffer (BioRad). Samples were heated to 95°C in a heat block for 5

min to linearise proteins. Samples were cooled to RT and were then stored at -20°C for future use.

SDS-polyacrylamide gel electrophoresis (SDS-PAGE)

SDS-PAGE was conducted using the BioRad Mini-PROTEAN system. Equal amounts of protein (10 μg) were loaded onto a 12.5 % polyacrylamide mini-gel in sample loading buffer and SDS-PAGE conducted by running the gel in tris-glycine running buffer at 100 volts for 90-120 min.

Protein transfer and western blotting

Western blotting was conducted by transferring the proteins on the acrylamide gels to Immobilon-P 0.45 μm Polyvinylidene fluoride (PVDF) membranes using a standard wet-transfer procedure. PVDF membranes were briefly dipped in 100 % methanol before being placed on top of each gel, surrounded by filter paper and sponges, and packed in a transfer electrophoresis tank. Transfer was performed at 4°C in Laemmli transfer buffer at 37 volts overnight. After the transfer procedure, the blots were blocked for non-specific background by incubating the PVDF membranes with 5 % skim milk in TBS for 2 h at room temperature. Membranes were then probed with the primary antibody diluted in 2 % skim milk in TBS for 1 h at room temperature and then washed three times (3×20 min) with TBST. Following the washing step, membranes were probed with a horseradish-peroxidase (HRP) conjugated, species appropriate secondary antibody diluted in 2 % skim milk in TBS for 1 h at room temperature. The membranes were again washed three times and visualised using a Western Lightning-ECL chemiluminescent substrate. The visualisation step was performed by exposing membranes to Fuji X-Ray Film and developed using an Agfa Benchtop Automated Developer.

Gene Silencing by Small Interfering RNA (siRNA)

A siRNA sequence was designed to knockdown Tpm1.8/9 (target sequence: 5'-GGAGCGGAAGCTGCGGGAAAC-3', Qiagen). A sequence previously reported (Cai et al., 2007) to knockdown mouse coronin 1B (target sequence: 5'-GTCATTGCCAGTGGATCAG-3', Sigma) was used to knockdown coronin 1B. A sequence previously reported (Bryce et al., 2005) to knockdown mouse cortactin (target sequence: 5'-GCATGAGTCTCAGAAAGAT-3', Sigma) was used to knockdown cortactin. A sequence previously validated to knockdown mouse non-muscle cofilin (Silencer[®]Select Pre-Designed siRNA ID: s63901, Ambion) was used to knockdown cofilin. A sequence previously validated to knockdown the mouse *TPM2* gene (Silencer[®]Select Pre-Designed siRNA ID: s75392, Ambion) was used to knockdown Tpm2.1. Finally, Allstars[®] non-silencing siRNA (Qiagen) was used as a negative control for all siRNA experiments.

Transient transfection of siRNA

MEF cells were plated onto 6-well plates at 1×10^5 cells/well and allowed to grow for 24 hr. siRNA was transfected using Lipofectamine[®] RNAiMAX reagent (Invitrogen) according to the manufacturer's instructions. Optimal knockdown of protein was achieved at a final concentration of 25 nM for Tpm1.8/9, coronin 1B and at 10 nM for cofilin and Tpm2.1 siRNA at 48 hr post-transfection.

Cell Imaging

Immunofluorescent staining

Cells were seeded on glass coverslips (Thermo Fisher, Waltham, MA) pre-treated with 50 $\mu\text{g}/\text{mL}$ fibronectin (Sigma) at 5×10^3 cells per cm^2 and allowed to spread for 6 h prior to fixing with paraformaldehyde (4% (w/v) in PBS). For Tpm antibody staining, cells

were permeabilised with chilled 100% methanol, for other antibody staining cells were permeabilised with 0.25 % TrionX-100 in PBS. Cells were then blocked with FBS (5% (v/v) in PBS) and stained with anti- α /1b, anti-CG1 (Schevzov et al., 2011), anti-cortactin (Sigma), anti-Arp2 (Abcam), anti-Arp3 (Sigma) anti-cofilin (Sigma) or anti-coronin 1B (Sigma), anti-TM311 (Sigma), anti- γ /9d (Schevzov et al., 2011), anti- δ /9d (Schevzov et al., 2011) or anti-paxillin to visualise Tpm1.8/9, Tpm2.1, cortactin, Arp2, Arp3, cofilin, coronin 1B, Tpm1.6/7/2.1, Tpm3.1/2, Tpm4.2 and paxillin respectively. Cells were thoroughly rinsed with PBS before secondary antibody staining with Alexa Fluor[®] 488-conjugated or Alexa Fluor[®] 568-conjugated antibody (Invitrogen) with target species as appropriate to relevant primary antibody host species. To Visualise F-actin, cells were fixed with paraformaldehyde (4% (w/v) in PBS), permeabilised with 0.25% Triton X-100 (v/v) in PBS), incubated with Atto-565-Phalloidin (Sigma) before being thoroughly rinsed with PBS. Coverslips were mounted using ProlongGold[®] anti-fade mounting medium containing DAPI (Invitrogen) to visualise nuclear material.

Microscopy and fluorescence quantification

Confocal images were acquired using an LSM780 laser scanning inverted microscope (Zeiss) equipped with an oil-immersion Plan apochromat 1.4-NA 100X objective lens, driven by the Zen software (Zeiss). Alexa-488 (Invitrogen), which has a maximum emission of 519 nm was excited at 488 nm and Alexa-568 (Invitrogen) and Atto-565 (Sigma), which have maximum emissions of 601 nm and 592 nm respectively, were excited at 561 nm. Image quantification was done using the JACoP Plugin (Bolte & Cordelieres, 2006) for ImageJ (NIH) to calculate the Pearson's co-localisation coefficient between the red and green channels as previously described (Bolte & Cordelieres, 2006). Pixel intensity values were calculated using the ImageJ (NIH) line scan function simultaneously between the two channels.

Live-cell imaging

Tpm1.8/9 and control siRNA-transfected cells were grown on a FluoroDish (World Precision Instruments) pre-treated with 50 µg/mL fibronectin (Sigma). Live-cell imaging was performed on an Eclipse Ti-E inverted microscope (Nikon) at 37°C in a humidified atmosphere with 5% CO₂ using differential interference contrast (DIC) imaging with a 40X (NA 0.95) Plan Apochromat air objective or by phase contrast illumination with a 20X (NA 0.45) S Plan Fluor air objective.

Random migration assay

Cells transfected with either control or Tpm1.8/9 siRNA were seeded sparsely (2×10^4 cells) on a FluoroDish (World Precision Instruments) pre-treated with 50 µg/mL fibronectin and allowed to adhere for 4 h before the start of imaging. Cells were imaged every 10 min for 8 hr using the 20X phase contrast objective and tracked using the Manual Tracking plugin for ImageJ software (NIH). Cells that divided or made contact with other cells during the experiment were not used for data analysis. Velocity was calculated as the total track distance divided by the total time (480 min). Persistence ratio was calculated as the linear distance between start and end points divided by the total track length.

Preparation of collagen gels

Collagen gels were prepared from Rat Tail Collagen I (Invitrogen) 3 mg/mL stock solution. Kept on ice, collagen was first neutralised with cold neutralisation buffer (500 µL per mL of collagen) before a suspension of cells previously transfected with either control or Tpm1.8/9 siRNA was added and to give a final cell density of 1×10^5 cells / mL and a final collagen concentration of 1.5 mg / mL. 200ul of the mix (containing 20,000 cells) was added per well to a 24-well plate which was gently swirled to coat the

surface evenly before being incubated at 37° C for 1 h. 300 µL of complete DMEM was then carefully added onto the top of each gel and the plate was then incubated for a further 15 h before imaging.

Imaging of cells in collagen gels

Cells were imaged every 10 min for 8 hr using the 20X phase contrast objective and tracked using the Manual Tracking plugin for ImageJ software (NIH). Cells that divided or made contact with other cells during the experiment were not used for data analysis. Velocity was calculated as the total track distance divided by the total time (480 min).

Kymography

For kymography, cells transfected with either control or Tpm1.8/9 siRNA were seeded sparsely (2×10^4 cells) on a FluoroDish pre-treated with 50 µg/mL fibronectin and allowed to adhere for 4 h before the start of imaging. Individual cells were imaged every 3 seconds for 10 min using the 40X DIC objective. Kymographs were generated using the ImageJ Kymograph plugin (NIH). Kymographs were analysed by drawing lines on protrusions and retractions and length and angle measurements were converted to rate and distance parameters using standard trigonometric calculations in Excel software (Microsoft Corporation, Redmond, WA).

Cell Morphometry

Cell Area was calculated in MEF cells stained for Arp2 using ImageJ (NIH). Following background subtraction the threshold function was used so that individual cells could be selected with the wand (tracing) tool, upon which area and perimeter (for use in calculating % cell edge containing Arp2) were calculated. Calculation of % cell edge containing Arp2 was done by drawing freehand Regions Of Interest (ROIs) on the Arp enrichment along the lamellipodia and calculating total length of the ROIs as a

percentage of total perimeter. Lamellipodial thickness was calculated in MEF cells stained with phalloidin by drawing straight-line ROIs across the clearly visible actin band designating the lamellipodium (from outside the cell to inside) many times per cell and calculating the average length of the ROIs. (total 15 cells per condition).

Focal adhesion morphometry

Cells transfected with either control or Tpm1.8/9 siRNA were seeded on glass coverslips (Thermo Fisher) pre-treated with 50 µg/mL fibronectin (Sigma) at 5×10^3 cells per cm² and allowed to adhere for 16 hr before being fixed and permeabilised as previously described. Cells were then incubated with the anti-paxillin antibody (Abcam) followed by Alexa Fluor[®]488 (Invitrogen) and coverslips mounted using Prolong Gold anti-fade mounting medium (Invitrogen). Confocal images were acquired using an LSM780 laser scanning inverted microscope (Zeiss) as previously described. Focal adhesion area was quantified using Image J. In Image J, the periphery of each cell was traced using the free-hand tool and the outside area was removed. The image was then changed to an 8-bit format and the threshold was auto-adjusted to remove background interference. After the scale of the image was entered, focal adhesion area was measured using the 'analyse particles' function.

Measurement of protein recruitment into lamellipodia

Cells were seeded on glass coverslips (Thermo Fisher) pre-treated with 50 µg/mL fibronectin (Sigma) at 5×10^3 cells per cm² and allowed to adhere overnight. Cells were then washed once with PBS and the medium was replaced with medium containing the Arp2/3 inhibitor, CK666 (Sigma) at 150 µM for 3 hr. The drug was then washed out by addition of pre-warmed drug-free medium and cells were fixed with paraformaldehyde (4% (w/v) in PBS) at exactly 5, 10, 20 or 30 sec and stained using antibodies against

Arp2, cortactin, coronin 1B, cofilin, paxillin or Tpm1.8/9 as previously described. For analysis, cells were observed using the 100x objective and scored according to having clear lamellipodial enrichment (equivalent to that of non-drug-treated cells) of the protein in question with > 100 cells per time-point analysed for each antibody.

Molecular Biology

Restriction endonuclease digestion

Restriction digests were set up in a total volume of 30 μ L containing plasmid DNA (1 μ g), 10-20 Units of restriction enzyme with 3 μ L of appropriate 10X buffer and nuclease free water to make up the volume. The reactions were incubated at 37° C for 1 h. Digested DNA products were analysed by gel electrophoresis using 1-2 % agarose gels in 1x Tris-acetate-EDTA (TAE) and visualised by post staining using Gel Red (Biotium) nucleic acid stain and imaging on a Bio-Rad gel doc system (Bio-Rad, Gladesville NSW).

Gel purification of DNA fragments

For the purification of DNA fragments required for ligation, digested plasmid DNA was electrophoresed using a 1.0 % low melt agarose gel. Fragments of interest were cut out of the gel under a UV light box (UVP inc, Scientifix P/L Clayton VIC) and the DNA was extracted and purified using the Wizard SV Gel purification kit as per the manufacturer's protocol.

Ligation of DNA fragments and bacterial transformation

DNA ligations were performed using T4 DNA ligase at 4 °C overnight. The ligation mixture was transformed into competent bacteria using a heat shock protocol. Heat shock competent XL1-Blue cells (prepared by Steve Palmer) were thawed quickly on ice. 5 μ L of ligation mixture was added to 50 μ L XL1-Blue cells and incubated on ice

for 30 min. The cells were then heated in a 42 °C water bath for exactly 30 seconds, and transferred back onto ice for 5 min before the addition of 950 µL SOC medium containing no antibiotic. After a 60 min recovery period with shaking at 37 °C, cells were centrifuged at 3000 RPM for 3 min to form a pellet which was then re-suspending in 100 µL SOC medium before being plated onto LB agar plates containing 100 µg/mL ampicillin.

Purification of plasmid DNA

For midiprep of DNA, single bacterial colonies were picked and grown overnight with shaking in 100 mL LB Medium containing 100 µg/mL ampicillin. DNA was then purified using a midiprep kit (Invitrogen) according to the manufacturer's instructions. The resulting DNA pellet was air dried for 5 min and resuspended in 100 µL TE (10 mM Tris, 0.1 mM EDTA). The concentration and purity of plasmid DNA was measured by UV spectrophotometry at A260 and A280.

Extraction of RNA

MEF cells previously transfected with either control, coronin 1B or cofilin siRNA growing on 10 cm plates were trypsinised, collected and washed with PBS. The pellets were resuspended in 1 mL of Tri-Reagent and samples were incubated at RT for 5 min before the addition of 200 µL of chloroform. The mixture was shaken vigorously for 15 seconds then allowed to stand at RT for 5 min. Samples were centrifuged at maximum speed for 15 min at 4 °C. The upper aqueous phase was transferred to a new tube and 0.5 mL isopropanol was added. Samples were mixed well, incubated at RT for 5 min then centrifuged at maximum speed for 15 min at 4 °C. The supernatant was discarded and the RNA pellets were washed with 1 mL of 80 % ethanol. The RNA pellets were mixed, centrifuged at maximum speed for 10 min at 4 °C and then air dried for 15 min

and resuspended in 30 μ L nuclease free water. RNA was quantified by spectrophotometry at 260nm, and the purity of the RNA was determined by measuring the A260 / A280 ratio.

Preparation of cDNA

cDNA for RT PCR and qPCR was synthesised from RNA using The *SuperScript® VILO™* cDNA Synthesis Kit (Invitrogen) for RT-qPCR as per the manufacturer's instructions. For a single reaction, 4 μ L 5X VILO™ Reaction Mix, 2 μ L 10X SuperScript® Enzyme Mix, 2 μ g RNA and RNase free water to 20 μ L were combined in a tube. The tube was then incubated at 25°C for 10 minutes before being incubated at 42°C for 60 minutes. The reaction was terminated at 85°C for 5 minutes and the cDNA was diluted 1 in 10 to yield a final concentration of 10 ng/ μ L).

qPCR

For quantitative PCR (qPCR) analysis, cDNA from control, coronin 1B or cofilin siRNA treated cells was amplified using SsoAdvanced™ Universal SYBR® Green Supermix (BioRad) along with the following DNA primers to produce an amplicon of 251 bps from Tpm1.8/9 mRNA and exclude genomic DNA. Forward (anchored in exon 1b of the *TPMI* gene): 5'-GTAGCAGCTCGCTGGAGG-3', Tm: 59.8 °C. Reverse (anchored in exon 3 of the *TPMI* gene): 5'-CTCATCTGCAGCCTTCTCG-3', Tm: 59.8 °C. A total of forty cycles were performed at 60 °C annealing on a Stratagene Mx3000P qPCR machine (Agilent Technologies). In order to establish qPCR conditions, standard curves were performed for the primer set as well as GAPDH (Forward:5'-CGCAAAGGTATGCACCTCAC-3'andReverse:5'-TCAGACCCATCCCGTAATCC-3') as a housekeeping gene. The amount of amplified cDNA was normalised to standard curves of amplified products from the housekeeping gene.

Standard PCR

Polymerase chain reaction (PCR) amplifications of DNA products up to 1 kb were routinely performed using Taq DNA polymerase. A total of 30 cycles were generally performed using a Bio-Rad C1000 PCR machine. Denaturation steps were performed at 94 °C for 30 seconds, annealing step temperatures were performed for 30 seconds at temperatures ranging between 52 - 62 °C depending on the T_m of the primer pair, and extension steps were performed at 72 °C for 2 min.

PCR products were run on a 1-2 % agarose gels in 1x Tris-acetate-EDTA and visualised either by post staining using ethidium bromide solution or by the addition of Gel Red nucleic acid stain into the agarose gel prior to setting. PCR products were imaged on a Bio-Rad gel doc system.

Statistical Analysis

All graphs were compiled using GraphPad Prism 6 software for Windows (GraphPad Software, Inc; La Jolla, CA). Results are expressed as mean \pm SEM of ≥ 3 independent experiments or as box and whisker plots. For statistical comparisons, results were analysed using Student's unpaired *t*-test assuming unequal variance. Values of $p < 0.05$ were considered statistically significant. It should be noted that for the Tukey box plots presented in Figure 6.3, whiskers indicate maximum and minimum values within 1.5 IQR, and outliers, whilst included in all statistical analyses, were not included on the plots for the sake of visual clarity.

Chapter Three

**Characterisation of the $\alpha/1b$ rat
monoclonal antibody and the
lamellipodial localisation of
Tpm1.8/9**

Chapter 3: Characterisation of the $\alpha/1b$ rat monoclonal antibody and the lamellipodial localisation of Tpm1.8/9

Introduction

The precise localisation of Tpm at the leading edge of cells has been a controversial topic in the literature with some studies reporting the absence of Tpm from lamellipodia (Blanchoin, Pollard & Hitchcock-DeGregori, 2001; Bugyi, Didry & Carlier, 2010; DesMarais et al., 2002; Gupton et al., 2005; Iwasa & Mullins, 2007; Koestler et al., 2013; Lazarides, 1976; Ponti et al., 2004; Skau et al., 2015), and others reporting the presence of Tpm at or near lamellipodia (Bryce, Schevzov & Gunning, 2003; Hillberg et al., 2006; Hsiao et al., 2015a; Lin, Hegmann & Lin, 1988; Schevzov et al., 2011). These opposing observations are partly due to the lack of availability of Tpm isoform specific antibodies and partly due to problems which may occur when using fluorescently tagged Tpm as the N- and C- terminus of Tpm have been shown to be crucial for fidelity of function (Bharadwaj et al., 2004; Martin, Schevzov & Gunning, 2010).

The initial motivation for this project was, in large part, founded on an observation by Schevzov et al., who, upon carrying out characterisation of a range of anti-Tpm antibodies, demonstrated that a sheep polyclonal $\alpha/1b$ antibody which recognises Tpm1.8 and Tpm1.9 (the immunogen for which was a single 18mer peptide at the C-terminal end of exon 1b of the human *TPM1* gene) stained the lamellipodium of primary mouse fibroblasts (Schevzov et al., 2011). Further applications of this antibody however were hindered by the fact that it tends to yield generally poor results when used for either immuno-staining (Figure 3.1 A) or Western blotting (Figure 3.1C). It

became apparent that, if any thorough investigation into the isoforms seen by this antibody (Tpm1.8 and Tpm1.9) were to be undertaken, a cleaner, more reliable antibody would need to be generated.

The $\alpha/1b$ rat monoclonal antibody was generated by ProMab Biotechnologies Inc. (Richmond, CA) by using the entire sequence of exon 1b of the mouse *Tpm1* gene as the immunogen with two 28mer peptides comprising of overlapping sequences (Figure 3.2 A). The purified rat ascites fluid proved to be much more useful for both immunostaining (Figure 3.1 B) and for Western blotting (Figure 3.1 D) in terms of visual clarity and was therefore used in all further experiments reported in this study. Staining using this new antibody also revealed these Tpm's to localise to the lamellipodium in mouse embryonic fibroblasts (Figure 3.1 B), further validating the initial observation (Schevzov et al., 2011) and also indicating a potential role for the tropomyosin isoforms Tpm1.8 and Tpm1.9 in the regulation of actin dynamics within this structure. It was also speculated at this point that more detailed experiments involving this antibody would likely shed some light on the controversy surrounding the presence of Tpm in the lamellipodium, as up until now, a suitable antibody specific to Tpm1.8 and Tpm1.9 was not readily available.

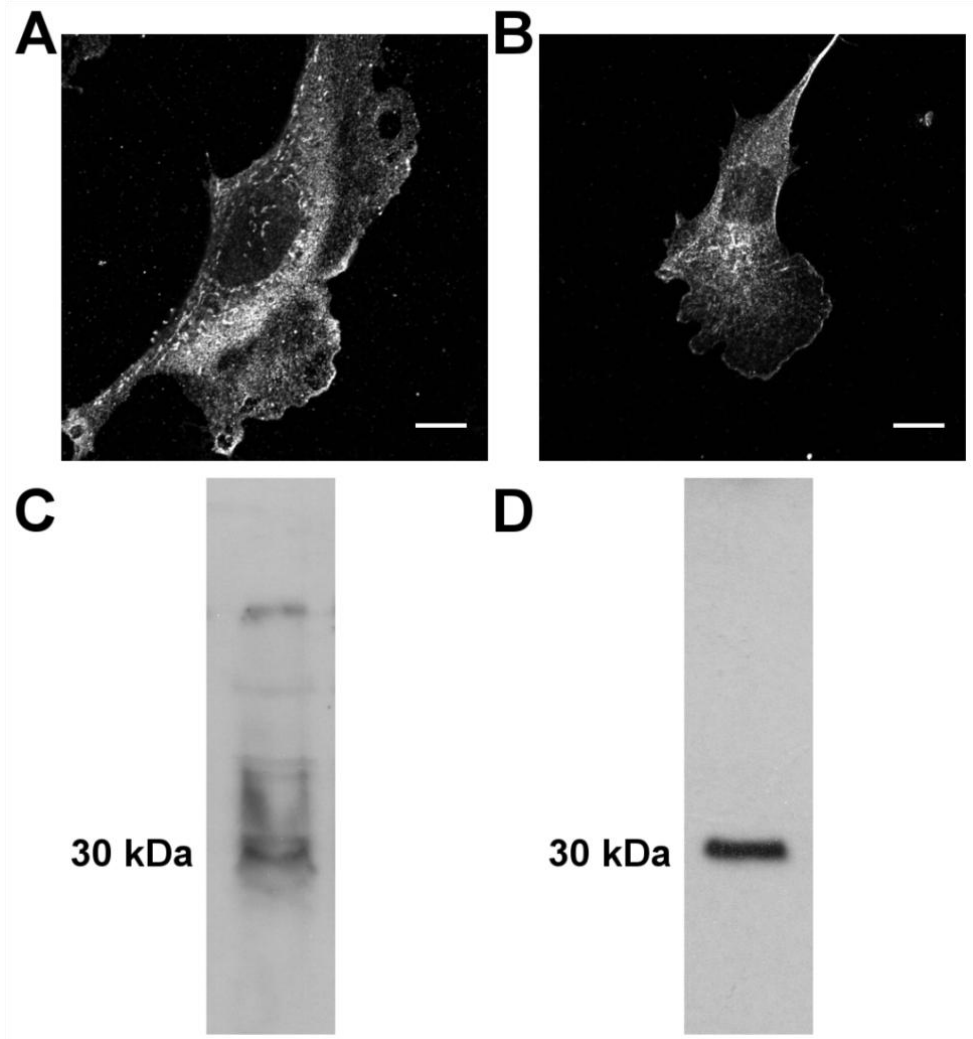


Figure 3.1. Difference in clarity between the sheep polyclonal and rat monoclonal $\alpha/1b$ antibodies.

- (A) Confocal image of a MEF cell stained using the $\alpha/1b$ sheep polyclonal antibody
- (B) Confocal image of a MEF cell stained using the $\alpha/1b$ rat monoclonal antibody
- (C) Western blot of MEF lysates probed with the $\alpha/1b$ sheep polyclonal antibody
- (D) Western blot of MEF lysates probed with the $\alpha/1b$ rat monoclonal antibody

As mentioned earlier, problems with fidelity of function are often faced when fusing fluorescent tags to Tpm's due to the end-to-end nature of their quaternary structure. Unfortunately, Tpm1.8 and Tpm1.9 proved to be no exception to this and several attempts were made at overcoming various problems associated with the generation of fluorescently tagged constructs. These issues are outlined in the 'Discussion' section of this chapter. But first, this chapter will report on the characterisation of the novel $\alpha/1b$ rat monoclonal antibody.

Results

Characterisation of the $\alpha/1b$ rat monoclonal antibody

To confirm specificity of the $\alpha/1b$ rat monoclonal antibody for Tpm1.8 and Tpm1.9, a panel of recombinant mouse Tpm proteins (as previously reported by Schevzov et al., (Schevzov et al., 2011)) comprised of isoforms representing all four *Tpm* genes was probed with the $\alpha/1b$ rat monoclonal antibody. Development of the blot probed with HRP linked anti-rat IgG secondary antibody revealed preferential detection of Tpm1.8 and Tpm1.9 (Figure 3.2 B). Minor cross reactivity is also observed with Tpm2.1 (Figure 3.2 B) which will be addressed later in this chapter. The most prominently detected Tpm isoforms, Tpm1.8 and Tpm1.9 will hereafter be referred to as Tpm1.8/9 as the only difference between the two isoforms is a single, alternatively spliced exon at 6a/6b (see Figure 1.5) and the two cannot be distinguished from one another by the antibody or by siRNA, both of which target the shared exon 1b. Interestingly, these Tpm's also share a similar amino-terminal exon/intron structure with Tpm1.12 (Geeves, Hitchcock-DeGregori & Gunning, 2014; Schevzov et al., 2011), an isoform found at the leading edge of neuronal cells (Bryce, Schevzov & Gunning, 2003). Coomassie staining of the membrane was carried out to demonstrate that protein was loaded into each well (Figure 3.2 C).

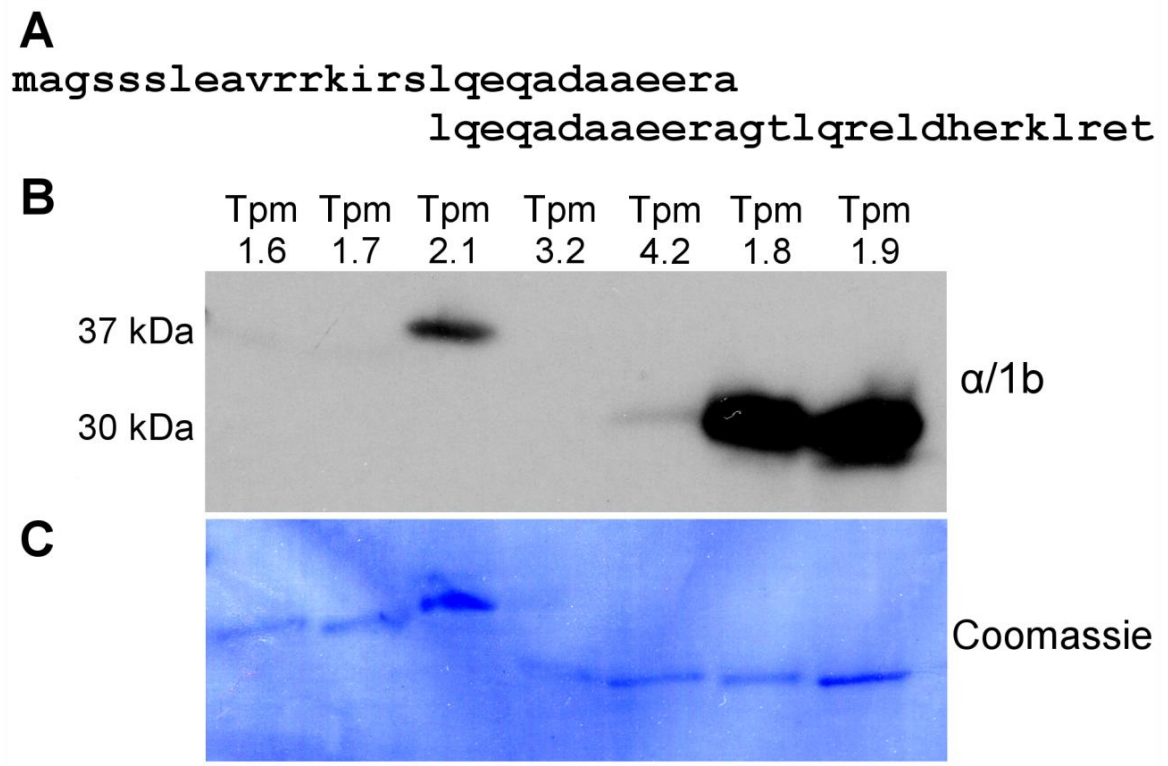


Figure 3.2. Characterisation of the $\alpha/1b$ rat monoclonal antibody.

(A) Overlapping peptides that span the entire exon 1b of the mouse *Tpm1* gene were used as the immunogen to generate the rat $\alpha/1b$ monoclonal antibody.

(B) Western blot of recombinant Tpm isoforms showing isoform specificity of the $\alpha/1b$ antibody for Tpm1.8 and Tpm1.9 with minor cross-reactivity with Tpm2.1.

(C) Coomassie staining of the membrane to demonstrate protein loading in each well.

Tpm1.8/9 display a unique cellular localisation compared to other Tpm isoforms

In order to demonstrate that the observed lamellipodial localisation of Tpm1.8/9 was unique when compared to other Tpm isoforms, the spatial distribution of a range of Tpm isoforms was assessed in MEF cells which had been previously shown to display characteristic features of leading edge protrusions (Coombes et al., 2015). The cells were grown on fibronectin-coated glass coverslips to promote spreading before fixation. The Arp2/3 complex was chosen as a marker for the lamellipodium as it is well established to localise to the leading edge where it nucleates the branched actin network responsible for lamellipodial protrusive force (Pollard & Borisy, 2003). Cells were co-immunostained with anti-Arp3 (to visualise Arp2/3) along with a range of anti-Tpm antibodies, each of which targets a specific exon of an individual *Tpm* gene, thus providing specificity for a subset of Tpm isoforms (Schevzov et al., 2011). The HMW Tpm isoforms from the *Tpm1* and *Tpm2* genes: Tpm1.6, Tpm1.7 and Tpm2.1 as detected with the TM311 antibody localise to actin stress fibres, which traverse the cell and were not detected in the lamellipodium (Figure 3.3 A, top panel). Similarly, the LMW isoforms from the *Tpm3* gene: Tpm3.1 and Tpm3.2, as seen by the $\gamma/9d$ antibody, also localised to stress fibres and were undetected in the lamellipodium (Figure 3.3 A, second panel). The $\delta/9d$ antibody, which recognises the LMW Tpm4.2 from the *Tpm4* gene, detected both stress fibres and transverse arcs (Figure 3.3 A, third panel), an observation consistent with work reported for human osteosarcoma cells (Tojkander et al., 2011). Finally, the low molecular weight isoforms from the *Tpm1* gene: Tpm1.8/9, as detected with the $\alpha/1b$ rat monoclonal antibody, display a unique cellular sorting pattern and are found predominantly enriched along the leading edge of the lamellipodium where they occupy the first micron from the cell edge along with Arp3 (Figure 3.3 A, bottom panel). This unique localisation is demonstrated by the

accompanying fluorescence plots shown in Figure 3.3 B. These were generated by simultaneous line-scans on the two image channels from outside the cell to inside and plotting fluorescence intensity against distance from the cell edge (defined as the first detected signal above background in the Arp3 channel). These plots provide information on the relative spatial distribution between the Arp2/3 complex and the subset of Tpm isoforms referred to in the relevant panel of Figure 3.3 A. Multiple line scans were taken for fifteen cells per antibody pair.

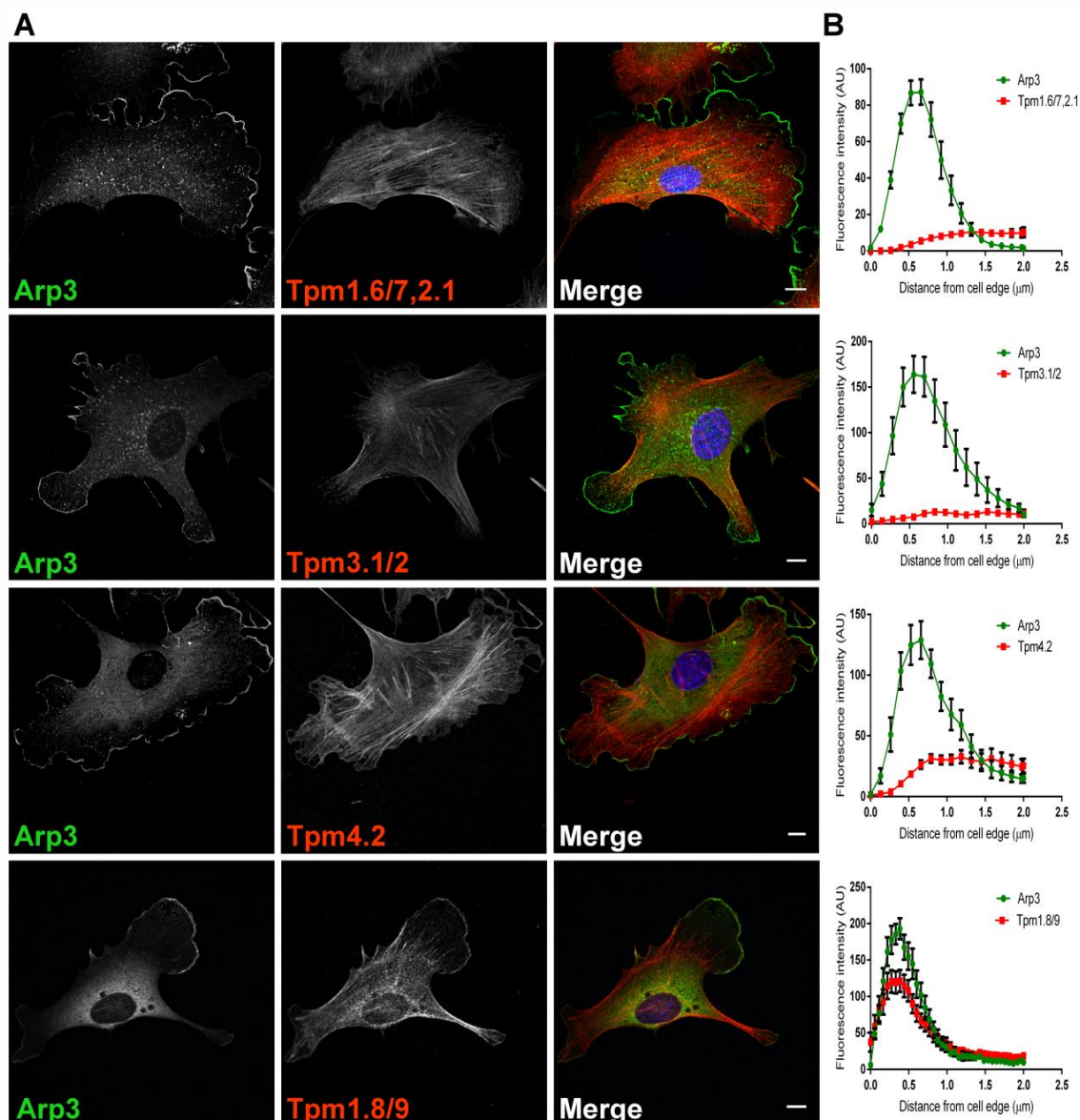


Figure 3.3. Tpm1.8/9 display a unique lamellipodial localisation compared to other Tpm isoforms.

(A) Representative confocal images of MEFs immunofluorescently stained using the anti-Arp3 antibody along with the TM311 (Tpm2.1, 1.6, 1.7), $\gamma/9d$ (Tpm3.1/2), $\delta/9d$ (Tpm4.2) and $\alpha/1b$ (Tpm1.8/9) antibodies. Merged images show Arp3 in green, Tpms in red and nuclei stained with DAPI (blue). Scale Bars = 10 μm .

(B) Quantification of the spatial distribution of Tpm isoforms relative to Arp3; Error bars = SEM; $n = 15$ cells for each plot, with fluorescence in arbitrary units (AU).

Cross-reactivity of the $\alpha/1b$ rat monoclonal antibody with Tpm2.1

Due to the observed slight cross-reactivity of the $\alpha/1b$ antibody with Tpm2.1 as well as Tpm1.8/9 (Figure 3.2 B), experiments were first carried out to ensure that the lamellipodial staining observed in Figure 3.3 was indeed due to Tpm1.8/9 enrichment and not Tpm2.1. MEF cells were treated with small interfering RNA (siRNA) specifically designed to knockdown the *Tpm2* gene and, due to Tpm2.1 being the only known isoform from the *Tpm2* gene, expression of Tpm2.1 (Figure 3.4 A). Cells were then stained using the $\alpha/1b$ rat antibody (Figure 3.4 B). It is demonstrated in Figure 3.4 B that the $\alpha/1b$ antibody still stains the lamellipodium even in the absence of Tpm2.1 protein, providing evidence that Tpm1.8/9 are enriched in lamellipodia of these cells, rather than Tpm2.1.

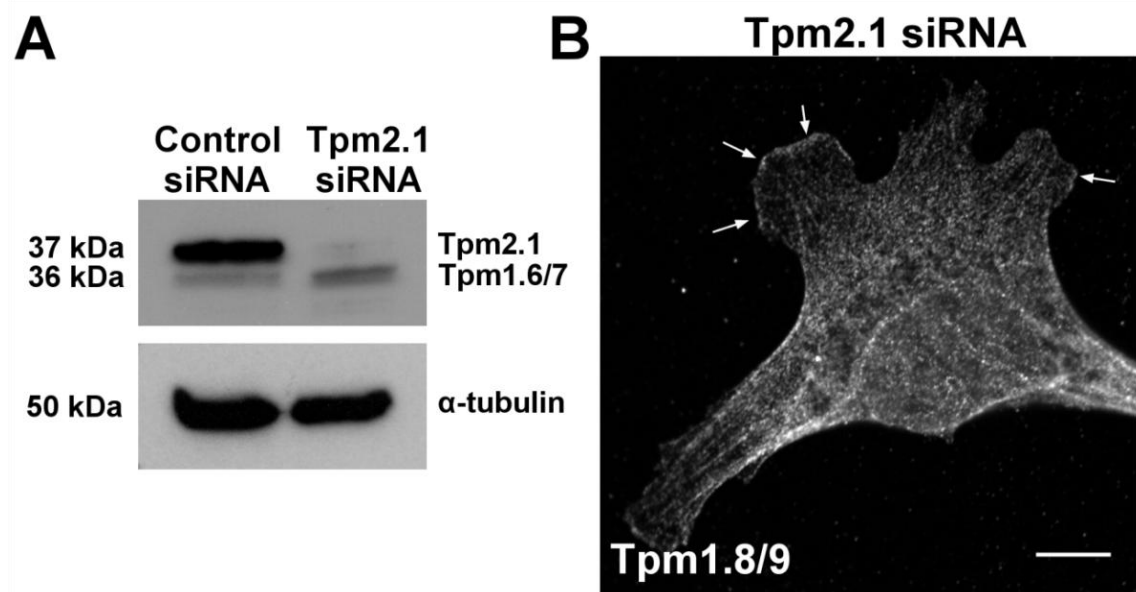


Figure 3.4. Tpm2.1 knockdown does not result in loss of lamellipodial staining.

(A) Western blot demonstrating successful knockdown using Tpm2.1 siRNA as detected using the TM311 antibody (Schevzov et al., 2011).

(B) Representative confocal image of a Tpm2.1 siRNA treated MEF cell stained for Tpm1.8/9. Arrows indicate that lamellipodial staining of Tpm1.8/9 is still present. Scale bar = 10 μ m.

In order to provide further evidence that any Tpm2.1 protein detected by the $\alpha/1b$ rat antibody is not present in the lamellipodium (it should also be noted that Tpm2.1 is not detected in MEF lysates via Western blot using this antibody, as demonstrated in Figure 3.1 D), MEFs were co-stained with $\alpha/1b$ and CG1 (an antibody specific for Tpm2.1 (Schevzov et al., 2011)). Figure 3.5 demonstrates that lamellipodial staining in MEFs by $\alpha/1b$ (Figure 3.5 A) is due to the presence of Tpm1.8/9 rather than Tpm2.1, which, as seen by CG1, is absent from the lamellipodium (Figure 3.5 B). Tpm2.1 is instead more prominent in stress fibres as has been previously reported (Schevzov et al., 2005; Schevzov et al., 2011; Temm-Grove et al., 1998).

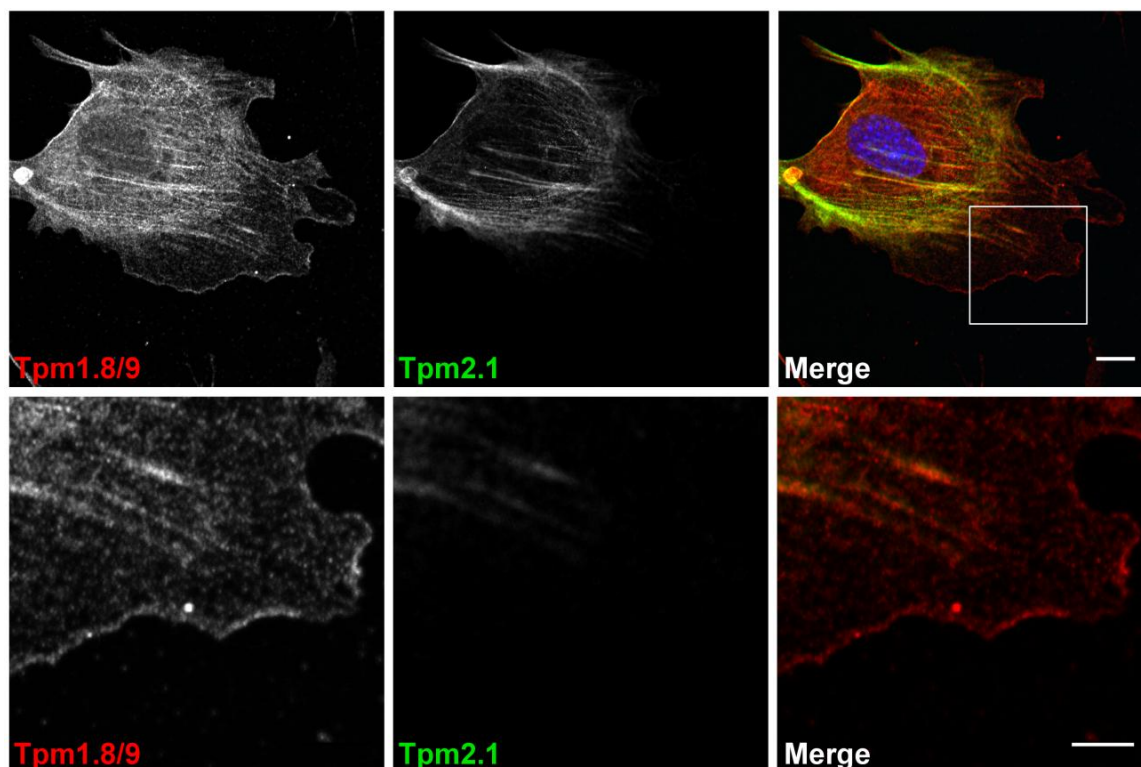


Figure 3.5. Tpm2.1 is not detected in the lamellipodium of MEF cells.

Upper panel: Representative confocal image of a MEF cell co-stained for Tpm1.8/9 and Tpm2.1, demonstrating that Tpm1.8/9 but not Tpm2.1 are present in the lamellipodium. Merged image shows Tpm1.8/9 in red, Tpm2.1 in green and the nucleus stained with DAPI in blue. Scale bar = 10 μm .

Lower Panel: 30 μm x 30 μm enlargement of the boxed region (in upper panel merge) showing, in detail, the presence of Tpm1.8/9 and absence of Tpm2.1 from the lamellipodium. Scale bar = 5 μm .

Confirmation of the lamellipodial localisation of Tpm1.8/9

To assess the lamellipodial localisation of Tpm1.8/9 in more detail, MEFs were co-stained with anti-Arp2 to detect the Arp2/3 complex as a marker for the lamellipodium and anti-cortactin to detect cortactin, a protein also known to localise to the lamellipodium (Weed et al., 2000) (Figure 3.6 A). This was done as a positive control for lamellipodial co-localisation as both of these proteins are present in the lamellipodium and directly interact with one another (Bryce et al., 2005; Weaver et al., 2002; Weaver et al., 2001). Next, MEFs were co-stained with α /1b and anti-Arp2 (Figure 3.6B). Finally, in order to examine these proteins in more detail, 3 μ m x 3 μ m enlargements (Figure 3.6C) of regions along the leading edge (indicated in the merge panel of Figure 3.6B) reveal that, although both are present in the lamellipodium, Tpm1.8/9 (red) and Arp2 (green) do not overlap significantly. This was confirmed quantitatively using Pearson's coefficient as previously described (Bolte & Cordelieres, 2006) (Figure 3.6C, final panel). Compared to the cortactin control, Tpm1.8/9 and Arp2 display a significantly lower level of co-localisation (R) from nine cells per group analysed, suggesting that Tpm1.8/9 and Arp2/3, although both present in the lamellipodium, associate with different populations of actin filaments. This observation is supported by in vitro studies which showed that binding of the Arp2/3 complex to actin filaments is inhibited by Tpm1.8 (Blanchoin, Pollard & Hitchcock-DeGregori, 2001), but interestingly, not the related Tpm1.12 (Bryce, Schevzov & Gunning, 2003; Kis-Bicskei et al., 2013a)

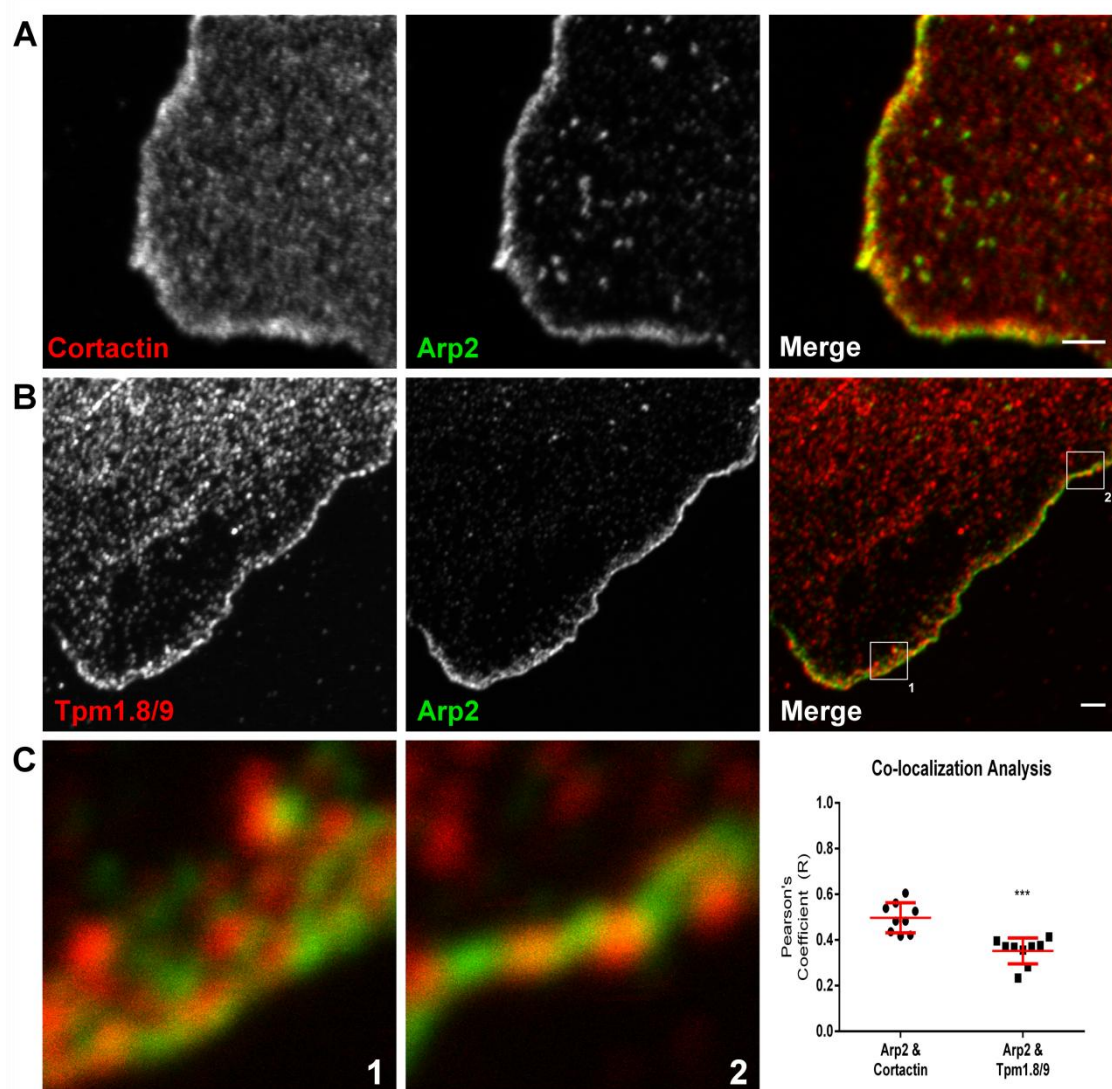


Figure 3.6. Tpm1.8/9 and Arp2/3 co-occupy the lamellipodium.

(A) 5x magnification of the lamellipodium of a MEF cell co-stained for cortactin and Arp2, used as a control to demonstrate that both of these proteins co-localise in the lamellipodium. Merged image shows cortactin in red and Arp2 in green. Scale bar = 2 μ m.

(B) 3x magnification of the lamellipodium of a MEF cell co-stained for Tpm1.8/9 and Arp2 to demonstrate that both of these proteins also occupy the lamellipodium. Merged image shows Tpm1.8/9 in red and Arp2 in green. Scale Bar = 2 μ m.

(C) 3 μ m x 3 μ m enlargements of the regions shown in the merge panel from (B), showing that, although both present in the lamellipodium, Tpm1.8/9 (red) and Arp2 (green) do not strongly overlap. This is demonstrated quantitatively by co-localisation analysis of the images by Pearson's coefficient, where compared to cortactin control (individual zooms not shown), Tpm1.8/9 and Arp2 display a significantly lower level of co-localisation (R). Error bars \pm SEM; n = 9; ***p < 0.001; Student's t-test.

Discussion

Tropomyosin in the lamellipodium

Cell migration consists of a well-defined cycle of coordinated steps beginning with protrusion of the leading edge. The major driving force behind leading edge protrusion is Arp2/3 mediated polymerisation of actin filaments. This results in the generation of a flat, sheet-like structure containing a dense network of branched actin filaments known as the lamellipodium (Pollard & Borisy, 2003). The stabilisation and disassembly of the actin network of the lamellipodium is co-ordinated by a defined network of proteins. These include cortactin, which has been shown to promote cell motility by stabilising newly generated filament branch points (Bryce et al., 2005; Weaver et al., 2001) and cofilin, which severs actin filaments (Bamburg, 1999). The exact molecular mechanisms underlying the way in which rapidly-treadmilling Arp2/3 filaments within the lamellipodium are mechanically coupled to actin filaments associated with more stable lamellipodia however remain unclear.

There is disagreement in the literature about the organisation of the actin network in the lamellipodium. Some studies have reported the existence of two spatially segregated zones composed of Arp2/3-branched filaments at the cell edge, and unbranched filaments immediately proximal to this zone (Iwasa & Mullins, 2007; Pollard & Borisy, 2003; Svitkina & Borisy, 1999; Svitkina et al., 1997; Vallotton & Small, 2009). Others have stated that these overlap and that both branched and unbranched filaments are present at the very leading edge (Small, 2015; Urban et al., 2010; Vinzenz et al., 2012).

Recent experiments indicate the importance of building multiple actin filament types in the same location to generate functional outcomes (Kee et al., 2015; Tojkander et al., 2011). Studies in a variety of systems support that Tpm isoforms are used to specify the

functional and molecular properties of actin filaments to allow the collaboration of different filament populations within the cell (Gunning et al., 2015). By a mechanism that is not yet well-understood, Tpm isoforms display extensive sorting, both at a tissue and intracellular level resulting in spatially distinct actin filament populations (Martin & Gunning, 2008; Martin, Schevzov & Gunning, 2010; Schevzov et al., 2008; Schevzov et al., 2005). If multiple populations of actin filaments are indeed present within the lamellipodium, it begs the question of how these are differentially regulated both spatially and temporally. One potential candidate molecule that may allow the cell to discriminate between different actin populations is Tpm.

Undeniably, the presence of Tpm in lamellipodia has been a disputed topic in the literature (Blanchoin, Pollard & Hitchcock-DeGregori, 2001; Bryce, Schevzov & Gunning, 2003; Bugyi, Didry & Carlier, 2010; DesMarais et al., 2002; Gupton et al., 2005; Hillberg et al., 2006; Hsiao et al., 2015a; Iwasa & Mullins, 2007; Koestler et al., 2013; Lazarides, 1976; Lin, Hegmann & Lin, 1988; Ponti et al., 2004; Skau et al., 2015), primarily due to the lack of Tpm isoform specific antibodies.

Summary of findings

This chapter reports on the characterisation of a novel anti-Tpm antibody ($\alpha/1b$) produced in rat. It was generated by two overlapping peptides spanning the entire exon 1b of the *Tpm1* gene as the immunogen. A panel of recombinant Tpm proteins comprised of isoforms representing all four *Tpm* genes was probed with the $\alpha/1b$ antibody. It preferentially detects isoforms Tpm1.8 and Tpm1.9 with minor cross reactivity with Tpm2.1. Tpm1.8/9 share a similar amino-terminal exon/intron structure with Tpm1.12 (Geeves, Hitchcock-DeGregori & Gunning, 2014; Schevzov et al., 2011), an isoform found at the leading edge of neuronal cells (Bryce, Schevzov & Gunning,

2003). MEFs were co-stained with $\alpha/1b$ and CG1 (an antibody specific for Tpm2.1) in order to demonstrate that lamellipodial staining in these cells is due to the presence of Tpm1.8/9 rather than Tpm2.1. MEFs were also co-stained $\alpha/1b$ and anti-Arp2. Enlargements of regions along the leading edge reveal that, although both are present in the lamellipodium, Tpm1.8/9 and Arp2/3 do not overlap significantly. Co-localisation was quantified using Pearson's coefficient, showing that, compared to a cortactin control, Tpm1.8/9 and Arp2/3 display a significantly lower level of co-localisation, suggesting that Tpm1.8/9 and Arp2/3 associate with different populations of actin filaments within the lamellipodium.

Problems associated with fluorescently-labelled Tpm1.8/9

Fluorescent protein fusion constructs can serve as a useful tool to study the function of proteins in living cells. This approach however requires that a bulky protein be fused to either the amino (N-) or carboxyl (C-) terminus of the protein of interest and, depending on the importance of either end for protein function, may result in the tagged protein no longer mimicking the function or cytosolic localisation of the endogenous protein.

Plasmids encoding for GFP (green fluorescent protein) fusions of both Tpm1.8 and Tpm1.9 already existed as reagents in the Gunning lab (PG421 and PG422 respectively, generated by Nicole Bryce, 2002). These plasmids feature a mammalian CMV promoter and, due to the orientation of the tropomyosin and the GFP in the plasmid, encode for GFP to be fused to the N-terminus of tropomyosin. Transfection of either of these constructs into MEF cells and subsequent confocal imaging of the fixed samples revealed that the subcellular localisation of both Tpm1.8 and Tpm1.9 GFP fusion proteins no longer resembled that of the native protein, as detected by the $\alpha/1b$ antibody. Rather, both were excluded from the lamellipodium and instead localised to stress fibres

in a similar pattern to β -actin (Figure 3.7), suggesting that the N-terminus is essential for normal function of these Tpms (as has been reported for other Tpms (Bharadwaj et al., 2004) and the GFP tag may be interfering with intracellular sorting.

Furthermore, the α 1b antibody doesn't properly label exogenous N-terminal GFP fused Tpm1.8 (Figure 3.8 A) or Tpm1.9 (Figure 3.8 B). These images also show that while the antibody stains endogenous Tpm1.8/9 in each case, the GFP-tagged proteins again, do not have access to the very periphery of the cell and appear as stress fibres (GFP-Tpm1.9 appears somewhat more peripheral than GFP-Tpm1.8). As the epitope for the antibody resides in the N-terminus of the Tpm molecule, it is possible that the GFP tag is blocking access of the antibody to its binding site on the protein.

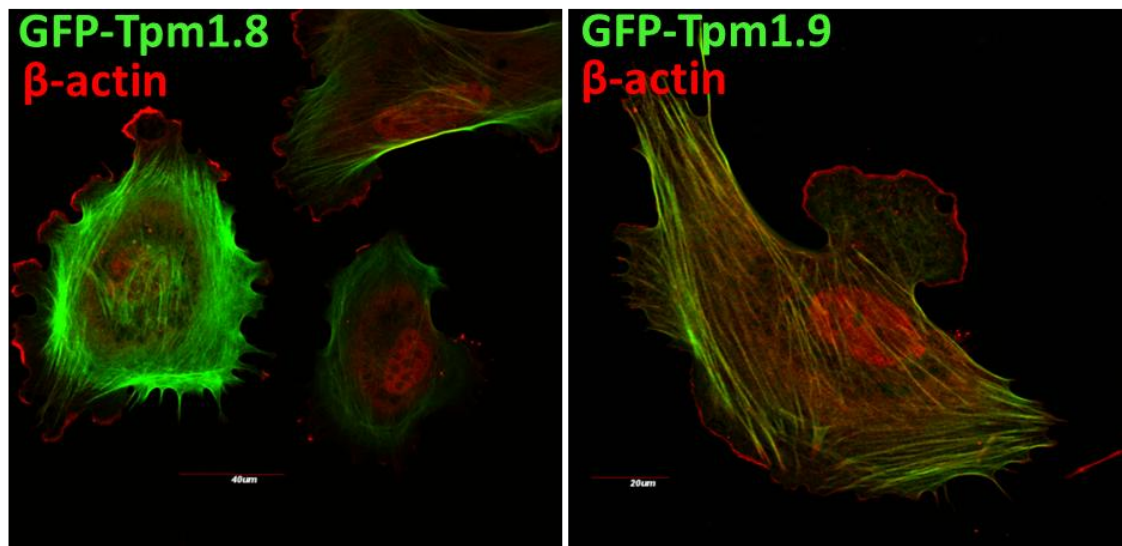


Figure 3.7. Incorrect sorting of tagged Tpms.

Representative confocal images of MEF cells stained for β -actin (red) following transfection with either PG421 (GFP-Tpm1.8, green, left panel) or PG422 (GFP-Tpm1.9, green, right panel)

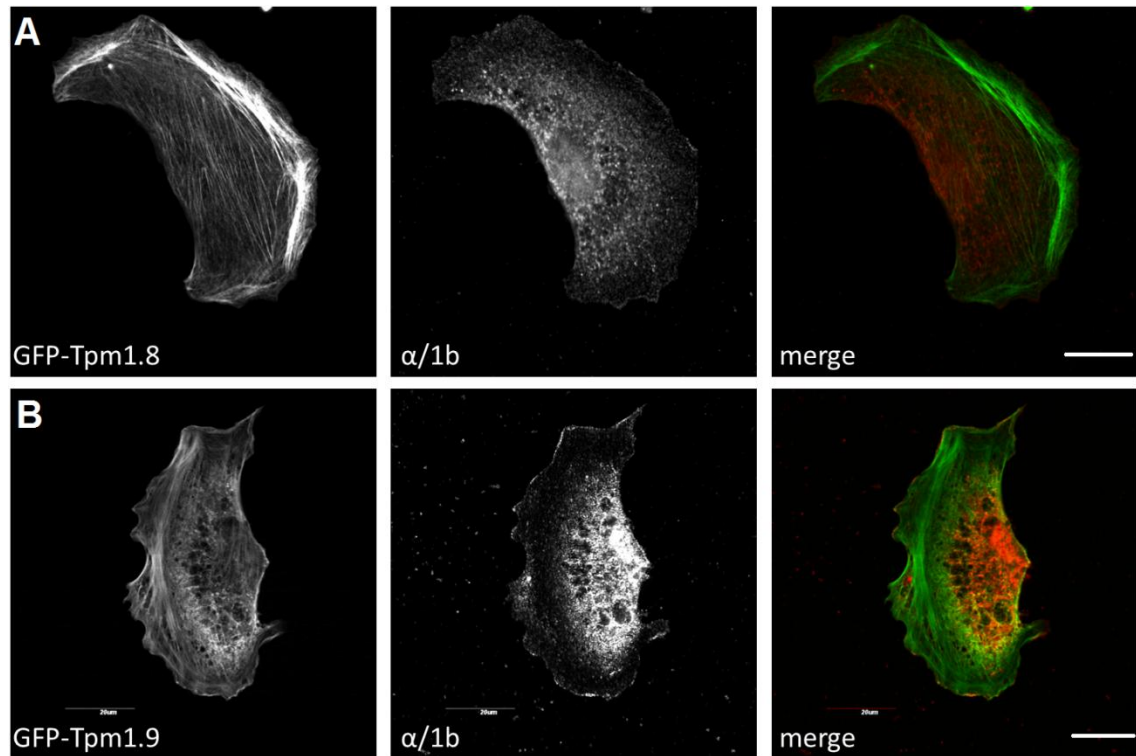


Figure 3.8. Failure of the $\alpha/1b$ to bind to exogenous Tpm1.8 or Tpm1.9.

(A) Confocal image of a PG421 transfected cell expressing GFP-Tpm1.8 co-labelled using the $\alpha/1b$ antibody.

(B) Confocal image of a PG422 transfected cell expressing GFP-Tpm1.9 co-labelled using the $\alpha/1b$ antibody.

Merged images show exogenous Tpm protein in green and endogenous protein detected with the $\alpha/1b$ antibody in red. Scale bars = 20 μm .

Two possible strategies could be employed in an attempt to rectify this scenario. Firstly, a linker sequence (the amino acid sequence which lies in an open reading frame between the protein of interest and the fluorescent protein) could be made longer, thus increasing the distance between the two and possibly circumventing any interference caused by the tag. Secondly, if it is indeed the N-terminus that is important for protein function, the plasmid can be re-designed so that the fluorescent protein becomes fused to the C-terminus of the protein of interest. Due to reagents already available in the lab and certain time constraints, that latter strategy was chosen. To achieve this, the commercially available vector pcDNA 3.1+ (Invitrogen) was chosen which for sub-cloning. This vector also utilised a mammalian CMV promoter but, due to the organisation of the MCS (multiple cloning site), it was possible to insert the DNA fragment encoding tropomyosin (Tpm1.8 was chosen in this instance) upstream of the fluorescent protein (in this case m-NeonGreen (mNG), which has similar spectral properties to GFP was chosen) resulting in a plasmid (PG538, generated by Simon Brayford, 2014) encoding a 57 kDa protein consisting of Tpm1.8 followed mNG-fused to the C-terminus with a 6-amino acid linker sequence between, followed by a stop codon (See Figure 3.9 for vector map).

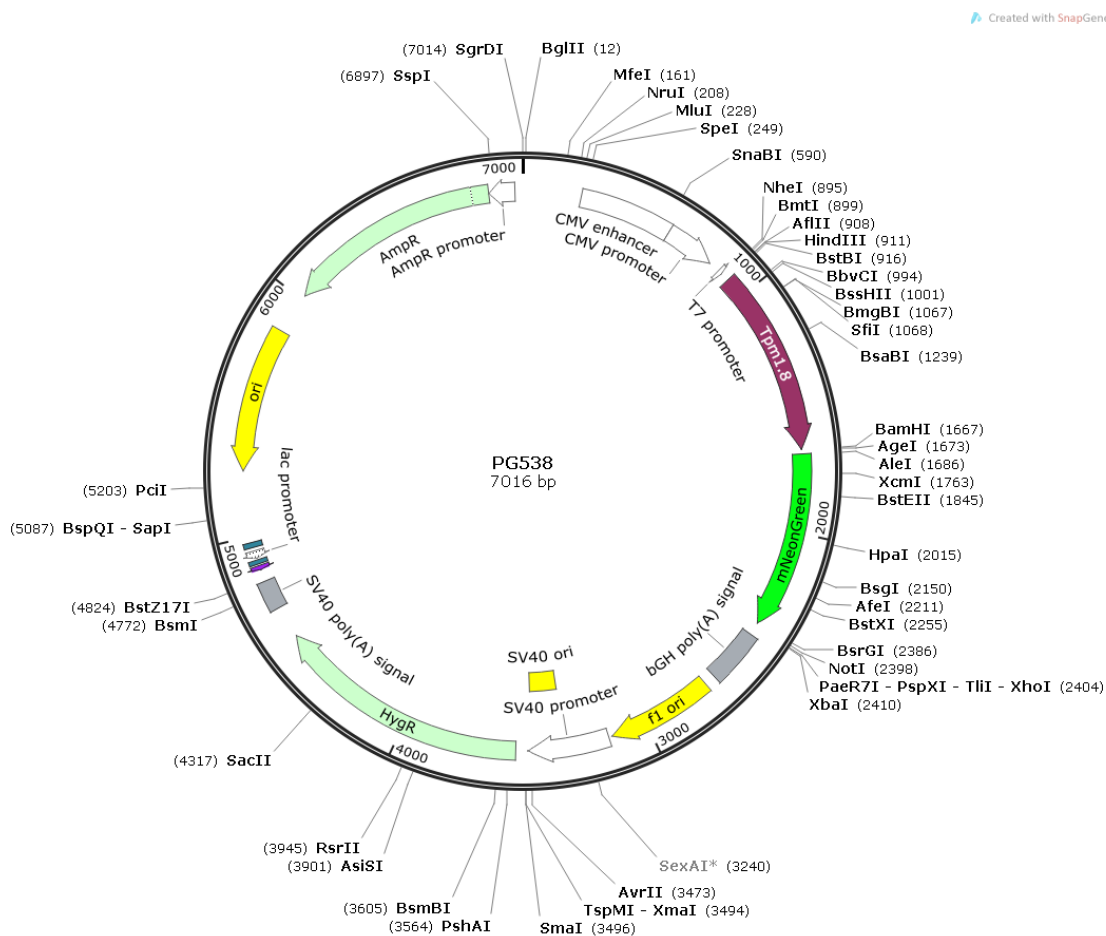


Figure 3.9. Vector map of PG538 showing the orientation of Tpm1.8 and m-NeonGreen relative to the mammalian CMV promoter.

(Created with SnapGene, GSL Biotech LLC, Chicago, IL)

Following transfection of MEFs with PG538, cell lysates were collected and analysed via Western blot first to check for expression of the fusion protein at the predicted molecular weight. Probing with the $\alpha/1b$ antibody reveals that, compared to wild-type MEFs, PG538 transfected MEFs express endogenous Tpm1.8/9 at 30 kDa as well as another band representing the Tpm1.8-mNG fusion protein at the predicted molecular weight of 57 kDa (Figure 3.10).

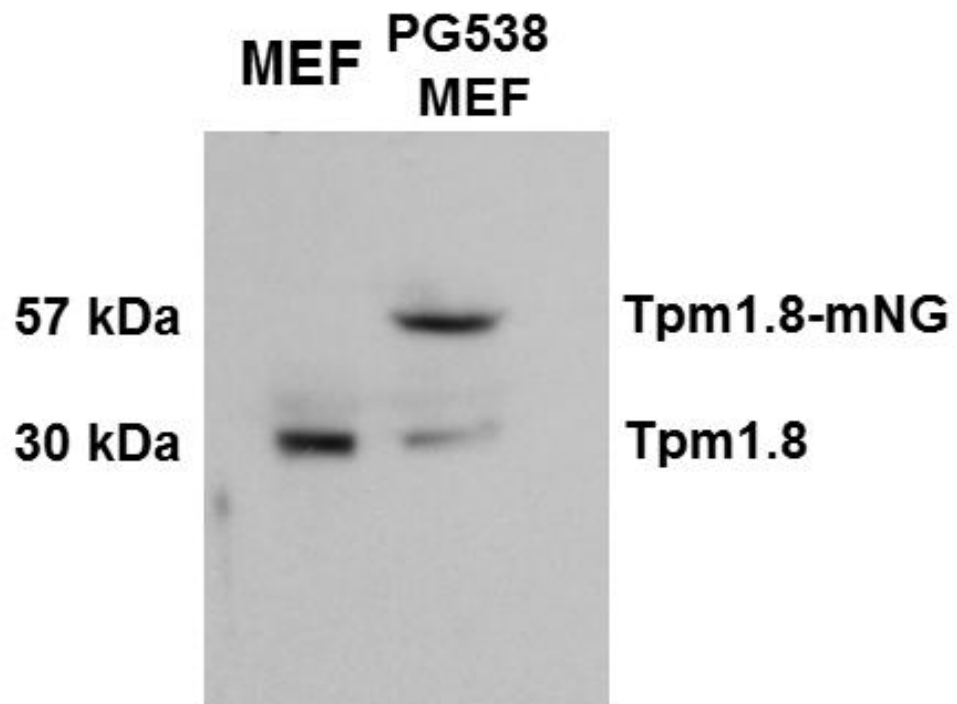


Figure 3.10. Western blot of MEF lysates and MEF lysates transfected with PG538 as probed with the $\alpha/1b$ antibody. As well as endogenous Tpm1.8/9 at 30 kDa, a band representing Tpm1.8-mNG can be seen at the predicted molecular weight of 57 kDa.

Finally, confocal images of MEFs transfected with PG538 show that the C-terminally tagged Tpm1.8 more closely resembles the cellular distribution of endogenous Tpm1.8/9, and is enriched in, and therefore has access to the lamellipodium (Figure 3.11 A). Furthermore, the $\alpha/1b$ antibody exhibits a more reliable recognition of the Tpm1.8-mNG protein than it does for the N-terminally-tagged variants (Figure 3.11 B). However, significant stress-fibre like structures are still present with this construct (Figure 3.11 A). Possible explanations for this could be either that the C-terminus also plays a role in true Tpm localisation (due to the head-to-tail interaction described in Figure 1.4) or that, under control of this particular promoter, the cell simply translates too much Tpm protein and this in turn saturates the actin filaments throughout the cytoplasm. Either way, based on this observation, it was concluded that biological function could not be faithfully reproduced using this construct and, as a result, planned knockout-rescue experiments were subsequently abandoned in favour of transient knockdown studies alone.

Concluding Remarks

In conclusion, the findings of this chapter provide a solution to the controversy found in the literature surrounding the presence of Tpm in the lamellipodium. These results also pave the way for a more detailed study into a potential mechanism of how Tpm and Arp2/3 networks may collaborate at the leading edge to regulate lamellipodial actin filaments. The next chapter will explore the cellular effects of siRNA-mediated gene silencing of Tpm1.8/9.

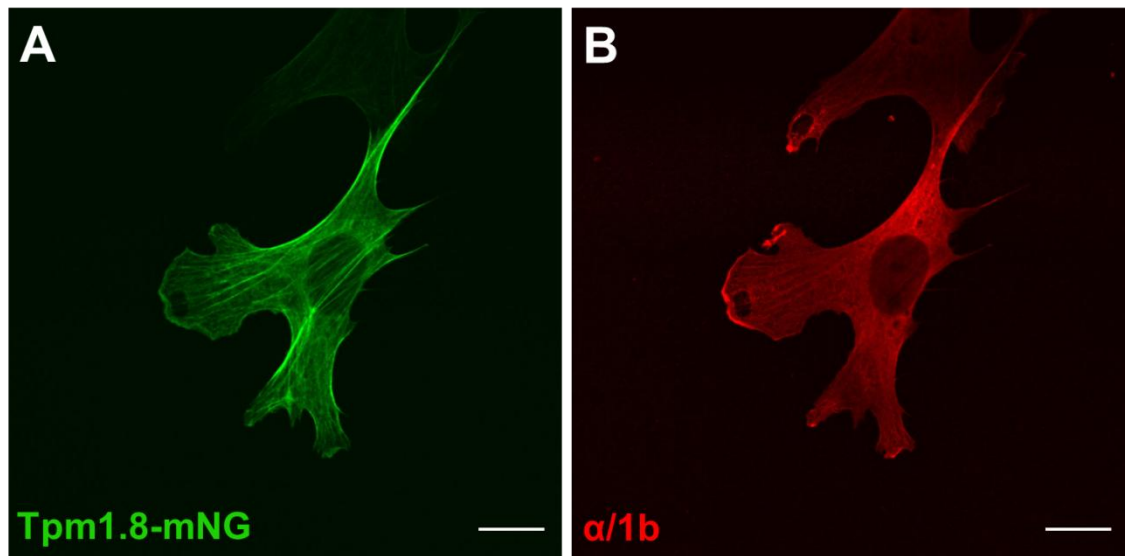


Figure 3.11. Cellular localisation and detection of Tpm1.8-mNG.

(A) Representative confocal image of a MEF cell transfected with PG538 (Tpm1.8-mNG, green)

(B) Confocal image of the MEF cell from (A) stained using the $\alpha/1b$ antibody (red) Scale Bar = 20 μm

Chapter Four

**siRNA knockdown of Tpm1.8/9
expression and its effect on cell
morphology and Arp2/3 activity**

Chapter 4: siRNA knockdown of Tpm1.8/9 and its effect on cell morphology and Arp2/3 activity

Introduction

Understanding cell motility will require detailed knowledge not only of the localisation of signalling networks regulating actin polymerisation but also of their dynamics. Unfortunately, many signalling networks are not amenable to such analysis, as they are frequently transient and dispersed. By contrast, the signalling pathways used by pathogens undergoing actin-based motility are highly localised and operate in a constitutive fashion (Backert, Feller & Wessler, 2008; Bhavsar, Guttman & Finlay, 2007; Frischknecht & Way, 2001; Munter, Way & Frischknecht, 2006; Pawson & Warner, 2007). Some researchers have taken advantage of this fact and, by examining the host-pathogen interaction have uncovered some useful new data on Arp2/3 regulatory proteins. For example, N-WASP, WIP, GRB2 and NCK are required to stimulate Arp2/3-dependent actin-based motility of vaccinia virus (Frischknecht et al., 1999; Moreau et al., 2000; Scaplehorn et al., 2002; Snapper et al., 2001), by exploiting this interaction, Weisswange and colleagues have shown that the turnover of N-WASP depends on its ability to stimulate Arp2/3-mediated actin polymerisation while conversely, disruption of the interaction of N-WASP with Grb2 increases its exchange rate, resulting in faster virus movement, suggesting that the exchange rate of N-WASP controls the rate of Arp2/3-dependent actin-based motility (Weisswange et al., 2009). Other work from this group has established that WIP acts as an essential link between Nck and N-WASP (Donnelly et al., 2013). Observations such as these provide

important insights into the hierarchy and connections in one of the major cellular signalling networks stimulating Arp2/3 complex-dependent actin polymerisation.

Much less is known about the role of tropomyosin in regulating Arp2/3 activity. There appears to be some conflicting reports with some studies demonstrating that Tpm inhibits binding of Arp2/3 to actin filaments (Blanchoin, Pollard & Hitchcock-DeGregori, 2001) and others reporting cooperative binding (Kis-Bicskei et al., 2013a). It is important to note that, while these studies were performed in cell-free systems, they also were looking at different Tpm isoforms. There is considerable evidence to support to idea that different Tpm isoforms confer different properties to the actin filaments they are associated with (Bryce, Schevzov, Ferguson, Percival, Lin, Matsumura, Bamburg, Jeffrey, Hardeman, Gunning, et al., 2003; Creed et al., 2008; Gunning et al., 2015; Gunning, O'Neill & Hardeman, 2008; P. W. Gunning et al., 2005). Very little is currently known about the interaction of Tpm and Arp2/3 in cells primarily because, up until the results reported in the previous chapter, the mere presence of Tpm in Arp2/3-rich areas of the cell such as the leading edge was doubted (DesMarais et al., 2002).

In the previous chapter, it was established that the tropomyosin isoforms Tpm1.8/9 are enriched in the lamellipodium of mouse fibroblasts together with the Arp2/3 complex. This observation strongly suggests that these Tpm isoforms play a role in the regulation of actin filaments within this cellular structure and in turn therefore, may regulate motility as the lamellipodium represents a key structure involved with many modalities of cell motility (Abercrombie, Heaysman & Pegrum, 1970a). Tpm1.8/9 and Arp2/3, whilst equally close to the leading edge, were also found not to strongly overlap with one another (Figure 3.6 C), suggesting that they may associate with different populations of actin filaments within the lamellipodium, and it has been demonstrated in

vitro that Tpm1.8 competes with Arp2/3 for binding sites on actin filaments (Blanchoin, Pollard & Hitchcock-DeGregori, 2001). In order to investigate what potential role Tpm1.8/9 may play in regulating Arp2/3 activity within the lamellipodium, a short interfering RNA (siRNA) gene silencing approach was employed. This method has been used extensively since its discovery to study the function of specific proteins by blocking their translation at the mRNA level (Fire et al., 1998). This chapter demonstrates that Tpm1.8/9 expression can be specifically silenced by siRNA, and uncovers a novel regulatory mechanism within the lamellipodium between Tpm1.8/9 and the Arp2/3 complex.

Results

Design of Tpm1.8/9 specific siRNA

In order to specifically knockdown expression of Tpm1.8/9, target DNA sequences for siRNA were chosen from exon 1b of the *Tpm1* mouse gene (Figure 1.5). Five unique candidate sequences were designed according to the siRNA design guidelines first described by Elbashir et al., (Elbashir et al., 2001). These custom oligonucleotides were synthesised by Qiagen (Melbourne, Australia). The sequences were then individually tested in MEF cells by transfecting each sequence at a final concentration of 25nM using Lipofectamine RNAiMAX (Life Technologies) according to the manufacturer's instructions. Following incubation for 48 h, cell lysates were harvested using RIPA buffer and subjected to SDS-PAGE and Western blotting before densitometry was performed. Of the five sequences, the one which provided the greatest degree of protein knockdown as revealed by Western blot (normalised to α -tubulin) was the sequence 5'-GGAGCGGAAGCTGCGGGAAAC-3 (Figure 4.1 A). This siRNA sequence was therefore used for all Tpm1.8/9 knockdown experiments described in this thesis.

AllStars negative control siRNA (Qiagen) was used as a negative control for all knockdown experiments described in this thesis.

Average reduction in Tpm1.8/9 protein levels achieved in MEFs using this siRNA sequence at 25nM, 48 h post transfection was calculated to be $80 \pm 2 \%$, $p < 0.0001$ compared to control (non-silencing) siRNA (Figure 4.1 B). This was calculated from triplicate repeats with each normalised to α -tubulin.

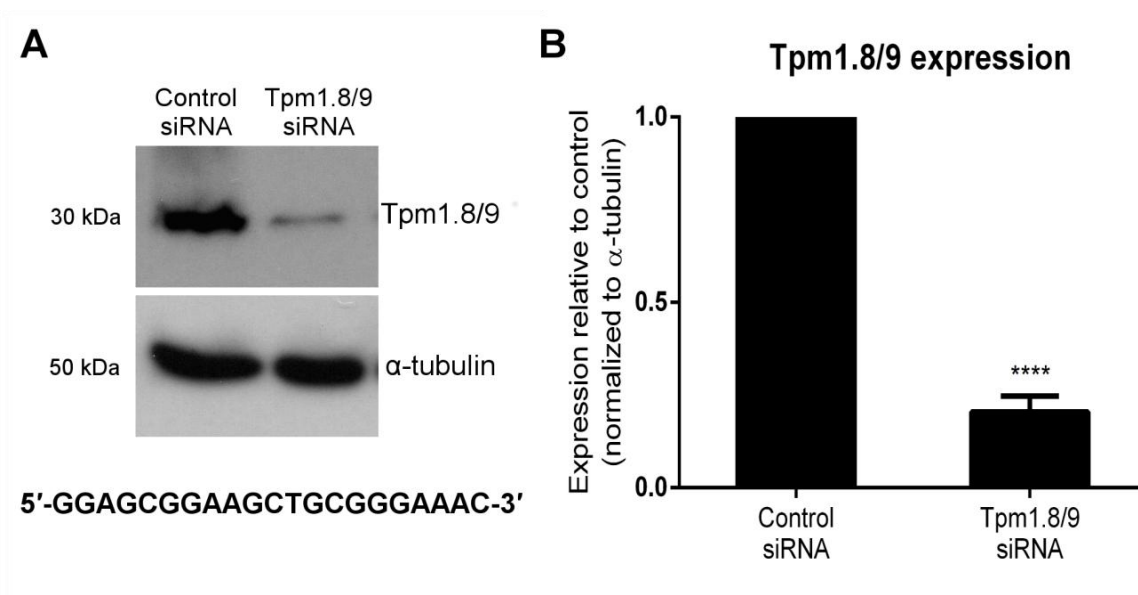


Figure 4.1. siRNA directed silencing of Tpm1.8/9 expression.

(A) Western blot analysis of Tpm1.8/9 expression in MEFs 48 hr post transfection with either control (non-silencing) or Tpm1.8/9 siRNA (target sequence shown below blot) with α -tubulin used as a loading control.

(B) Relative Tpm1.8/9 protein expression levels were determined by densitometry following normalisation to α -tubulin. Error bars = SEM; n = 3; ****p < 0.0001; Student's t-test.

In order to confirm the specificity of the siRNA for Tpm1.8/9, the expression levels of other Tpm isoforms were examined following treatment of Tpm1.8/9 siRNA (Figure 4.2A). Densitometry of triplicate repeats found no significant change in the relative protein levels of Tpm1.6/7, 2.1, 3.1/2 or 4.2 in the Tpm1.8/9 knockdown cell lysates compared to control (Figure 4.2 B). This shows that the siRNA sequence is specific to knocking down Tpm1.8/9 and that no compensatory increase in expression of other Tpm is occurring as a result.

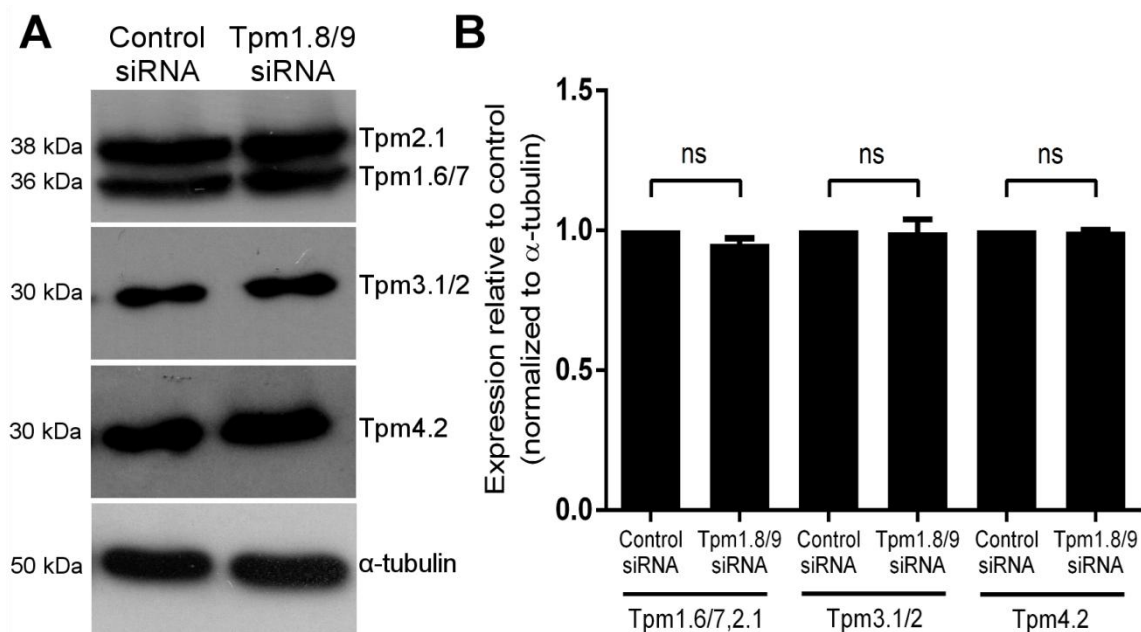


Figure 4.2. Knockdown of Tpm1.8/9 results in no compensatory expression of other Tpm isoforms.

(A) Representative western blot of control and Tpm1.8/9 siRNA-treated cell lysates probed with the TM311 (Tpm2.1, 1.6, 1.7), γ /9d (Tpm3.1/2), δ /9d (Tpm4.2) and α -tubulin antibodies.

(B) Quantification of the expression levels of different Tpm isoforms normalised to α -tubulin, relative to control. Error bars = SEM; n = 3; ns = no significant difference. Student's t-test.

To confirm that the siRNA sequence would have the desired and expected effect on Tpm1.8/9 protein localisation in situ, immunofluorescence staining of MEFs with the $\alpha/1b$ antibody post siRNA transfection was performed. Figure 4.3 demonstrates the absence of Tpm1.8/9 from the lamellipodium following Tpm1.8/9 siRNA treatment (Figure 4.3 B) when compared to MEFs treated with control (non-silencing) siRNA (Figure 4.3 A). This experiment also provides further evidence of the lamellipodial localisation of Tpm1.8/9 and the specificity of the $\alpha/1b$ antibody described in chapter 3.

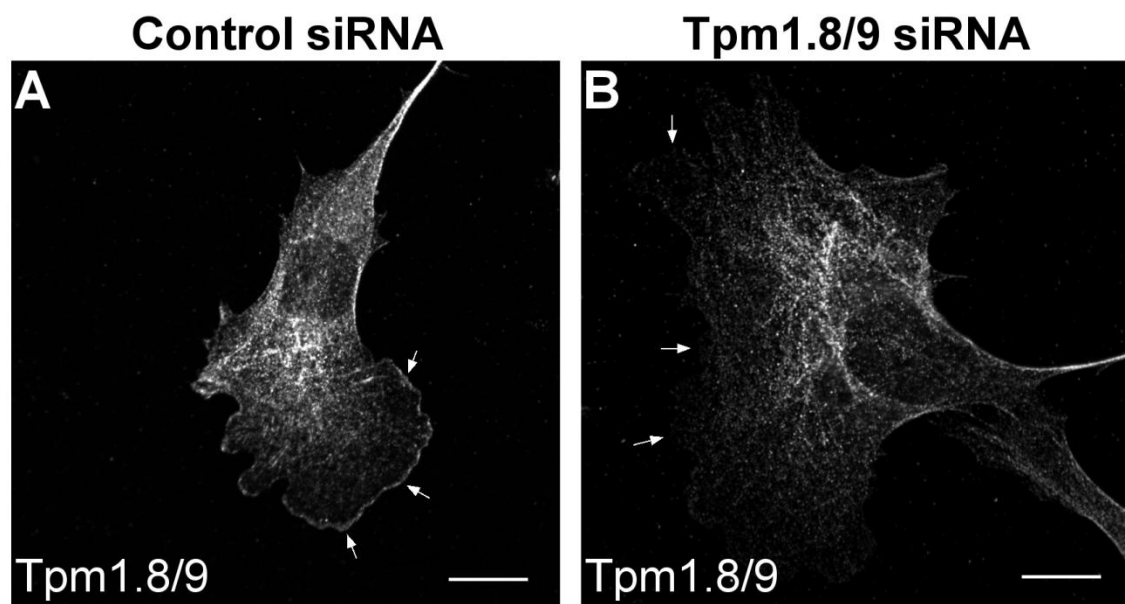


Figure 4.3. Knockdown of Tpm1.8/9 leads to its depletion from the lamellipodium.

Representative confocal images of MEFs 48 hr post transfection with either control (non-silencing) siRNA (A) or Tpm1.8/9 siRNA (B), immunofluorescently stained with the $\alpha/1b$ antibody. Arrows indicate loss of Tpm1.8/9 from the lamellipodium following knockdown. Scale bars = 10 μm .

Tpm1.8/9 knockdown results in increased peripheral Arp2/3

Following the observation that Arp2/3 and Tpm1.8/9 appear to associate with different actin filament populations within the lamellipodium (Figure 3.6 C), it was postulated that Tpm1.8/9 may have an antagonistic effect on the binding of Arp2/3 to actin filaments, a property of Tpm1.8 that has been previously demonstrated in vitro (Blanchoin, Pollard & Hitchcock-DeGregori, 2001). To test this in MEFs, cells were stained for Arp2/3 (by staining with anti-Arp2) in both control (Figure 4.4 A) and Tpm1.8/9 siRNA-treated cells (Figure 4.4 B). The acquired confocal images were then analysed to measure both total cell area and percentage of the cell perimeter that contains Arp2. Whilst no significant change in average cell area was observed ($2019 \pm 177 \mu\text{m}^2$ in control versus $2404 \pm 136 \mu\text{m}^2$ in Tpm1.8/9 knockdown) (Figure 4.4 C), there was a significant increase in the percentage of the cell edge that contains Arp2 in the Tpm1.8/9 knockdown cells ($42 \pm 2 \%$) compared to control cells ($27 \pm 2 \%$) (Figure 4.4 D). These data suggest that the transient knockdown of Tpm1.8/9 results in an increased ability of the Arp2/3 complex to bind to actin filaments at the cell edge and therefore spread along the cell periphery.

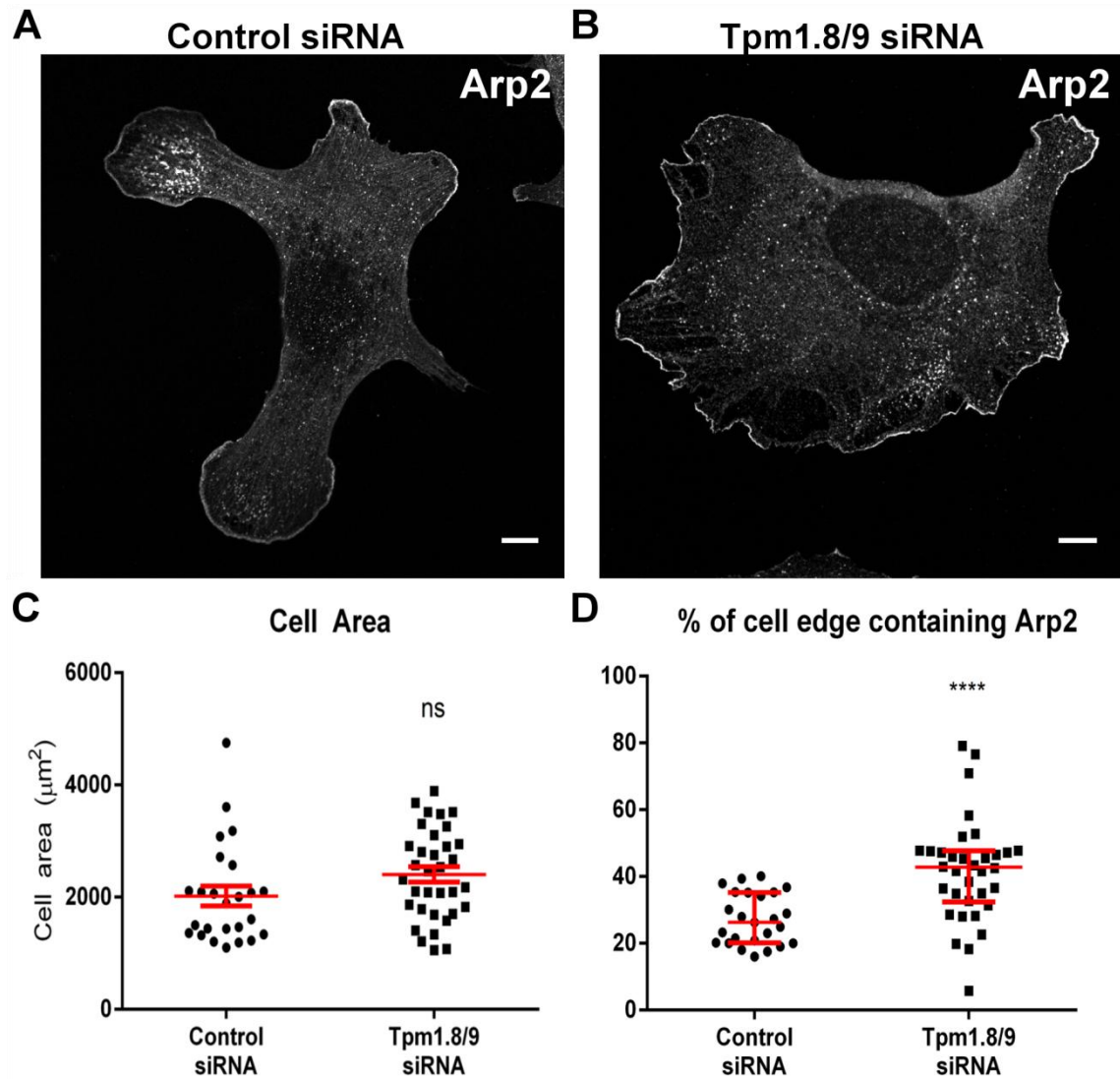


Figure 4.4. Tpm1.8/9 knockdown results in an increase in peripheral Arp2/3.

MEFs stained for Arp2, 48 h post transfection with either control siRNA (A) or Tpm1.8/9 siRNA (B). Scale bars = 10 μm .

(C) Quantitation of image analysis showing no significant difference in cell area in Tpm1.8/9 siRNA treated cells compared to control. Error bars \pm SEM; $n = 25$; ns = not statistically significant; Student's t-test.

(D) Quantitation of image analysis showing % of cell edge containing Arp2 is significantly increased in Tpm1.8/9 knockdown cells. Error bars \pm SEM; $n = 25$; **** $p < 0.0001$; Student's t-test.

Tpm1.8/9 knockdown results an increased lamellipodial thickness

As activity of the Arp2/3 complex is responsible for the generation of a dense, branched actin network, it was postulated that its increased activity, due to reduced inhibition by Tpm1.8/9, should also lead to a thicker lamellipodium due to an increased abundance of branched, F-actin at the leading edge. The lamellipodium is clearly identifiable as an F-actin rich band, as probed by phalloidin in fibroblasts (Dawe et al., 2003).

The width or thickness of the lamellipodium was measured in control (Figure 4.5 A) and Tpm1.8/9 knockdown cells (Figure 4.5 B). Lamellipodial thickness was calculated by drawing lines across the phalloidin-stained actin band at the leading edge from outside the cell inward. This was repeated many times per cell and the average length of the lines was used as the average lamellipodial thickness per cell. Analysis of 15 cells from each group revealed that lamellipodia were, on average, significantly thicker in the Tpm1.8/9 knockdown cells ($1.0 \pm 0.08 \mu\text{m}$) than those in the control group ($0.54 \pm 0.02 \mu\text{m}$) (Figure 4.5 C).

Together, these data suggest that Tpm1.8/9 regulates actin filaments at the leading edge such that, if Tpm1.8/9 is transiently removed, Arp2/3 is able to bind to more actin filaments along the cell edge, resulting in more filament branching and thicker lamellipodia.

Finally, in order to assess whether this apparent lamellipodial regulatory mechanism could be manipulated in the other direction, we examined the effects of Arp2/3 inhibition on Tpm1.8/9 levels.

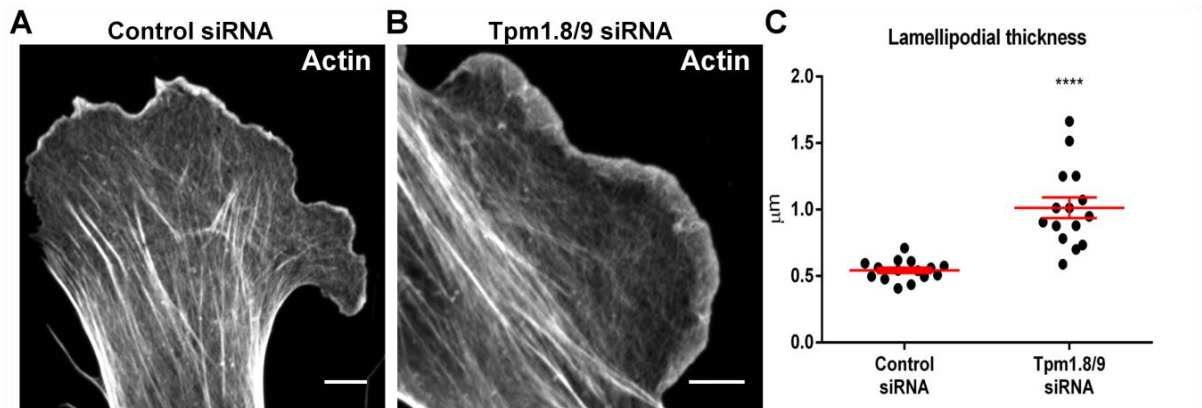


Figure 4.5. Tpm1.8/9 knockdown results in increased lamellipodial thickness.

(A) 2.0 x magnification confocal image of a MEF cell stained for Phalloidin, 48 h post transfection with control siRNA. Scale bar = 5 µm.

(B) 2.6 x magnification confocal image of a MEF cell stained for Phalloidin, 48 h post transfection with Tpm1.8/9 siRNA. Scale bar = 5 µm.

(C) Quantitation of image analysis showing lamellipodial thickness is significantly increased in Tpm1.8/9 knockdown cells. Error bars \pm SEM; n = 15; ****p < 0.0001; Student's t-test.

Arp2/3 inhibition results in an increase in Tpm1.8/9 protein levels

Rather than an siRNA approach, the commercially available small molecule Arp2/3 inhibitor, CK666 (Sigma) was used to examine the effects of loss of Arp2/3 activity on Tpm1.8/9. Using a time-course assay, it was found that Tpm1.8/9 levels were significantly increased compared to vehicle (DMSO) control after 6 h exposure to CK666 at 150 μ M (Figure 4.6) further indicating a regulatory relationship between Arp2/3 and Tpm1.8/9 whereby if Tpm1.8/9 is silenced, Arp2/3 activity increases (Figures 4.4 and 4.5) and conversely, if Arp2/3 is inhibited, Tpm1.8/9 expression is transiently increased (Figure 4.6).

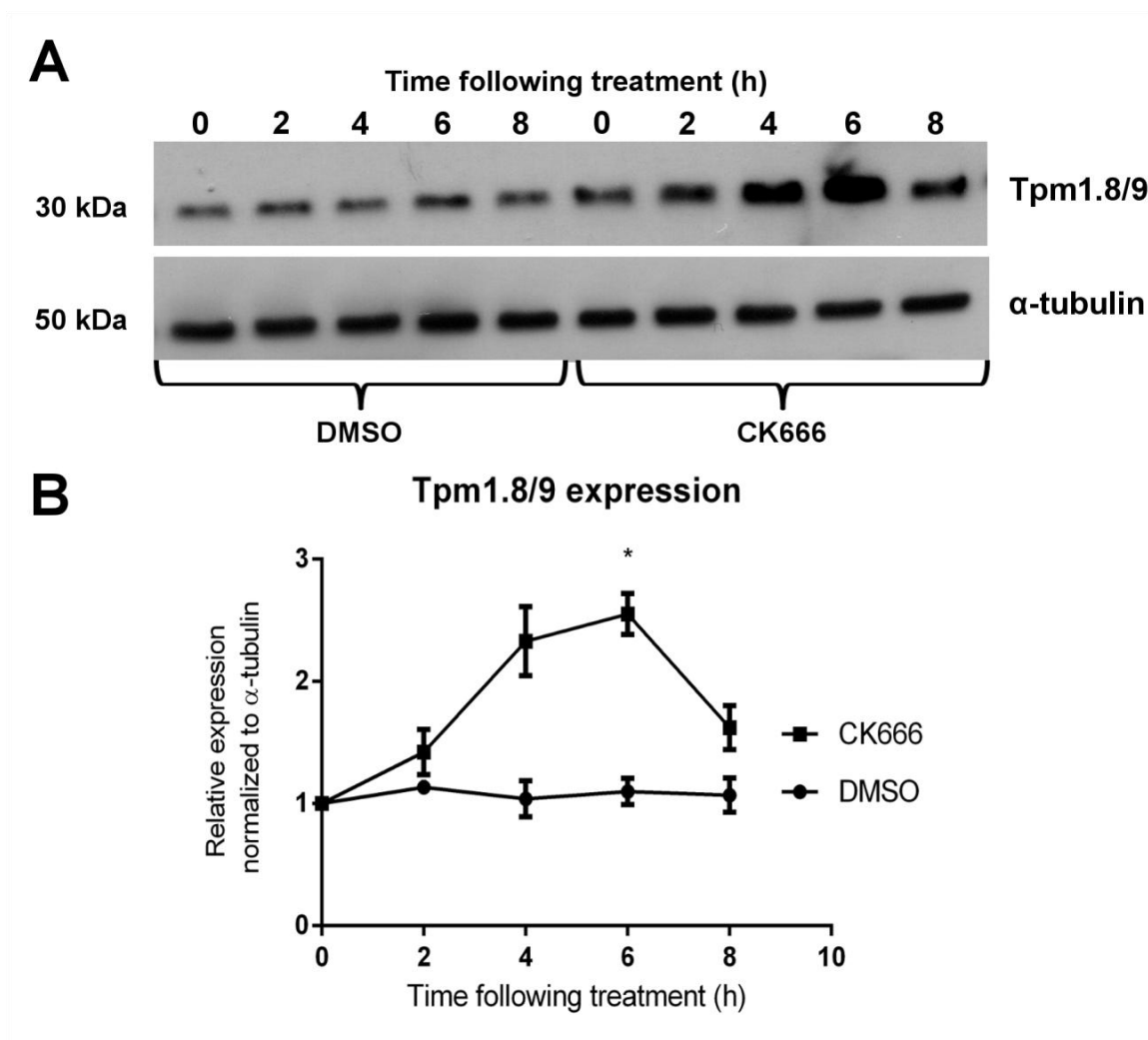


Figure 4.6. Arp2/3 inhibition leads to an increase in Tpm1.8/9 protein.

(A) Western Blot showing Tpm1.8/9 protein levels at 2 h time points following CK666 treatment compared to DMSO vehicle control. α -tubulin was used as a loading control.

(B) Quantitation of western blots in (A) showing an increase in Tpm1.8/9 protein levels (normalized to α -tubulin) post-CK666 treatment with a statistically significant increase at 6 h post-treatment. Error bars \pm SEM; n = 3; *p<0.05; Student's t-test.

Unsurprisingly, cells treated with CK666 for this time period also lose their characteristic lamellipodia due to Arp2/3 activity suppression. Interestingly however, despite the observed increase in protein level, Tpm1.8/9 are not redistributed to other cellular structures such as stress fibres (Figure 4.7), indicating that Tpm1.8/9 are strictly lamellipodial isoforms of tropomyosin.

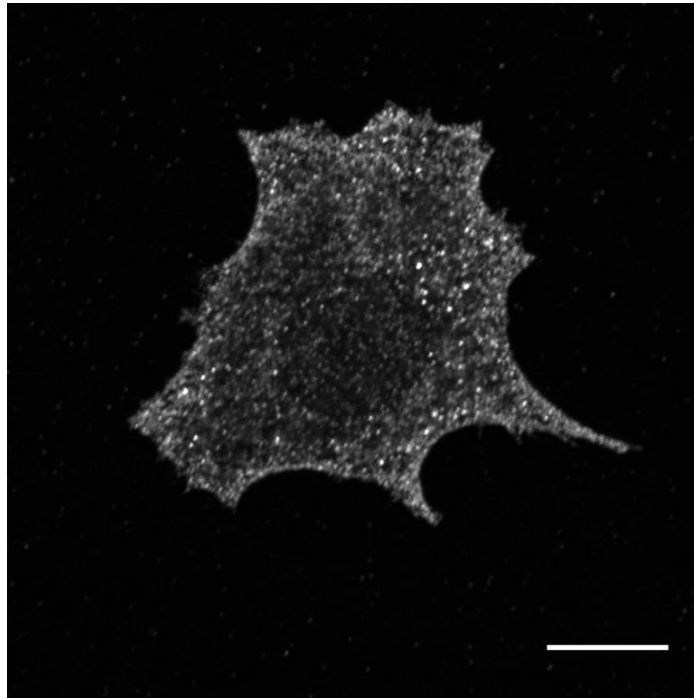


Figure 4.7. Representative confocal image of a MEF cell following 6 h CK666 treatment.

Staining for Tpm1.8/9 demonstrates that Tpm1.8/9 are not re-distributed to stress fibres. Scale bar = 10 μm .

Discussion

There is controversy in the literature about the organisation of the actin network at the leading edge. Some studies have reported the existence of two spatially segregated zones composed of Arp2/3-branched actin filaments at the cell edge, and unbranched filaments being contained immediately proximal to this zone (Iwasa & Mullins, 2007; Pollard & Borisy, 2003; Svitkina & Borisy, 1999; Svitkina et al., 1997; Vallotton & Small, 2009). Others have stated that these overlap and that both branched and unbranched filaments are present at the very leading edge (Small, 2015; Urban et al., 2010; Vinzenz et al., 2012).

Regulating the dynamics of two distinct actin networks

Due to the biochemical incompatibility of Arp2/3 and most Tpm, early reports suggested that Tpm was absent from the leading edge (Blanchoin, Pollard & Hitchcock-DeGregori, 2001; DesMarais et al., 2002). This model however does not take into account all possible isoforms of Tpm. It has since been proposed that two molecularly distinct actin networks overlap at the leading edge, and that persistent advancement of the cell relies on the underlying lamella rather than the lamellipodium (Lim et al., 2010; Ponti et al., 2004). This model is supported by the observations that cell migration is possible without a lamellipodium (Gupton et al., 2005) and that Arp2/3 is dispensable for chemotaxis (Wu et al., 2012). An important consideration however is an understanding of how multiple actin filament populations could co-exist in the same cellular region yet be differentially regulated.

Summary of Findings

In the previous chapter, it was demonstrated that Arp2/3 and Tpm1.8/9 associate with different actin filaments at the leading edge. In this chapter, it is demonstrated that

Tpm1.8/9 expression can be specifically silenced using an siRNA knockdown approach and that knockdown of Tpm1.8/9 results in an increase in both the peripheral localisation of Arp2/3 and its actin-branching activity. Together, these data suggest that Tpm1.8/9 play an inhibitory role protecting actin filaments from Arp2/3-mediated branching, providing regulation to the organisation of actin filaments within the lamellipodium. If unbranched actin filaments are indeed present at the leading edge alongside the branched Arp2/3 network, then these results present a logical mechanism for how these two distinct actin populations may be chemically insulated from one another, whilst occupying the same cellular structure.

A higher level of actin filament regulation

Inhibition of Arp2/3 using CK666 results in an increase in Tpm1.8/9 protein levels however, as shown in Figure 4.7, even at increased levels, Tpm1.8/9 is not enriched in stress fibres or at the cell periphery. This tells us two things, firstly that Tpm1.8/9, regardless of cytosolic concentration, has no affinity for the type of actin filaments found to occupy stress fibres (and therefore a more likely reason for the abnormal sorting seen with fluorescently tagged Tpm1.8/9 is due to direct interference of the tag itself, as discussed in chapter 3) and secondly, that something about Arp2/3 inhibition means the actin filaments at the cell periphery are no longer able to incorporate Tpm1.8/9. Perhaps, rather than Tpm1.8/9 and Arp2/3 simply engaging in a competition for actin filaments at the cell edge, it could be possible that Arp2/3 filaments are acquired first, and that these are subsequently re-modelled in order to be competent to incorporate Tpm1.8/9, which then functions to protect those actin filaments from further branching and perhaps even cofilin-mediated disassembly. In fact, it has recently been shown in vitro that severing of Arp2/3-generated actin networks by cofilin results in the generation of new pointed ends, to which the *Drosophila*-derived Tpm, Tm1A

preferentially binds and that these two sets of actin filaments; a Tpm-coated set and a Tpm-free set, that is competent to bind Arp2/3, can then be stably maintained in vitro because they are insulated from one another (Hsiao et al., 2015b). These findings point toward a potential mechanism of how branched actin filaments at the leading edge of cells may in fact be re-modelled to include Tpm.

The mechanisms underlying the generation of Tpm1.8/9-containing actin filaments will be explored in more detail in Chapter 6. The next chapter will look at the functional outcomes of Tpm1.8/9 knockdown on whole cell motility, leading edge dynamics and the formation and maturation of focal adhesions.

Chapter Five

**The effects of Tpm1.8/9
knockdown on cell motility,
lamellipodial persistence and
focal adhesions**

Chapter 5: The effects of Tpm1.8/9 knockdown on cell motility, lamellipodial persistence and focal adhesions

Introduction

Migration plays a vital role for most cells and is essential for processes such as immune response, wound healing or embryogenesis. This process is also dysregulated in metastatic disease. Metastatic disease is the leading cause of cancer-related mortality (Fidler, 2002). During the initial stages of metastasis, cancer cells migrate away from the primary tumour site through surrounding tissue and towards nearby vasculature and lymph vessels. Following successful invasion and migration, tumour cells progress to secondary sites and establish ectopic tumour growth. This results in a range of associated pathologies that ultimately lead to the death of the patient (Fidler, 2002; Poste & Fidler, 1980). Owing to the critical role of invasion and migration in metastasis, there has been considerable interest in targeting cancer cells' migration machinery as a novel therapeutic approach. However, it has become clear that cancer cells use a range of motility modes to migrate and invade (Friedl, 2004). Indeed the ability of cancer cells to switch between motility modes has likely contributed to the low efficacy of some anti-metastatic therapies (Coussens, Fingleton & Matrisian, 2002; Kruger et al., 2001).

Distinct individual cell motility modes, termed mesenchymal and amoeboid migration, have been revealed through the use of *in vivo* and three-dimensional (3D) collagen gel culture systems (Wolf et al., 2003). Mesenchymal migration is characterised by cell elongation and branching, polarised protrusions in the direction of migration. The chief properties that define mesenchymal migration include activation of the small GTPase Rac (Sanz-Moreno et al., 2008; Yamazaki, Kurisu & Takenawa, 2009) targeted

expression of matrix metalloproteases (Sahai & Marshall, 2003; Wolf et al., 2003) and the regulated formation and disassembly of integrin receptor-mediated extracellular matrix adhesions mediated by the activity of Src kinase (Carragher et al., 2006; Wolf et al., 2003). In contrast, amoeboid migration is characterised by rounded cell morphology and is associated with non-apoptotic plasma membrane blebbing (Sahai & Marshall, 2003). Rapid expansion and contraction allow amoeboid cells to squeeze through an obstructing matrix, and this is highly dependent on actomyosin contractility (Friedl & Wolf, 2010; Sahai & Marshall, 2003; Sanz-Moreno et al., 2008). The migration of amoeboid cells is facilitated by the RhoA GTPase effector molecule Rho-associated kinase (ROCK), independent of matrix metalloprotease activity and less dependent on integrin receptor adhesion to the extracellular matrix (Carragher et al., 2006; Friedl & Wolf, 2003).

Regardless of the form of cell migration, a complex mechanism must be strictly regulated. Many processes in substrate sensing, adhesion formation and generation of tracking forces are just some of the early events that need to be interactively combined to an overall working system (Geiger & Bershadsky, 2001; Geiger, Spatz & Bershadsky, 2009; Gupton & Waterman-Storer, 2006). Most eukaryotic cells migrate by using a motility cycle. During classic amoeboid cell migration, the motility cycle includes actin polymerisation-driven formation of a protrusion in the new direction of migration, attachment to the substratum, generation of traction force and retraction of the tail. These events are dependent on actomyosin-mediated contractile force production and the actin cytoskeleton, which is dynamic and undergoes repeated cycles of actin polymerisation and depolymerisation in a spatially and temporally coordinated pattern (Bravo-Cordero et al., 2013). Furthermore, the cytoskeleton has an essential role in establishing the internal cell architecture that controls cell migration. Other forms of

movement such as blebbing (Charras & Paluch, 2008) and rolling (Daubon et al., 2012) have been described, but the importance of actin polymerisation in these rare forms of motility is not well understood. Indeed, the involvement of tropomyosin in even the simplest types of cell motility has not yet been extensively studied. Therefore, this chapter presents a series of experiments using RNAi to elucidate the role of Tpm1.8/9 in lamellipodial dynamics, cell adhesion and migration in both two- and three-dimensions.

In the previous chapter, it was demonstrated that siRNA knockdown of Tpm1.8/9 resulted in elevated Arp2/3 activity, resulting in thicker lamellipodia. Due to the production of the lamellipodium being an important step in cell migration across a two-dimensional (2D) substratum and the apparent role for Tpm1.8/9 in regulating actin filaments within the lamellipodium, the next logical set of experiments was to measure a variety of parameters associated with cellular motility and compare these between Tpm1.8/9 and control siRNA-treated cells. Firstly, this chapter looks at the simple migration patterns exhibited by MEF cells moving randomly across a 2D surface coated with a thin layer of fibronectin, to more closely mimic a biological environment and enhance cell traction. Next, this chapter compares this to the cells' ability to move through a 3D matrix composed of collagen. It is well established that cells utilise differing motility phenotypes depending on whether they are moving in a two or three-dimensional way and also depending upon the composition of the extracellular matrix. This chapter then investigates the role of Tpm1.8/9 in the regulation of membrane dynamics at the cell edge. This is done by generating kymographs from movies of individual cells in order to derive parameters such as speed, distance and persistence of protrusions and retractions. Finally, this chapter examines the role of Tpm1.8/9 in the generation and maturation of focal adhesions by MEF cells on 2D, fibronectin coated

surfaces. This is done using various cell and adhesion morphometry techniques in fixed cells treated with either control or Tpm1.8/9 siRNA.

Results

Tpm1.8/9 knockdown affects random, 2D cell migration

To measure the effect of Tpm1.8/9 suppression on single cell migration, random cell motility was measured. Cells were seeded on fibronectin-coated glass fluorodishes and allowed to adhere before being imaged. Individual cells were then manually tracked to generate traces (five representative of which from each group are shown in Figure 5.1 A and B) from which measurements such as whole cell velocity and cell persistence (a measure of directionality, defined as vectoral distance between start and end points divided by total track length) can be calculated. Cells treated with Tpm1.8/9 siRNA had a significant reduction in the average velocity of migration ($0.28 \pm 0.01 \mu\text{m}/\text{min}$ in knockdown cells; $n = 74$, compared to $0.45 \pm 0.02 \mu\text{m}/\text{min}$ in control cells; $n = 79$, $p < 0.0001$) (Figure 5.1 C) coupled with a significant decrease in the directional persistence ratio (0.28 ± 0.02 in knockdown cells; $n = 74$, compared to 0.37 ± 0.03 in control cells; $n = 79$, $p < 0.05$) (Figure 5.1 D). These data suggest that Tpm1.8/9 play an important role in cell motility and also in the cells' ability to setup directional cues for effective movement. This assay however doesn't provide much mechanistic insight into the observed migration defect, nor does it provide information on whether these Tpm's are solely involved in cells which migrate using a lamellipodium, as is seen with MEFs in 2D or whether they play a role in cell movement in a 3D matrix.

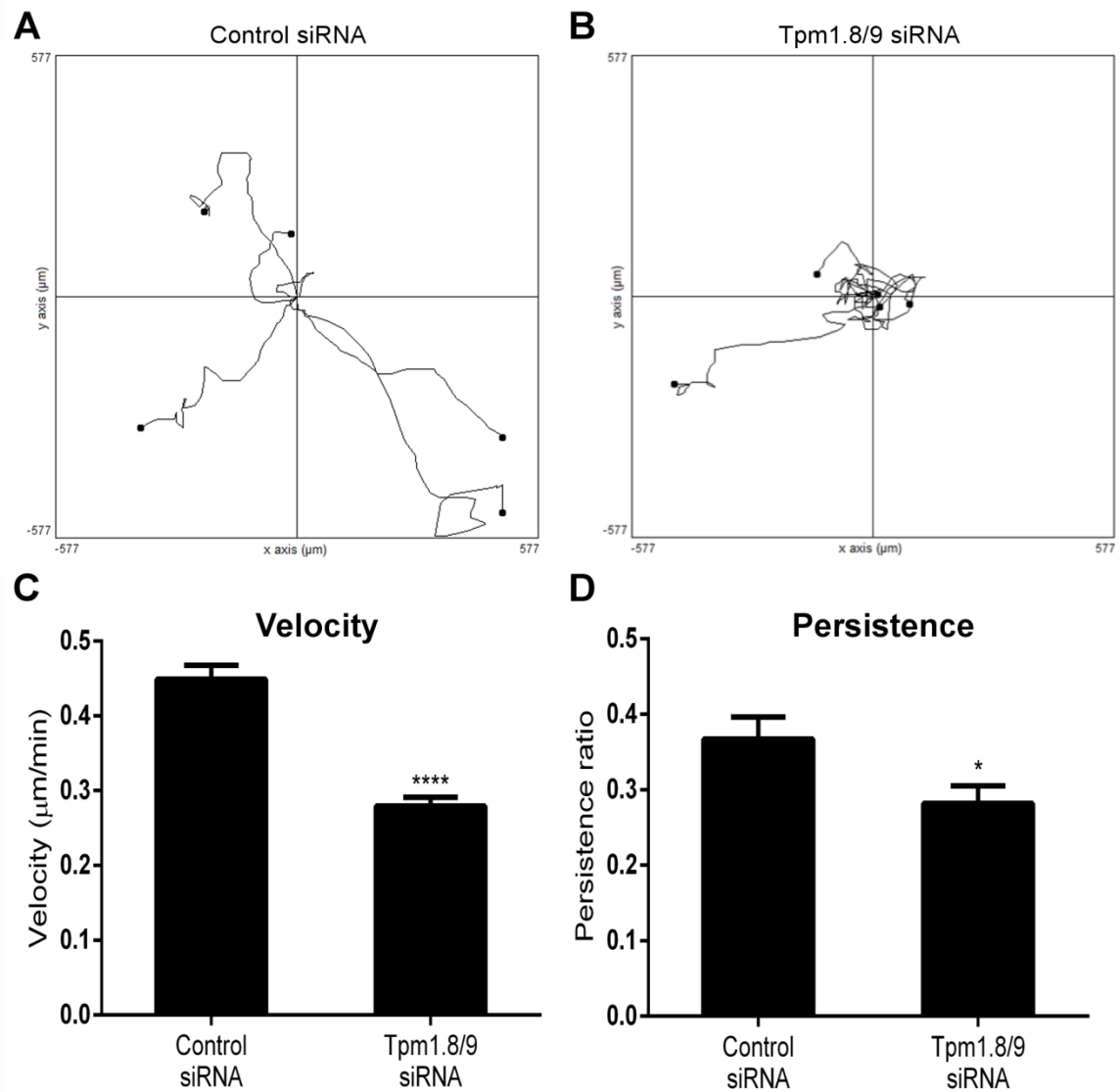


Figure 5.1. Tpm1.8/9 knockdown affects random cell migration.

(A and B) Random migration traces for control and Tpm1.8/9 siRNA-treated cells (five representative cells from each condition are shown).

(C and D) Histograms show average (control, $n = 79$ cells; Tpm1.8/9 siRNA, $n = 74$ cells) cell velocity and persistence ratio (vectoral distance over total distance travelled). Error bars = SEM; $n = 4$, * $p < 0.05$, **** $p < 0.0001$; Student's t-test.

Tpm1.8/9 knockdown does not affect 3D random cell migration

In order to investigate whether Tpm1.8/9 play a role in a cell's ability to migrate through a 3D matrix, the random migration assay described above was repeated with the exception that this time, prior to imaging, the cells were first embedded in a gel composed of Type I rat-tail collagen. Once set, imaging was carried out in the same manner as for the 2D assay, and cells were again manually tracked, and their average velocity in the x-y plane was calculated. Directionality in this case was not included as movement in the z direction could not be accounted for in this particular assay. Notably, cells moving through this environment exhibited a very different shape compared to those in 2D. Cells in this assay clearly adopted a mesenchymal motility phenotype with characteristic elongation and branching, polarised protrusions in the direction of migration (Figure 5.2 A). Secondly, no significant difference in cell velocity was measured between cells treated with control siRNA ($0.221 \pm 0.006 \mu\text{m}/\text{min}$; $n = 105$) and cells treated with Tpm1.8/9 siRNA ($0.21 \pm 0.01 \mu\text{m}/\text{min}$; $n = 142$) ($p = 0.38$) (Figure 5.2 B). This result suggests that Tpm1.8/9 may be specifically involved in the regulation of cell motility phenotypes that utilise the production of lamellipodia as their initial step and, as shown in Figure 5.2 A, cells moving through the 3D collagen matrix do not exhibit these cellular structures and instead appear to extend long, highly polarised protrusions. This result also provides further support to the findings reported in chapters 3 and 4 where Tpm1.8/9 are specifically recruited to lamellipodia

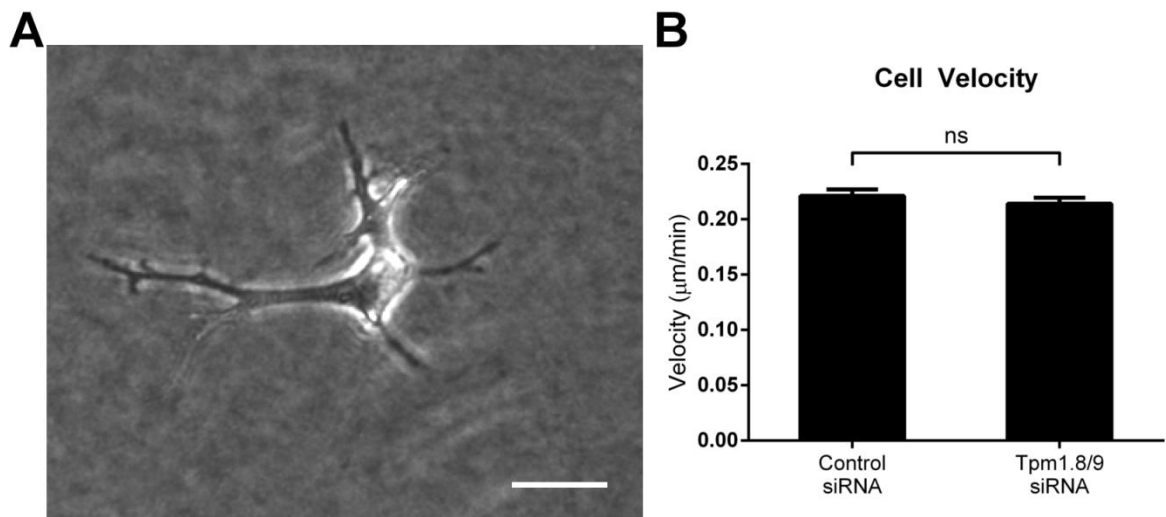


Figure 5.2. Tpm1.8/9 knockdown does not impact 3D random cell migration.

(A) Representative phase contrast image of a control siRNA-treated MEF cell migrating through a collagen gel matrix. Scale bar = 20 μm

(B) Histogram showing average (control, $n = 105$ cells; Tpm1.8/9 siRNA, $n = 142$ cells) cell velocity. Error bars = SEM; $n = 3$, ns = not statistically significant ($p > 0.05$); Student's t-test.

Tpm1.8/9 knockdown results in more dynamic, less persistent lamellipodia

To further investigate the observed deficit in 2D cell migration following the knockdown of Tpm1.8/9, leading edge dynamics was evaluated by the generation of kymographs from 10 min movies of active lamellipodia (Figure 5.3 A). Analysis of the resulting kymographs (Figure 5.3 B) revealed that protrusion velocity was significantly increased in Tpm1.8/9 siRNA-treated cells ($3.16 \pm 0.08 \mu\text{m}/\text{min}$) compared to control cells ($2.09 \pm 0.05 \mu\text{m}/\text{min}$, $p < 0.0001$) (Figure 5.3 C). This was coupled with a significant increase in retraction velocity in Tpm1.8/9 siRNA-treated cells ($3.93 \pm 0.12 \mu\text{m}/\text{min}$) compared to control cells ($2.79 \pm 0.14 \mu\text{m}/\text{min}$, $p < 0.0001$) (Figure 5.3 D). These observations are comparable to those previously reported where the leading edges of tropomyosin depleted *Drosophila* S2 cells were more dynamic than untreated cells and underwent rapid protrusion and retraction (Iwasa & Mullins, 2007).

Protrusion persistence, a measure of lamellipodial stability, was significantly reduced in Tpm1.8/9 siRNA-treated cells ($0.58 \pm 0.02 \text{ min}$) compared to control cells ($1.49 \pm 0.05 \text{ min}$, $p < 0.0001$) (Figure 5.3 E), as was average protrusion distance ($1.07 \pm 0.03 \mu\text{m}$ in Tpm1.8/9 knockdown cells compared to $2.22 \pm 0.06 \mu\text{m}$ in control cells, $p < 0.0001$) (Figure 5.3 F). Together, these results suggest that knockdown of Tpm1.8/9 results in lamellipodia that are more dynamic (i.e. protrude and retract faster, Figure 5.3 C and D respectively), but are, by some underlying mechanism relating either directly or indirectly to Tpm1.8/9, less stable, resulting in a reduction in the persistence and distance of protrusions (Figure 5.3 E and F respectively).

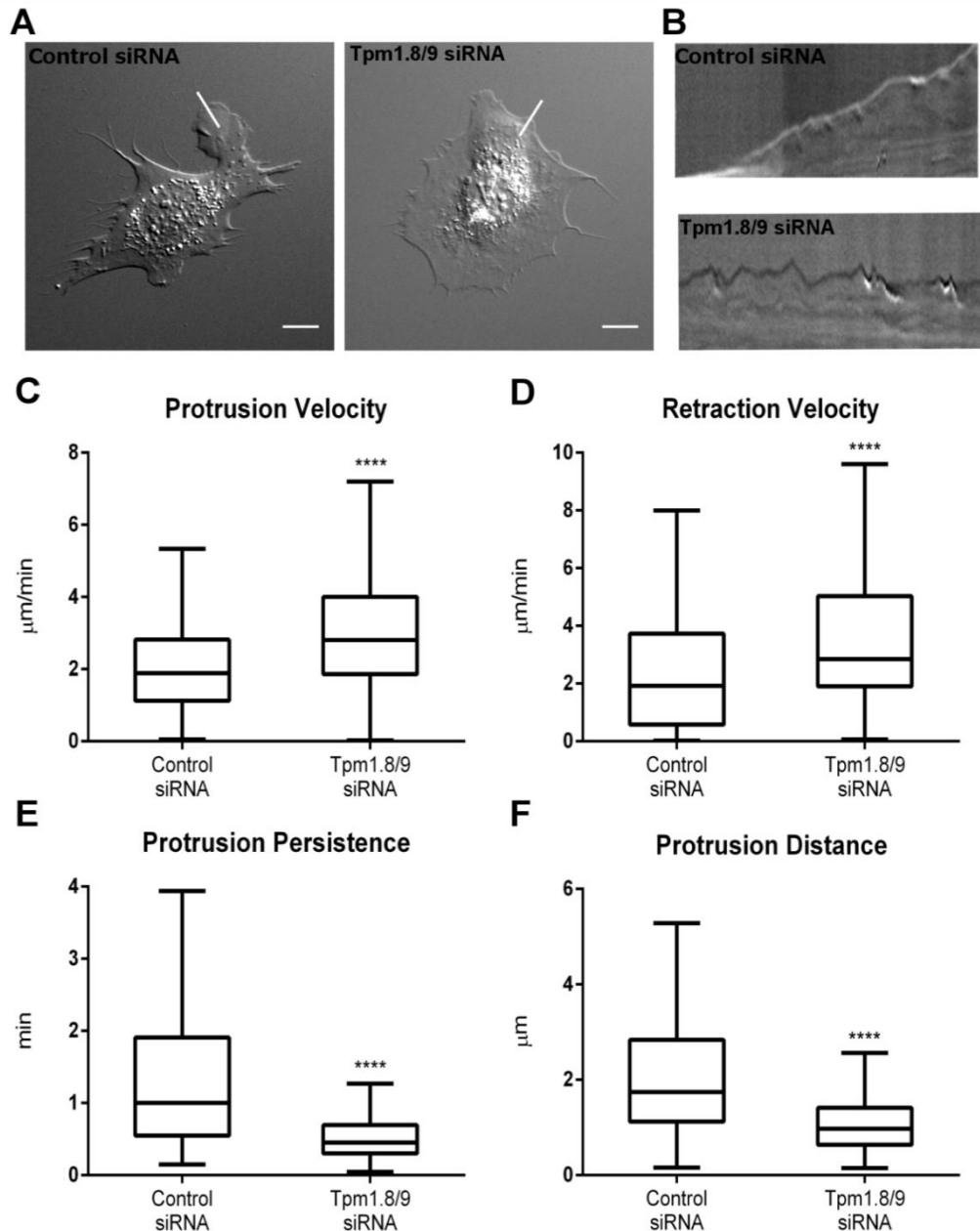


Figure 5.3. Impaired protrusion persistence in Tpm1.8/9 knockdown cells.

(A) Individual final frames from representative 10 min DIC movies of control and Tpm1.8/9 siRNA-treated cells. Lines indicate typical regions chosen to generate kymographs. Scale bars = 10 μm .

(B) Resulting kymographs show lamellipodial activity over 10 min along the lines in respective DIC images.

(C – F) Quantification of kymographs (control, $n = 228$ kymographs generated for 30 cells; Tpm1.8/9 siRNA, $n = 181$ kymographs generated for 23 cells) showing the velocity of protrusions (C), velocity of retractions (D), the persistence (E) and the distance (F) of protrusions. For Tukey box plots, whiskers indicate maximum and minimum values within 1.5 IQR, the box represents the 25th-75th quartile, and the line indicates the median. $n = 4$; **** $p < 0.0001$; Student's t-test.

Knockdown of Tpm1.8/9 results in the formation of fewer focal adhesions

It was postulated that the deficit in whole cell motility and lamellipodial persistence observed in the Tpm1.8/9 knockdown cells (Figures 5.2 and 5.3) may be due to a reduced ability of the cell to produce substratum adhesions as it is well established that lamellipodial dynamics and directional persistence are profoundly influenced by cell-substratum adhesions (Huttenlocher, Ginsberg & Horwitz, 1996; Ponti et al., 2004). To test this, control and Tpm1.8/9 siRNA-treated cells were allowed to adhere to fibronectin-coated glass coverslips before being fixed and immuno-stained for paxillin (Figure 5.4 A). Confocal images were then subjected to analysis to determine the average size and number of focal adhesions per cell. The knockdown of Tpm1.8/9 had no significant impact on the average size of the adhesions ($p = 0.32$; $n = 15$) (Figure 5.4 B), but a significant decrease in the average number of paxillin-based focal adhesions per cell was observed (77.47 ± 6.00 in control and 35.47 ± 3.05 in Tpm1.8/9 siRNA-treated cells, $p < 0.0001$; $n = 15$) (Figure 5.4 C). A comparable observation has previously been made in PtK1 epithelial cells overexpressing skeletal muscle Tpm, where a significant increase in paxillin detected adhesions were seen closer to the leading edge (Gupton et al., 2005). Collectively, these data suggested at first that assembly of focal adhesions at the leading edge requires Tpm and in particular the isoforms Tpm1.8/9. However it is important to note that focal adhesions begin life as nascent adhesions at the very leading edge of cells, and that these differ in size, shape and molecular composition from mature adhesions found deeper in the cell body. As this particular assay only addresses the total number of adhesions per cell, it was decided that a more sensitive assay would be required if the influence of Tpm1.8/9 on focal adhesion assembly were to be properly assessed. Furthermore, this assay did not allow for measurement of adhesions relative to area.

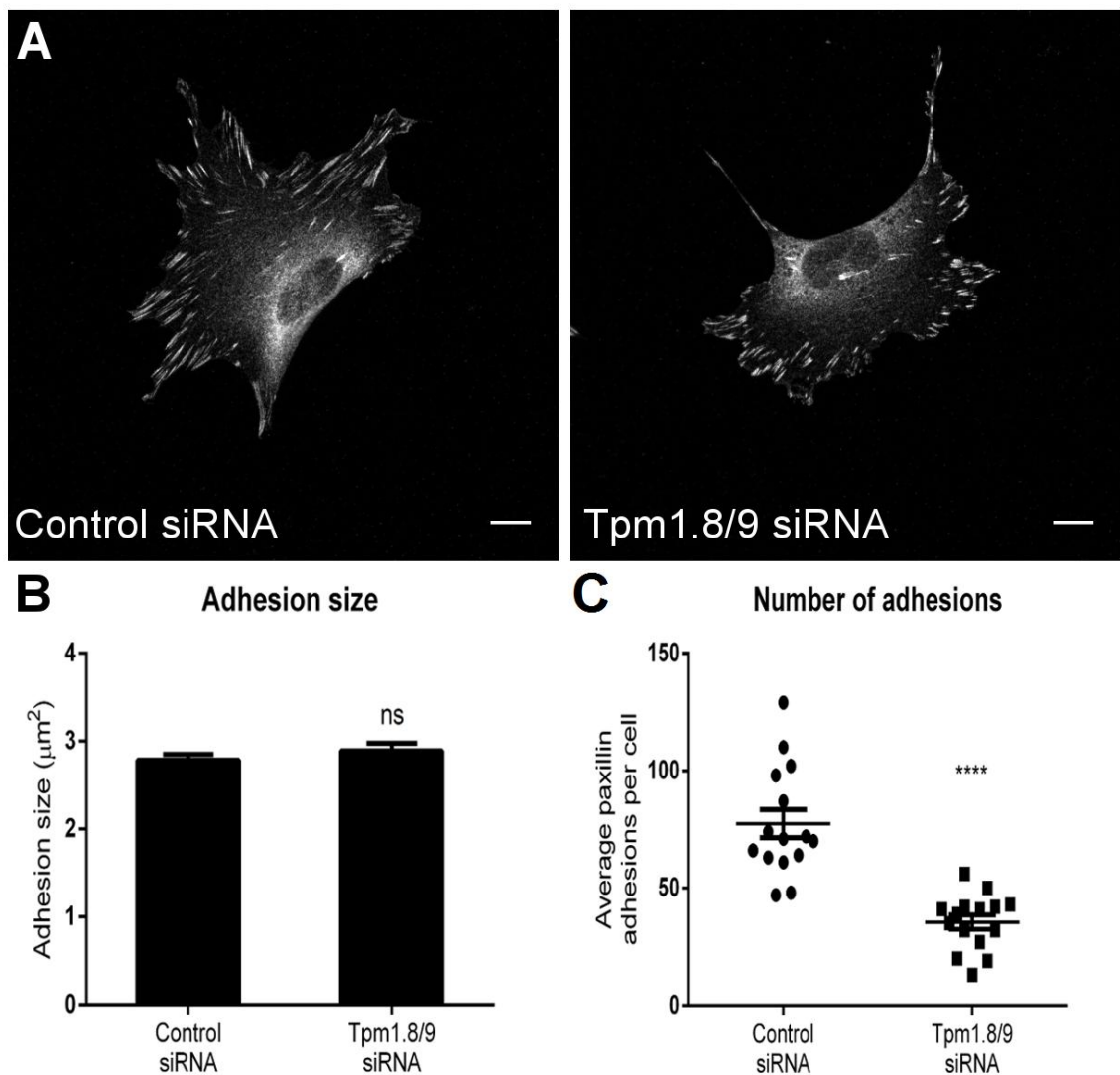


Figure 5.4. Knockdown of Tpm1.8/9 disrupts the formation of focal adhesions.

(A) Control or Tpm1.8/9 siRNA-treated cells were seeded on coverslips for 16 hr before being fixed and stained for paxillin. Scale Bars = 10 μm .

(B) Histogram showing the average size of paxillin-based focal adhesions in control and Tpm1.8/9 siRNA-treated cells. Error bars = SEM; $n = 15$ cells per group; ns = not statistically significant ($p < 0.05$); Student's t-test.

(C) Scatterplot showing the average number of paxillin-based focal adhesions in control and Tpm1.8/9 siRNA-treated cells. Error bars \pm SEM; $n = 15$ cells per group; **** $p < 0.0001$; Student's t-test.

Knockdown of Tpm1.8/9 disrupts the maturation of focal adhesions

In order to investigate the influence of Tpm1.8/9 on any differences between mature adhesions and the formation of nascent adhesions at the leading edge, the lamellipodium needs to be distinguished from the rest of the cell. To accomplish this, as was done previously, the Arp2/3 complex was used to demark the lamellipodium (Figure 3.3). Control and Tpm1.8/9 siRNA-treated cells were allowed to adhere to fibronectin-coated glass coverslips before being fixed and then co-stained for both Arp2 and paxillin. Acquired confocal images from both experimental groups were then subjected to the following image analysis technique: Firstly, in the Arp2 channel, a region of interest (ROI) was carefully drawn to encompass the clearly visible enrichment of Arp2 and hence the lamellipodium. This ROI was then transferred to the other image channel so that it now overlaid the lamellipodium in the paxillin channel. Thresholding was then performed so that the background was removed and only the adhesions were visible. The particles present within this ROI, representing nascent adhesions, were then analysed to determine their number (per μm^2) as well as their size and circularity. To measure mature adhesions, the same procedure was followed only the ROI was drawn to exclude the Arp2 enrichment and hence included all of the cell except for the lamellipodium. Particles detected within this region were therefore defined as mature adhesions.

The analysis of the paxillin-based adhesions of nine cells transfected with either control siRNA (Figure 5.5 A) or Tpm1.8/9 siRNA (Figure 5.5 B) showed that there was no significant difference in the average number of lamellipodial, nascent adhesions per μm^2 ($p = 0.95$) (Figure 5.5 C). In contrast however, Tpm1.8/9 siRNA-treated cells displayed significantly fewer mature adhesions (0.022 ± 0.004 per μm^2 ; $n = 9$) compared to control siRNA-treated cells (0.052 ± 0.002 per μm^2 ; $n = 9$) ($p < 0.0001$) (Figure 5.5 D).

This parallels the result presented in the previous assay whereby fewer total adhesions were measured per cell (Figure 5.4 C). No significant change was observed in the average size of either nascent adhesions ($p = 0.5525$) (Figure 5.5 E) or mature adhesions (Figure 5.5 F). This also corresponds to the results of the previous assay whereby no significant change to adhesion size was observed (Figure 5.4 B). Finally, it is well established that, as focal adhesions mature, their shape changes from small, round, dot-like structures (nascent adhesions) to large, elongated structures (mature focal adhesions) (Balaban et al., 2001; Galbraith, Yamada & Sheetz, 2002; Riveline et al., 2001). Therefore circularity can be used as a measure of adhesion maturity. Circularity was measured using the following equation where A = area; P = perimeter (Horzum, Ozdil & Pesen-Okvur, 2014):

$$circularity = \frac{4\pi A}{P^2}$$

While there was no significant change measured in the average circularity of nascent adhesions between control and Tpm1.8/9 knockdown cells ($p = 0.42$) (Figure 5.5 G), the mature adhesions of the Tpm1.8/9 siRNA-treated cells were significantly more circular (less elongated) (0.26 ± 0.01) compared to the control siRNA-treated cells (0.20 ± 0.01) (Figure 5.5 H).

Together, these data suggest that, whilst not required for the initiation of nascent adhesion formation, Tpm1.8/9-actin filaments are required at the leading edge to facilitate the maturation of nascent adhesions into mature focal adhesions via a mechanism that as yet remains unclear.

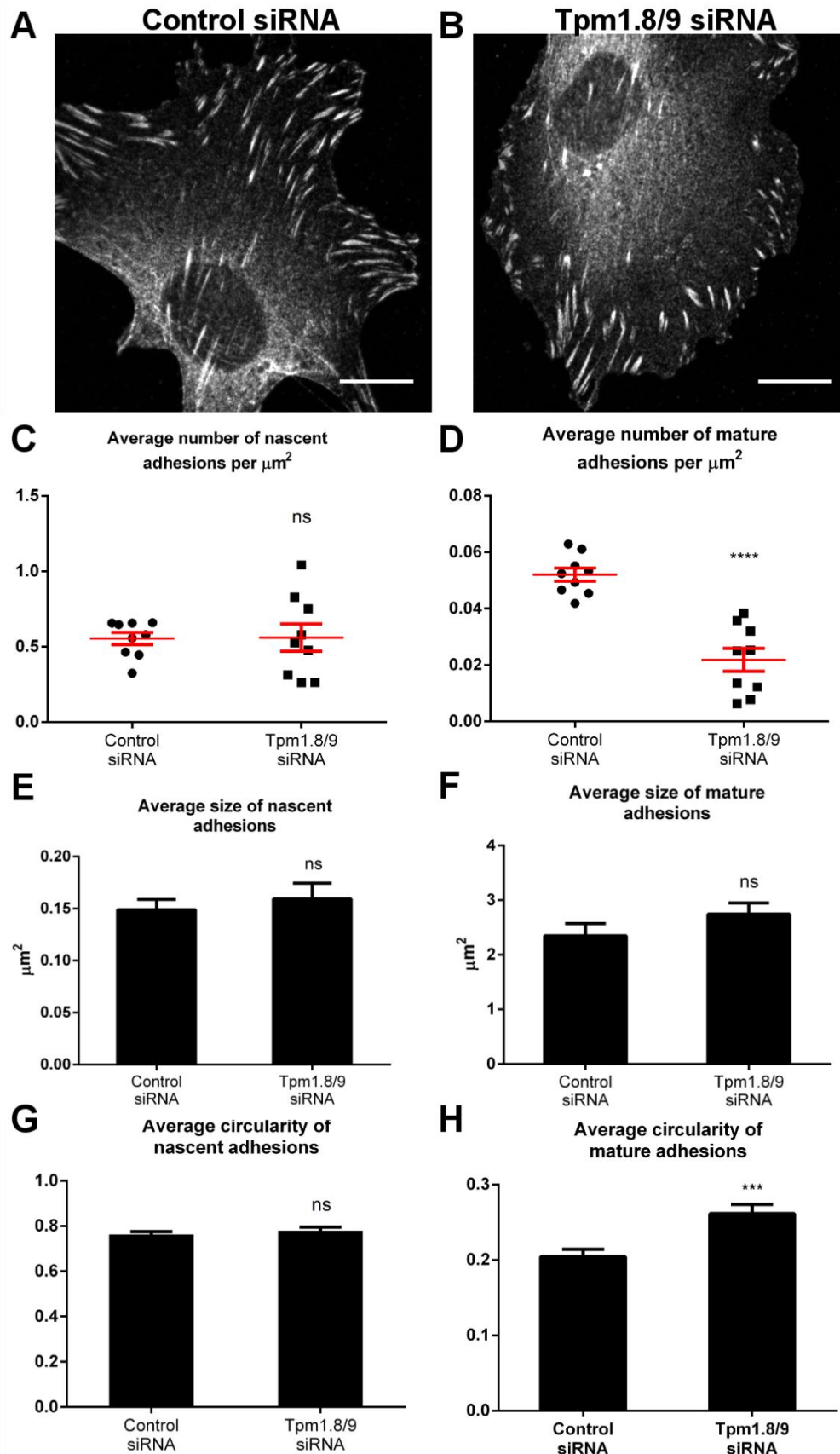


Figure 5.5. (Legend on next page)

Figure 5.5 (previous page). Knockdown of Tpm1.8/9 disrupts the maturation of focal adhesions.

(A and B) Representative confocal images of MEF cells stained for paxillin following transfection with either control (A) or Tpm1.8/9 siRNA (B). Scale bars = 10 μ m.

(C and D) Scatterplots showing the average number of nascent (C) and mature (D) paxillin-based focal adhesions per μ m². Error bars \pm SEM; n = 9 cells per group; ns = not statistically significant ($p > 0.05$); **** $p < 0.0001$; Student's t-test.

(E and F) Histograms showing the average size of nascent (E) and mature (F) paxillin-based focal adhesions. Error bars = SEM; n = 9 cells per group; ns = not statistically significant ($p > 0.05$); Student's t-test.

(G and H) Histograms showing the average circularity of nascent (G) and mature (H) paxillin-based focal adhesions. Error bars = SEM; n = 9 cells per group; ns = not statistically significant ($p > 0.05$); *** $p < 0.001$; Student's t-test.

Discussion

Migration is a widely studied function in cells due to its involvement in cancer metastasis and subsequent increased mortality associated with various types of cancer (Fidler, 2002; Poste & Fidler, 1980). Cytoskeletal tropomyosins in cell migration are much less well studied but potentially represent a point for chemotherapeutic intervention in metastatic disease. Lamellipodia are characteristic protrusions associated with cell motility which, up until the present study, have largely been thought to be tropomyosin-free. This is a likely contributing factor for the lack of experimental data in the literature surrounding the role of cytoskeletal tropomyosins in regulating cellular motility. In previous chapters, it was established that the non-muscle Tpm isoforms Tpm1.8/9 are indeed enriched in the lamellipodium of mouse embryonic fibroblasts where they regulate Arp2/3 activity. The main premise of this chapter is to explore what role these Tpm's play in regulating the various modalities of cell motility by examining the functional outcomes of their knockdown in various assays.

Summary of findings

In this chapter, it is demonstrated that Tpm1.8/9 play a role in regulating focal adhesion maturation, lamellipodial persistence and migration speed across a 2D fibronectin-coated substratum. While all three of these processes suffered a significant defect following siRNA-directed knockdown, cells moving through a 3D, collagen gel were unaffected. Furthermore, cells moving in 3D clearly exhibit a more elongated shape and lack lamellipodia, suggesting that cells moving in this type of environment do so with a different phenotype that does not rely heavily on Tpm1.8/9. This result further serves to suggest that Tpm1.8/9 are proteins specifically involved in regulating the lamellipodium.

Relationship between lamellipodial persistence and whole-cell motility

Despite an incomplete reduction in Tpm1.8/9 expression (79.5 ± 2.1 %, Figure 4.1 B), numerous cellular processes crucial in mediating migration are severely affected. A clear example of this is the initiation of motility, as seen from the random migration assay whereby cells are allowed to migrate without the influence of external chemotactic stimuli. Tpm1.8/9 knockdown severely affected their overall speed and directional persistence. This lack of migration efficiency is likely due to several factors including effects on the ability of the lamellipodium to protrude persistently.

Analysis of the kymographs generated from movies taken of individual protrusions revealed a dramatic increase in the speed of protrusions and retractions following Tpm1.8/9 knockdown. It is important to remember from chapter 4 that Tpm1.8/9 knockdown results in an increase in Arp2/3 activity. Therefore, rather than a defect in the formation of protrusions, which is driven by Arp2/3, Tpm1.8/9 knockdown cells successfully generate protrusions, which rapidly extend, but then quickly retract again. The defect therefore, appears to lie in the stability of these lamellipodial protrusions. This is supported by the accompanying reduction in the persistence and overall distance of protrusions which again suggests that lamellipodial stability is affected by Tpm1.8/9 knockdown. One possible explanation for why Tpm1.8/9 are required for lamellipodial persistence may be that persistence of lamellipodia relies on effective generation of adhesions to the substratum.

Relationship between efficiency of focal adhesion production and lamellipodial persistence

A logical necessity for lamellipodial persistence is that, in a series of highly temporally-regulated events; Arp2/3 drives the initial membrane protrusion then, some form of

adhesion to the underlying substratum must occur or else it immediately retracts, either passively or via active depolymerisation of the protrusive actin filaments. The fact that Tpm1.8/9-deficient cells suffer a defect in lamellipodial persistence suggests that Tpm1.8/9-coated actin filaments must in some way play a role in the formation of substratum adhesions. Indeed, staining of whole cells for paxillin reveals that Tpm1.8/9 knockdown cells do possess fewer substratum adhesions overall.

Upon closer assessment of this data however, one arrives at the question of whether there is a direct relationship between Tpm1.8/9 actin filaments and paxillin recruitment itself, or rather if simply stabilising individual actin filaments by inhibiting excessive branching and severing (which would surely result in the overly dynamic structures described in Figure 5.3) would be sufficient to affect a downstream response, namely more mature focal adhesions.

Given that Tpm1.8/9 staining shows that these isoforms are really only present at the very leading edge, it is difficult to imagine a way in which these Tpm1.8/9s could be directly influencing paxillin-rich structures several tens of microns away in the trailing lamella. Therefore the latter supposition seems to be more probable, such that the role of Tpm1.8/9 is to stabilise actin filaments of the protruding lamellipodium long enough that proper adhesion to the underlying substratum can occur before retraction takes place.

Relationship between Tpm1.8/9 and focal adhesion maturation

Finally, it is demonstrated in Figure 5.5 that there is no significant loss in the formation of nascent adhesions in the Tpm1.8/9 knockdown cells. This further suggests that Tpm1.8/9 are not directly involved in the recruitment of paxillin. Instead, it appears that that early, paxillin-based contacts still begin to form in the absence of Tpm1.8/9.

However, as the observation that fewer mature adhesions exist in these cells suggests, the deficit lies in the ability of these early complexes to turn over and become bona-fide focal adhesions. Further support of this suggestion lies in the shape measurements of the mature focal adhesions which were significantly less elongated, a well-established measure of focal adhesion maturity.

Together these data suggest that, following initiation by Arp2/3, Tpm1.8/9 are recruited to the leading edge to stabilise the actin network so that these actin filaments may facilitate maturation of early focal complexes into mature focal adhesions to drive lamellipodial-based cell motility. The exact mechanisms underlying this process remain unclear, but there is evidence that the actin bundling protein, α -actinin orchestrates the maturation of nascent adhesions (Beningo et al., 2001; Choi et al., 2008; Schäfer et al., 2010; Zaidel-Bar et al., 2003). At this stage, one can only speculate as to whether Tpm1.8/9-coated actin filaments play a direct role in the recruitment of α -actinin (or some other actin bundling or cross-linking protein) as an intermediary for subsequent adhesion maturation. With ever increasing advancement in single molecule and super-resolution microscopy techniques, the answer is likely on the horizon.

One important question that remains, is how the actin network at the leading edge is organised. As shown in chapter 3, Arp2/3 and Tpm1.8/9 occupy different actin filament populations within the lamellipodium. If Arp2/3 initialises the branched actin network within the lamellipodium, and Tpm1.8/9 are required for stabilisation of lamellipodia, then what exactly is the mechanism behind how these Tpm1.8/9-actin filaments come to be? This will be the focus of the next chapter.

Chapter Six

Mechanistic insight into the generation of Tpm1.8/9 actin filaments in the lamellipodium

Chapter 6: Mechanistic insight into the generation of Tpm1.8/9 actin filaments in the lamellipodium

Introduction

In previous chapters, this thesis has reported that the Tpm isoforms 1.8/9 are enriched in the lamellipodium of fibroblasts as detected with a novel isoform-specific monoclonal antibody. RNAi-mediated silencing of Tpm1.8/9 leads to an increase of Arp2/3 accumulation at the cell periphery and a decrease in the persistence of lamellipodia and cell motility, a phenotype consistent with cortactin and coronin 1B-deficient cells (Bryce et al., 2005; Cai et al., 2007). An important question therefore remains. What is the relationship between Tpm1.8/9, cortactin, and coronin 1B at the leading edge and how do these proteins collaborate with the Arp2/3 complex to enhance lamellipodial persistence?

As mentioned earlier, there is controversy in the literature about the organisation of the actin network at the leading edge. Some studies have reported the existence of two spatially segregated zones composed of Arp2/3-branched filaments at the cell edge, and unbranched filaments immediately proximal to this zone (Iwasa & Mullins, 2007; Pollard & Borisy, 2003; Svitkina & Borisy, 1999; Svitkina et al., 1997; Vallotton & Small, 2009). Others have stated that these overlap and that both branched and unbranched filaments are present at the very leading edge (Small, 2015; Urban et al., 2010; Vinzenz et al., 2012). The formation of a linear array of actin filaments at the leading edge would need to be governed by a precise sequence of appearance of other actin binding proteins following activation of the Arp2/3 complex. The focus of this chapter will be to investigate Arp2/3, cortactin, coronin 1B, cofilin and Tpm1.8/9 in this

sequence of events and how these proteins collaborate to ultimately give rise to an actin network that is both protrusive, yet stable enough to provide persistent lamelleipodial advancement. First, a brief outline of what is known about the relationships of these leading edge proteins will be provided followed by the outcomes of the final set of experiments of this thesis and finally, a discussion which will examine these findings in the context of the literature.

Cortactin

Activation of the Arp2/3 complex occurs in response to various signals, including growth factors, Src family kinases, and Rho GTPases, and is mediated by direct binding of nucleation-promoting factors (NPFs) (Pollard & Borisy, 2003). Members of the Wiskott Aldrich Syndrome protein (WASp) family are the best-characterised NPFs (Millard, Sharp & Machesky, 2004). A less well understood activator of Arp2/3 complex is cortactin, known to bind and activate Arp2/3 complex in vitro (Urano et al., 2001; Weaver et al., 2001; Weed et al., 2000). Cortactin activates Arp2/3 complex via a mechanism involving interactions with F-actin (Urano et al., 2001; Weaver et al., 2001), whereas WASps interact with G-actin (Millard, Sharp & Machesky, 2004). Cortactin also enhances N-WASp activation of Arp2/3 complex in pyrene-actin-polymerisation assays (Urano et al., 2001; Weaver et al., 2001) and stabilises Arp2/3-nucleated branched-actin networks in vitro by inhibiting debranching (Weaver et al., 2001).

A role for cortactin in regulating actin branching is further substantiated by its cellular localisation to dynamic actin assembly sites such as lamellipodia (Daly, 2004). Notably, unlike WASp proteins that localise primarily on membranes, cortactin is more directly localised to cytosolic dynamic actin (Daly, 2004; Millard, Sharp & Machesky, 2004; Zettl & Way, 2001). Cortactin binds Arp2/3 complex via an N-terminal acidic domain,

homologous to that of WASp proteins, and it binds to actin filaments (F-actin) via a tandem-repeats domain (Weed et al., 2000). Under certain circumstances, cortactin and N-WASp can bind simultaneously to Arp2/3 complex, accounting for their synergy in activation of actin assembly. The interaction of cortactin with Arp2/3 does not inhibit Arp2/3 activation by N-WASp, despite competition for a common binding site located on the Arp3 subunit (Weaver et al., 2002; Weaver et al., 2001).

Finally, cortactin has been shown to promote cell motility by selectively enhancing lamellipodial persistence and adhesion assembly, at least in part through interactions with the Arp2/3 complex and actin filaments (Bryce et al., 2005).

Coronin 1B and cofilin

Coronins are highly-conserved F-actin binding proteins (Utrecht & Bear, 2006). Functional studies in *Dicytostelium* amoeba, fibroblasts and thymocytes indicate that coronins play an important role in lamellipodial protrusion, whole-cell motility and chemotaxis (Cai et al., 2005; de Hostos et al., 1993; Foger et al., 2006; Mishima & Nishida, 1999). Mammalian coronin 1B is ubiquitously expressed and localises to the leading edge of migrating fibroblasts (Cai et al., 2005; Mishima & Nishida, 1999). The interaction of coronin 1B with the Arp2/3 complex is regulated by phosphorylation of Serine 2 via PKC, where phosphorylation of Ser2 reduces the interaction with Arp2/3 and diminishes cell motility (Cai et al., 2005; Foger et al., 2006).

Cofilin controls actin filament turnover at the leading edge and at other cellular locations (Bamburg, 1999). Mechanistically, cofilin severs and potentially enhances depolymerisation of filaments by cooperatively binding along the sides of actin filaments and inducing conformational changes in filament structure (Bamburg, McGough & Ono, 1999). *In vivo*, cofilin regulates the dynamics of actin-based

structures such as stress fibres, dendritic spines and lamellipodia (Dawe et al., 2003; Hotulainen et al., 2005).

The activity of cofilin is regulated in a variety of ways including phosphorylation, PIP2 binding, intracellular pH changes and interactions with binding partners such as AIP1 (Bamburg, 1999). Phosphorylation of cofilin-serine 3 by LIM Kinase leads to decreased F-actin binding and inactivation of cofilin (Stanyon & Bernard, 1999). Dephosphorylation of Serine 3 on cofilin enhances F-actin binding and activates its severing/depolymerisation activity (Agnew, Minamide & Bamburg, 1995). Two classes of phosphatases act on cofilin; Chronophin and the Slingshots (Huang, DerMardirossian & Bokoch, 2006). Chronophin, is a Serine phosphatase that plays an important role in cytokinesis (Gohla, Birkenfeld & Bokoch, 2005). Slingshot is a family of atypical Serine/Threonine protein phosphatases that in mammals includes Slingshot-1, -2 and -3 (Niwa et al., 2002; Ohta et al., 2003). The long isoform of Slingshot-1 (SSH1L) functions during chemotaxis of hematopoietic cells (Nishita et al., 2005).

Considerable evidence suggests that the activities of Arp2/3 complex and cofilin are coordinately regulated at the leading edge of motile cells. Early studies using correlative microscopy suggested a model for actin assembly and turnover within lamellipodia in which Arp2/3-dependent filament nucleation at the front of lamellipodia was balanced by cofilin-dependent depolymerisation at the rear (Svitkina & Borisy, 1999). More recent studies using quantitative fluorescence speckle microscopy in epithelial cells suggested that Arp2/3 complex and cofilin activities within lamellipodia may be coupled (Ponti et al., 2005). A molecular connection has since been described between the Arp2/3 complex and cofilin activities at the leading edge of motile cells whereby coronin 1B influences cofilin activity via a SSH1L-dependent mechanism to drive the

turnover of branched filaments to establish a new network of F-actin (Cai et al., 2008; Cai et al., 2007).

Finally, it has recently been shown in a cell-free system that cofilin-mediated severing of Arp2/3 actin networks results in the generation of new pointed ends to which the *Drosophila* derived tropomyosin Tm1A can bind (Hsiao et al., 2015a). The findings of this study point toward a potential mechanism of how branched actin filaments at the leading edge may in fact be re-modelled in cells to include Tpm. The focus of this chapter therefore is how coronin 1B and its downstream effector cofilin are involved in the remodelling of Arp2/3-actin networks in MEF cells to include Tpm1.8/9.

Results

Arp2/3 and cortactin occupy newly formed lamellipodia, whereas coronin 1B and Tpm1.8/9 recruitment is delayed

The formation of a linear array of actin filaments at the leading edge must be governed by the precise sequence in the appearance of actin binding proteins following activation of the Arp2/3 complex. Cortactin and coronin 1B cooperate to drive the turnover of branched filaments to establish a new network of F-actin at the leading edge (Cai et al., 2008; Cai et al., 2007; Hsiao et al., 2015a; Weaver et al., 2001). To determine whether Tpm1.8/9-containing actin filaments are implicated in the formation of this F-actin network, the Arp2/3 inhibitor CK666 was used to abolish the lamellipodium. Upon washout of the inhibitor, Arp2/3 activity is rapidly restored and formation of new lamellipodia can be synchronised (Liu et al., 2013; Nolen et al., 2009). Cells are then fixed at specific time points following washout of the inhibitor, and stained using antibodies against candidate proteins. Cells are then scored according to the incidence of enrichment of each candidate protein along the leading edge of these newly-formed

lamellipodia. After 5 seconds of washout of the inhibitor, Arp2 staining can be seen at the very tips of newly formed lamellipodia (Figure 6.1 A). This is consistent with the well established role of Arp2/3 in the initiation of lamellipodia (Bailly et al., 1999; Gupton et al., 2005; Kis-Bicskei et al., 2013b; Wu et al., 2012). Strikingly, Tpm1.8/9 is absent from these structures at this early timepoint (Figure 6.1 A). However, after 30 seconds, some enrichment of Tpm1.8/9 is clearly visible at the periphery of cells (Figure 6.1 B). The time course of appearance of other actin binding proteins was also examined (Figure 6.1 C). Cortactin is rapidly recruited following the re-activation of Arp2/3 although not quite to the same extent as Arp2. This is also consistent with the role of cortactin in the stabilisation of Arp2/3-nucleated actin filaments at the leading edge (Bryce et al., 2005; Weaver et al., 2001). In contrast, significantly fewer cells displayed coronin 1B enrichment at the leading edge at 5 or 10 seconds after CK666 washout, with enrichment seen in the majority of cells after 30 seconds of washout. Collectively, these data indicate that coronin 1B and Tpm1.8/9, while not essential for initiation of lamellipodial protrusion, may play a role in the maintenance and persistence of lamellipodia by generating and stabilising the F-actin network. Finally cofilin, which is present fairly homogeneously throughout the cell, including the lamellipodium, in both migrating and non-migrating fibroblasts (Dawe et al., 2003), was enriched at the very earliest of timepoints closely following that of Arp2/3. Cofilin is activated via dephosphorylation by protein phosphatase slingshot homolog 1 (SSH1L) which is directed to the lamellipodium by coronin 1B (Cai et al., 2007). It is therefore likely that, although cofilin is present in early lamellipodia, it is not until the later recruitment of coronin 1B/SSH1L that cofilin is activated, and begins severing the Arp2/3 network, as has been described in a cell-free system (Hsiao et al., 2015a).

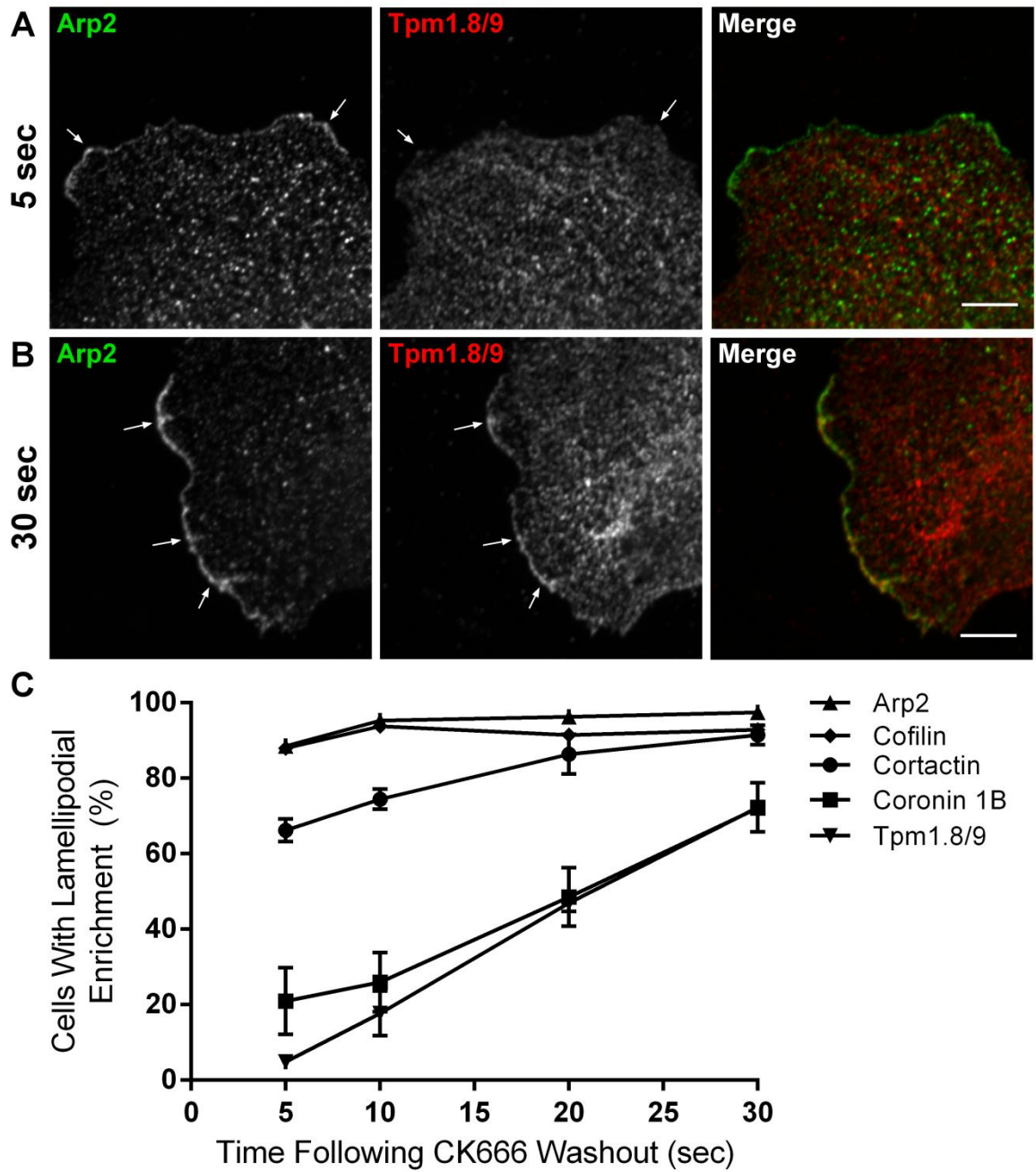


Figure 6.1. (legend on following page)

Figure 6.1 (previous page). Sequence of appearance of other actin binding proteins following activation of the Arp2/3 complex.

Cells were treated with the Arp2/3 inhibitor CK666 at 150 μ M for 3 hr, the inhibitor was then washed out and cells fixed at 5, 10, 20 or 30 sec.

(A) Representative confocal image of a newly formed lamellipodium in a MEF cell (3 x magnification), co-stained for Arp2 (green) and Tpm1.8/9 (red) at 5 seconds following washout of CK666. Scale bar = 5 μ m.

(B) Representative confocal image of a newly formed lamellipodium in a MEF cell (3 x magnification), co-stained for Arp2 (green) and Tpm1.8/9 (red) at 30 seconds following washout of CK666. Scale bar = 5 μ m.

(C) Quantitation shown as a percentage of cells displaying lamellipodial enrichment of the relevant protein at the various time-points following drug washout; Error bars \pm SEM; n > 100 cells per antibody per time-point. n = 3.

Cortactin knockdown does not affect Tpm1.8/9 localisation or protein levels

The next aim was to determine which of the candidate proteins from the previous assay were required for the recruitment of Tpm1.8/9 to newly-formed lamellipodia. The first candidate chosen was cortactin due to previous studies reporting similar motility defects in seen cortactin-deficient cells (Bryce et al., 2005). Firstly, we selected a siRNA sequence previously shown to knockdown cortactin (Bryce et al., 2005). Western blot of MEF lysates treated with this siRNA sequence were shown to exhibit successful knockdown of cortactin protein compared to control, as probed with the anti-cortactin antibody along with α -tubulin as a loading control (Figure 6.2 A). Next, to determine if cortactin knockdown had any effect on Tpm1.8/9 protein levels, cell lysates treated with cortactin siRNA were probed with the α /1b antibody (Figure 6.2 B). Densitometry from triplicate repeats revealed that there was no significant change to the protein expression of Tpm1.8/9 in the cortactin knockdown cells compared to control ($p = 0.0785$) (Figure 6.2 D). Finally, due to the earlier observation that cortactin is recruited to the leading edge significantly earlier than Tpm1.8/9, it was hypothesised that cortactin may be required for Tpm1.8/9 recruitment to the lamellipodium. To test this, control and cortactin siRNA-treated cells were stained using the α /1b antibody, and examined for lamellipodial enrichment of Tpm1.8/9 (Figure 6.2 C). It was observed that both control and cortactin siRNA-treated cells exhibited strong lamellipodial Tpm1.8/9 staining, suggesting that cortactin is not required for Tpm1.8/9 recruitment into lamellipodia. This was confirmed quantitatively by scoring the cells from each group and calculating the percentage of cells which displayed lamellipodial enrichment of Tpm1.8/9. It was found that there was no statistically significant difference in the number of cells which displayed lamellipodial enrichment of Tpm1.8/9 between control and cortactin siRNA-treated cells ($p = 0.7828$) (Figure 6.2 E).

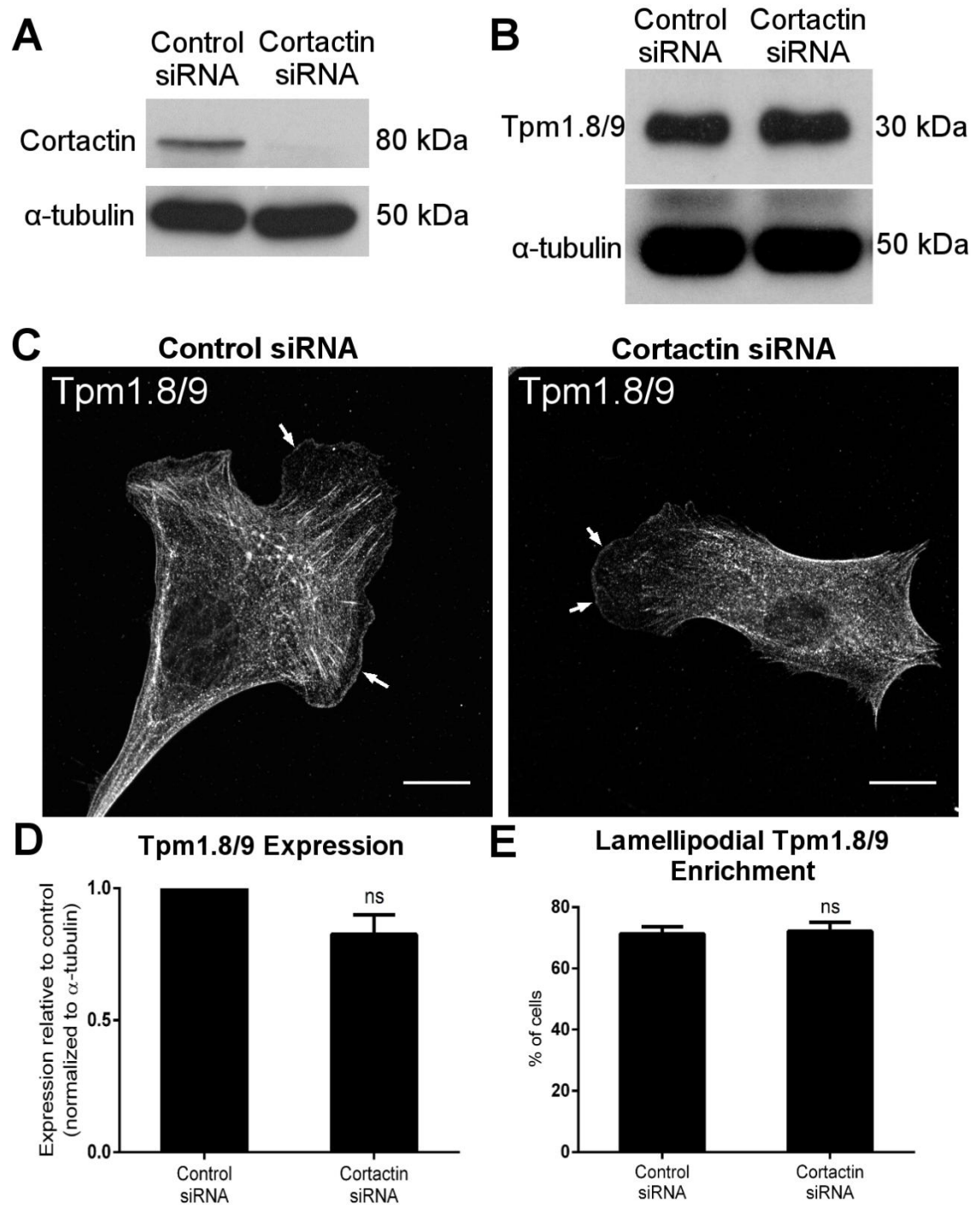


Figure 6.2. (legend on following page)

Figure 6.2 (previous page). Cortactin knockdown has no significant impact on the localisation or expression levels of Tpm1.8/9

(A) Western blot analysis of MEF lysates 48 hr post transfection with either control or cortactin siRNA, probed with the anti-cortactin and anti- α -tubulin antibodies.

(B) Western blot analysis of MEF lysates 48 hr post transfection with either control or cortactin siRNA, probed with α /1b and anti- α -tubulin antibodies.

(C) Representative confocal images of MEFs 48 hr post transfection with either control or cortactin siRNA, immunofluorescently stained with the α /1b antibody. Arrows indicate Tpm1.8/9 enrichment in the lamellipodium. Scale bars = 10 μ m.

(D) Relative protein levels were determined by densitometry from triplicate repeats normalised to α -tubulin and are represented in the histogram. Error bars = SEM; ns = no significant difference; Student's t-test.

(E) Quantification as a percentage of cells which display Tpm1.8/9 enrichment in lamellipodia. n > 200 cells per condition. Error bars = SEM; ns = no significant difference; Student's t-test.

Tpm1.8/9 is depleted from the leading edge following knockdown of coronin 1B or cofilin

Because of the co-recruitment of Tpm1.8/9 and coronin 1B observed in newly formed lamellipodia (Figure 6.1 C), it was postulated that coronin 1B and/or active cofilin may be required for Tpm1.8/9 targeting to lamellipodial actin filaments. To test this we used siRNA sequences previously shown to knockdown coronin 1B (Cai et al., 2007) or its downstream effector cofilin (Commercially available Silencer[®]Select Pre-Designed siRNA ID: s63901, Ambion, Carlsbad, CA). First, to test the coronin 1B siRNA sequence, lysates from MEFs treated with control or coronin 1B siRNA were probed with the anti-coronin 1B antibody along with anti-GAPDH as a loading control. Western blot of MEF lysates treated with this siRNA sequence were shown to exhibit successful knockdown of coronin 1B protein compared to control (Figure 6.3 A). Next, to test the cofilin siRNA sequence, lysates from MEFs treated with control or cofilin siRNA were probed with the anti-cofilin antibody along with anti- α -tubulin as a loading control. Western blot of MEF lysates treated with this siRNA sequence were shown to exhibit successful knockdown of cofilin protein compared to control (Figure 6.3 B).

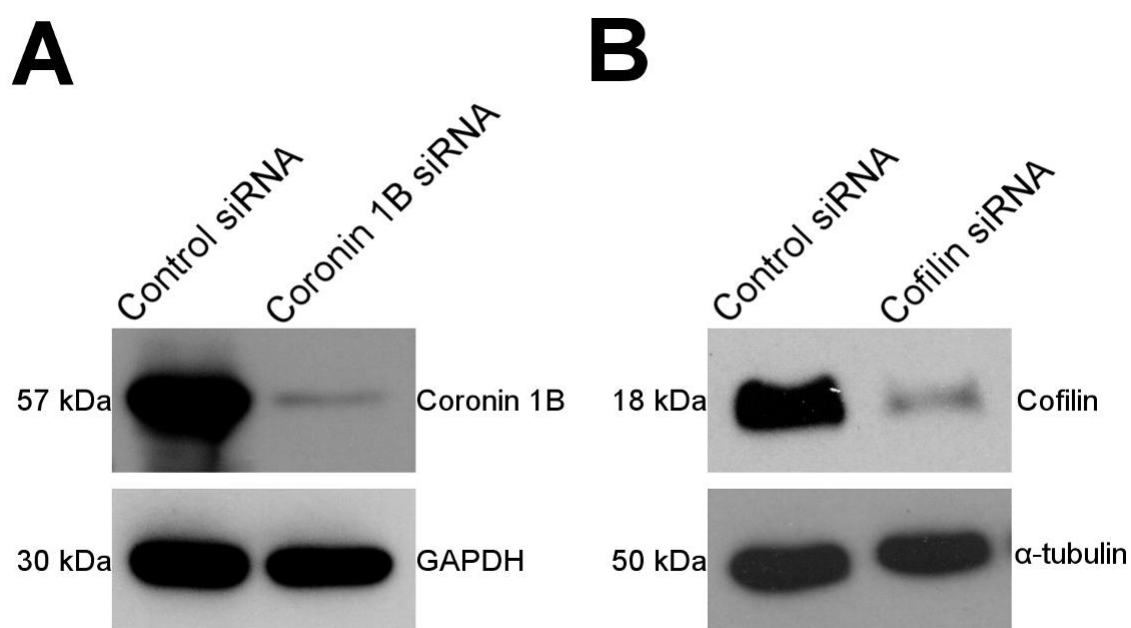


Figure 6.3. Confirmation of gene silencing by Coronin 1B and cofilin siRNA.

(A) Western blot demonstrating successful knockdown of Coronin 1B compared to control

(B) Western blot demonstrating successful knockdown of Cofilin compared to control

To determine if either coronin 1B or its downstream effector cofilin were required for Tpm1.8/9 recruitment into lamellipodia, MEFs were treated with either control, coronin 1B or cofilin siRNA sequences (Figure 6.3) following which cells were fixed and co-stained with the $\alpha/1b$ antibody to visualise Tpm1.8/9 and with phalloidin to visualise F-actin. Confocal images of the cells demonstrate that, compared to control, both coronin 1B and cofilin-deficient cells lack lamellipodial staining of Tpm1.8/9 (Figure 6.4 A). Phalloidin staining acted as a control to demonstrate that F-actin is still abundant within lamellipodia (Figure 6.4 B), showing that the reduction in Tpm1.8/9 seen is due to it being depleted from the leading edge, rather than loss of branched networks.

Quantification of Tpm1.8/9 enrichment in lamellipodia by cell-scoring as described earlier showed that significantly fewer cells displayed lamellipodial enrichment of Tpm1.8/9 in the coronin 1B (24.6 ± 2.0 %, $p < 0.0001$) and cofilin (16.0 ± 3.3 %, $p < 0.0001$) siRNA knockdown cells compared to control cells (71.3 ± 1.3 %) (Figure 6.4 C). These results suggest that both coronin 1B and its downstream effector cofilin are required for Tpm1.8/9 incorporation into the lamellipodium.

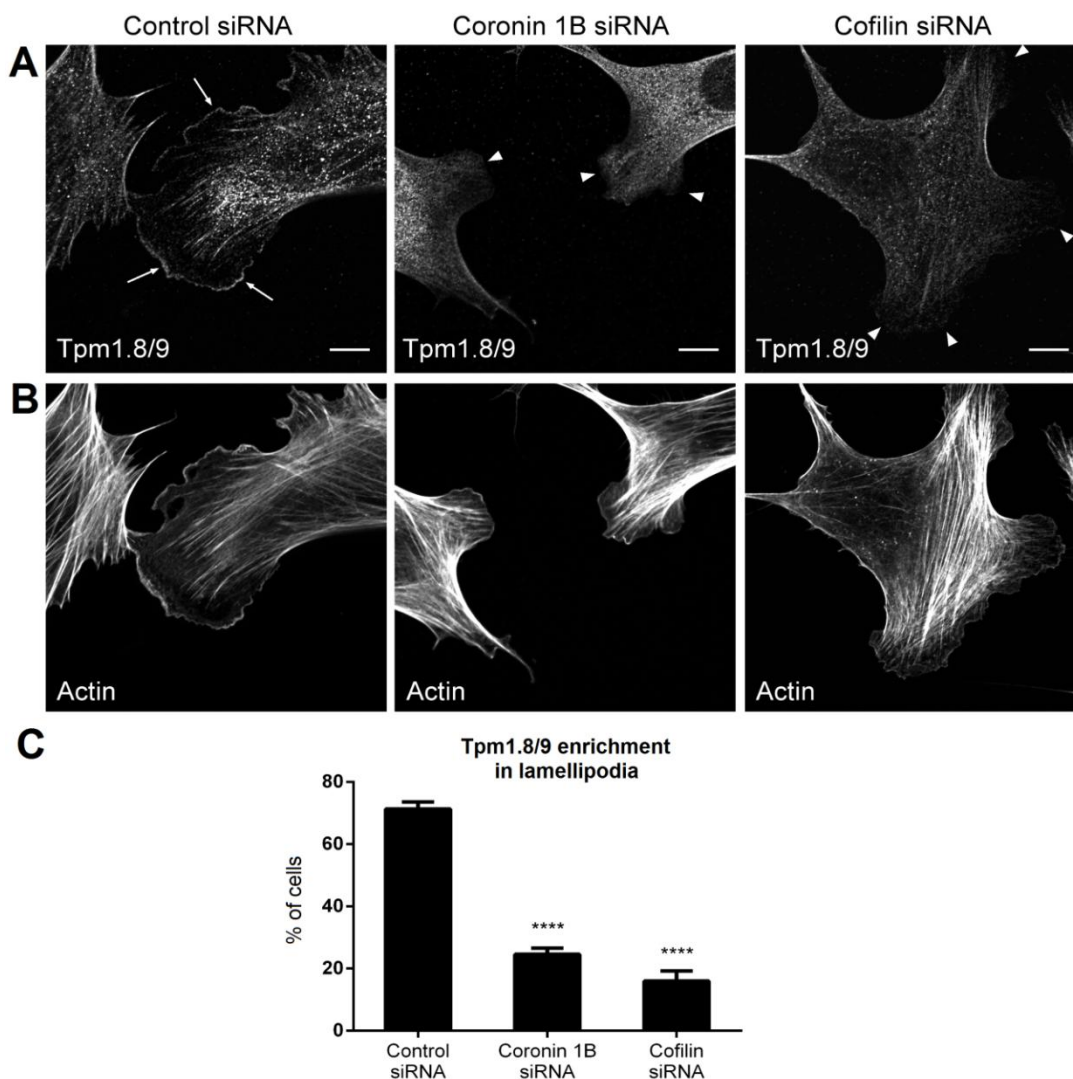


Figure 6.4. Coronin and cofilin knockdown removes Tpm1.8/9 from the leading edge.

(A) Tpm1.8/9 staining of control, coronin 1B or cofilin siRNA-treated MEF cells. Arrows indicate lamellipodial enrichment of Tpm1.8/9 and arrow heads indicate lack of enrichment. Scale bars = 10 μ m

(B) Phalloidin staining control, coronin 1B or cofilin siRNA-treated MEF cells from (A) to demonstrate that the reduction in Tpm1.8/9 seen is due to it being depleted from the leading edge, rather than a lack of signal

(C) Quantification as a percentage of cells which display Tpm1.8/9 enrichment in lamellipodia. $n > 300$ cells per condition. Error bars \pm SEM; $n = 3$; **** $p < 0.0001$; Student's t-test.

Tpm1.8/9 protein levels are reduced following knockdown of coronin 1B or cofilin

It was hypothesised that the lack of Tpm1.8/9 seen at the leading edge following the knockdown of coronin 1B or cofilin could potentially be as a result of protein degradation. To test this, MEF lysates treated with either control, coronin 1B or cofilin siRNA were probed with the $\alpha/1b$ antibody along with anti- α -tubulin as a loading control. The resulting Western blot indicates that Tpm1.8/9 protein levels are reduced following knockdown of either Coronin or cofilin (Figure 6.5 A). Densitometry of triplicate repeat Western blots reveals a significant reduction in the overall levels of Tpm1.8/9 following the knockdown of coronin 1B (65.1 ± 11.4 %, $p < 0.001$) or cofilin (83.2 ± 3.4 %, $p < 0.0001$) relative to control (Figure 6.5 B). This defective protein accumulation could be a result of increased degradation, or of defective protein synthesis. A similar result has been previously reported where Tpm gene expression is altered in response to altered actin gene expression (Schevzov et al., 1993). Firstly, mRNA levels were tested, followed by an investigation into a potential degradation mechanism.

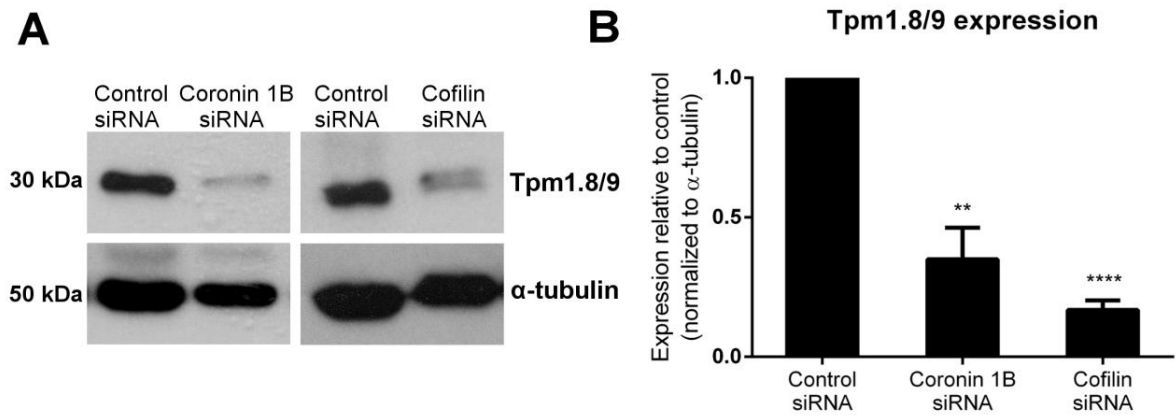


Figure 6.5. Coronin and cofilin knockdown results in a decrease in Tpm1.8/9 protein.

(A) Western blot analysis of Tpm1.8/9 expression in MEFs 48 hr post transfection with either control, coronin 1B or cofilin siRNA. α -tubulin represents a loading control.

(B) Relative protein levels were determined by densitometry from triplicate repeats normalised to α -tubulin and are represented in the histogram. Error bars \pm SEM; ** $p < 0.005$, **** $p < 0.0001$; Student's t-test.

mRNA levels remain constant following coronin 1B or cofilin knockdown

To determine whether the reduction in Tpm1.8/9 levels was accompanied by a change in Tpm1.8/9 mRNA, qPCR analysis was performed on cells transfected with either control, coronin 1B or cofilin siRNA. Primers were designed that were anchored in exon 1b and neighbouring exon 3 to produce an amplicon of 251 bps and exclude genomic DNA. Cells were re-suspended in TRI Reagent[®] (Sigma), shaken with chloroform and RNA extracted from the aqueous layer using isopropanol. First-Strand cDNA synthesis was performed using SuperScript[®] VILO[™] cDNA Synthesis Kit (Invitrogen) according to the manufacturer's instructions. Real-Time PCR was performed using SsoAdvanced[™] Universal SYBR[®] Green Supermix (BioRad, Hercules, CA). Primers for GAPDH were also included as a housekeeping gene. DNA copy number was determined for both genes using the standard curve method. No significant change between control, coronin 1B and cofilin siRNA-treated cells was observed in the mRNA levels for Tpm1.8/9 as revealed by qPCR (Figure 6.6), this result further suggests that Tpm1.8/9 protein is being continuously translated, but is being degraded when it cannot bind as effectively to actin filaments in the lamellipodium.

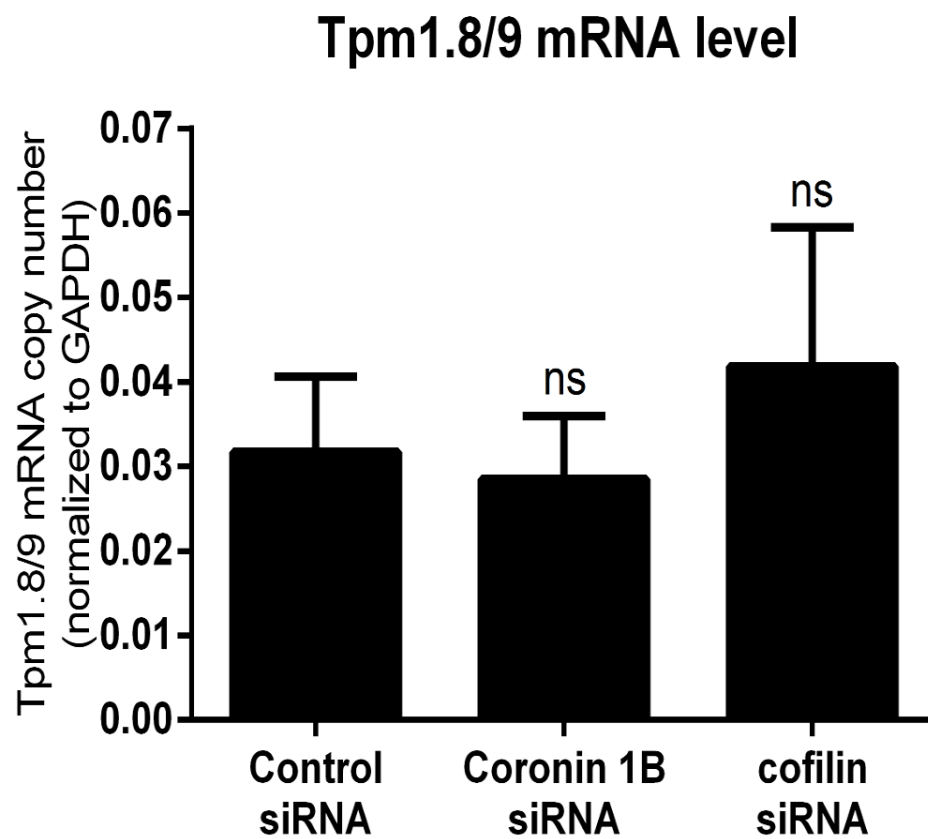


Figure 6.6. mRNA levels remain constant following coronin 1B or cofilin knockdown.

qPCR analysis of Tpm1.8/9 mRNA taken from cDNA generated from either control, coronin 1B or cofilin siRNA treated cells, normalised to GAPDH; Error bars = SEM; n = 2; ns = not statistically significant; Student's t-test.

Tpm1.8/9 is not degraded by the 26S Proteasome

Much of the protein degradation in cells is performed by the proteasome, a protein complex that uses ATP-dependant proteolysis to degrade proteins tagged with ubiquitin, and therefore targeted for degradation (Tanaka, Waxman & Goldberg, 1983). The total 26S proteasome consists of a core, barrel-shaped 20S particle, and two 19S regulatory caps (Cheng, 2009). To investigate whether Tpm1.8/9 degradation is mediated by the 26S proteasome, the proteasome inhibitor MG132 was used. Cells were transfected with either control, coronin 1B or cofilin siRNA before being either left untreated, or treated with 20 μ M MG132 for 6 hours. Protein lysates from treated and untreated cells were separated by SDS-PAGE, and blots were probed with the α /1b antibody along with anti- α -tubulin as a loading control. To confirm that MG132 was successful at inhibiting the proteasome at this concentration and treatment time, the same lysates from both treated and untreated cells were later run together on a separate gel and probed for Hsp70, a chaperone that is known to be degraded by the 26S proteasome. As expected, the MG132-treated samples showed increased levels of Hsp70 compared to untreated samples (Figure 6.7, lower panel). There was however no apparent restoration of Tpm1.8/9 protein levels following MG132 treatment compared to untreated cells. (Figure 6.7, upper panel) suggesting that Tpm1.8/9 is not degraded by the proteasome.

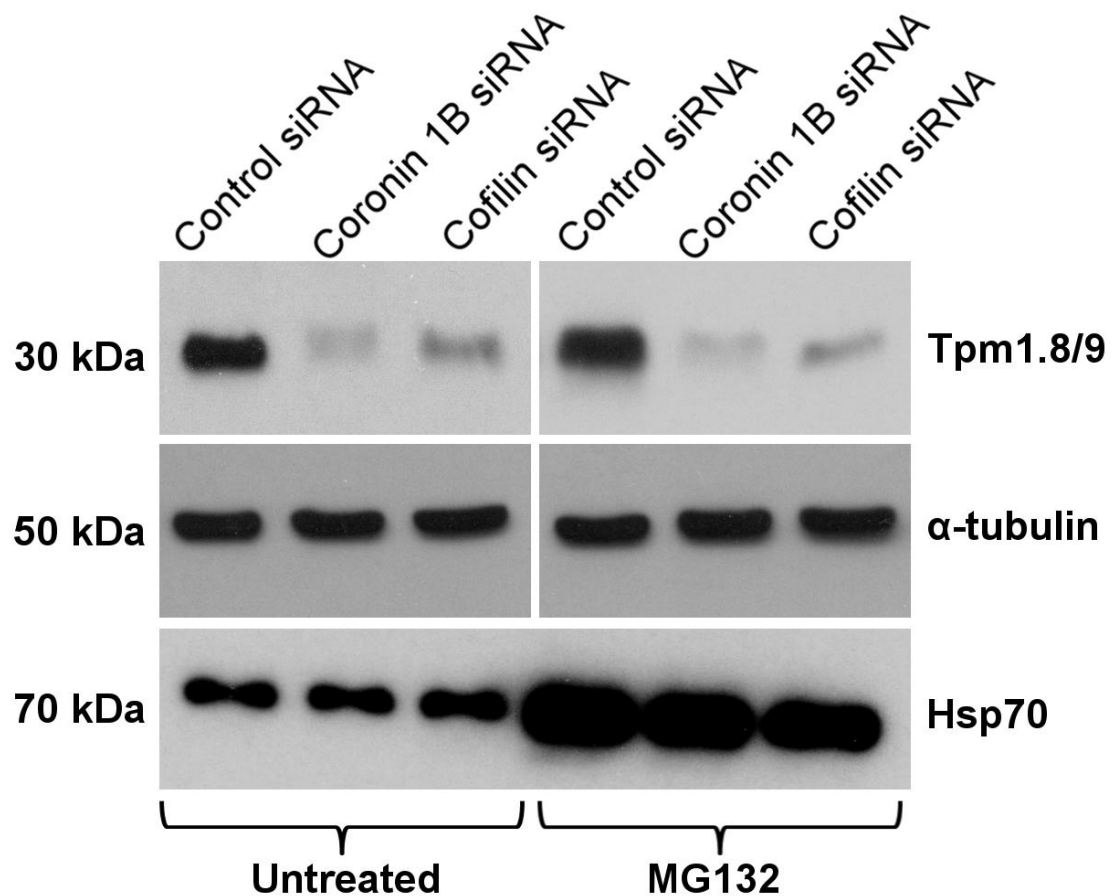


Figure 6.7. Tpm1.8/9 is not degraded by the 26S Proteasome.

Western blot showing degradation of Tpm1.8/9 protein following siRNA knockdown of either coronin 1B or cofilin compared to control siRNA in untreated cells (top left panel). Treatment with proteasome inhibitor MG132 does not restore Tpm1.8/9 protein levels (top panel, right). α -tubulin was used as a loading control for both experiments (middle panel). The same lysates from the upper panels were then run together on a separate gel and probed for Hsp70 to demonstrate successful inhibition of the proteasome (lower right panel) compared to lysates from untreated cells (lower left panel).

Discussion

Cell motility is a process that requires the precise spatial and temporal control of individual components of the cytoskeleton to achieve efficient directional movement. The composition of the lamellipodium has long been an area of debate in the literature in terms of the way the actin filament network is organised. Earlier reports suggested that the leading edge was divided into distinct zones of branched and unbranched actin filaments (Iwasa & Mullins, 2007; Pollard & Borisy, 2003; Svitkina & Borisy, 1999; Svitkina et al., 1997), more recently however, electron tomography has revealed that both branched and unbranched actin filaments are present throughout the lamellipodium (Small, 2015; Urban et al., 2010; Vinzenz et al., 2012). These findings raise an important question - how can multiple actin filament populations co-exist in the same cellular region yet be differentially regulated?

Collaboration of distinct actin networks

Recent experiments have indicated the importance of building multiple actin filament types in the same location to generate functional outcomes (Kee et al., 2015). Studies in a variety of systems have indicated that Tpm isoforms can be used to specify the functional and molecular properties of actin filaments to allow the collaboration of different filament populations within the cell (Gunning et al., 2015). Tpm isoforms display extensive intracellular sorting, resulting in spatially distinct actin-filament populations (Martin & Gunning, 2008). While the exact mechanisms which control isoform sorting in mammalian cells remain to be fully understood, the prevailing model is that Tpm's tend to be located in structures based on local demand (Schevzov et al., 2008; Schevzov et al., 1993) rather than via the presence of an intrinsic targeting signal (Martin, Schevzov & Gunning, 2010). This model is supported by the result displayed in Figure 4.7 whereby, upon inhibition of Arp2/3 by CK666, Tpm1.8/9, despite being

present in larger amounts, does not appear to simply accumulate elsewhere (such as stress fibres).

Summary of findings

This chapter demonstrates that, following re-activation of Arp2/3, protrusive activity is rapidly restored, with Arp2/3 and cortactin being rapidly recruited into new lamellipodia. Conversely, recovery of coronin 1B and Tpm1.8/9 is delayed, suggesting a need for coronin 1B directed remodelling of the Arp2/3-actin network to incorporate Tpm1.8/9. RNAi mediated knockdown of coronin 1B or cofilin resulted in the depletion of Tpm1.8/9 from the leading edge and also caused its subsequent degradation suggesting that, upon removal of the source of the correct type of actin filaments, Tpm1.8/9 cannot be incorporated into the lamellipodium and are instead degraded.

Intracellular degradation of proteins serves a number of functions including the removal of damaged or abnormal proteins, prevention of unwanted accumulation of proteins or to regulate cellular processes by removing enzymes, regulatory or structural proteins. This is usually achieved in two ways; via a ubiquitin-dependent process that targets unwanted proteins to the 26S proteasome, or the autophagy-lysosomal pathway which is a more non-selective process and utilises a large number of proteases. In figure 6.7 it was demonstrated, using the proteasome inhibitor MG132, that Tpm1.8/9 are not degraded by the 26S proteasome. This result is supported by similar findings in which Tpm3.1 was also not degraded by the 26S proteasome (Martin, 2010). This result may indicate that these isoforms are instead degraded by an as-yet unidentified protease as part of the autophagy-lysosomal pathway, a mechanism of degradation which has yet to be explored for tropomyosins.

These findings, taken together with other recent advances allows us to build a conceptual model for how multiple actin filament networks can be generated and maintained at the leading edge.

Previous work has identified coronin 1B as a link between cofilin and the Arp2/3 complex, that controls actin remodelling in many cell-types by directing SSH1L to the leading edge where it activates cofilin. (Cai et al., 2008; Cai et al., 2007). It has also recently been shown that severing of Arp2/3-generated networks by cofilin results in the generation of new pointed ends to which the *Drosophila*-derived Tpm, Tm1A, preferentially binds, generating two sets of actin filaments. One is Tpm-coated and the other Tpm-free that is competent to bind Arp2/3. They can be stably maintained in vitro because they are insulated from each another (Hsiao et al., 2015a). These findings point toward a potential mechanism of how branched actin filaments may be re-modelled in cells to include Tpm.

Proposed mechanism of generation of Tpm1.8/9-containing actin filaments at the leading edge

The findings presented in this chapter offer a novel mechanism of how Tpm isoforms allow multiple actin filament populations to collaborate at the leading edge. Activated Arp2/3 complex nucleates a new filament on the side of an existing filament, forming a branched junction. Cortactin associates with Arp2/3-containing branches, protecting them from spontaneous disassembly. Coronin 1B targets Arp2/3-containing actin branches in an antagonistic fashion with cortactin. It has been shown that coronin 1B binds Slingshot 1L, the activating phosphatase of cofilin (Cai et al., 2007). Recruitment of Slingshot 1L by coronin 1B brings it into close proximity to F-actin, an essential cofactor for its activation. Slingshot 1L activation leads to local dephosphorylation and

activation of cofilin. Locally activated cofilin severs the Arp2/3 branch junctions, allowing the exposed pointed ends of filaments to become coated with Tpm1.8/9. This in turn provides the stability needed to prevent the collapse of filaments either passively or via further severing. In the absence of coronin 1B therefore, SSH1L is not recruited, cofilin is not activated and fewer free pointed ends to which Tpm can bind are created. Tpm is subsequently degraded and therefore depleted from the leading edge, an observation also seen following the knockdown of cofilin. As a result of reduced Tpm levels, the presence of more stable, unbranched filaments is diminished and lamellipodial persistence is impaired, along with whole-cell motility.

While this model asserts that linear actin filaments seen in lamellipodia of motile cells begin life as branched actin filaments, the origin of the initial mother filament from which Arp2/3 nucleates daughter filaments remains unclear but one possible explanation is the activity of a formin-family protein. It has been reported that RNAi-mediated silencing of the Diaphanous-related formin FMNL2 decreases the rate of lamellipodial protrusion and, accordingly, the efficiency of cell migration (Block et al., 2012). Whether this is a direct indication of FMNL2 nucleating the mother filament remains to be seen but interestingly, in yeast, specific formin-family members dictate which Tpm isoform will associate with a particular actin filament (Johnson, East & Mulvihill, 2014). At this stage, one can only speculate as to whether a specific formin builds a Tpm1.8/9 coated actin filament in mammalian cells.

In conclusion, the tropomyosin isoforms Tpm1.8/9 are specifically recruited to the leading edge of migrating cells where they promote lamellipodial persistence by facilitating the transition from a branched actin network to a more stable actin network

in order to achieve a persistent state of protrusion coupled to cellular attachment for effective lamellipodial-based cell migration.

The next and final chapter will provide a generalised discussion encompassing all the findings and ideas presented in this thesis and reflect on their significance in the context of the literature.

Chapter Seven

General Discussion

Chapter 7: General Discussion

Outcomes and significance of the study

This study encompasses an investigation into the functional role of the cytoskeletal tropomyosin isoforms; Tpm1.8/9 in regulating cell migration. This is significant due to the role for cell migration in metastatic cancer. An incomplete understanding of the processes governing cell migration exists in the literature and it is therefore of considerable interest to further develop knowledge of the underlying mechanisms that regulate cell migration, with the vision that novel drug targets may be revealed, leading to better chemotherapeutic agents which inhibit cancer metastasis.

The primary results of this study show that Tpm1.8/9 are required for effective lamellipodial-based cell migration. This novel finding represents a potential point for intervention to disable, at least in some cell-types, migratory potential. Although this is still a far-cry from an anti-cancer drug target, inhibition of this process via a small-molecule may one day prove to be a useful research tool, and it should be noted that the small-molecule inhibition of other Tpm isoforms is already being enthusiastically adopted both for this purpose as well as being further investigated and indeed developed for future use in the clinic (Stehn et al., 2013).

The other major outcome of this study is of significance on a more academic level. One doesn't have to look very far to notice a lack of consensus among experts in the field on both the subject of the organisation of the leading-edge actin filament network, and the presence of tropomyosins within this region. The results reported in this study not only provide solutions to some of the disagreement, but also serve as a broader paradigm for how multiple actin filament types can be differentially regulated to achieve a singular outcome for the cell.

Tropomyosin at the leading edge

The initial focus of this project was to confirm lamellipodial enrichment of Tpm1.8/9. This was based on the observation that Tpm1.8/9 appeared to accumulate near the cell periphery in MEFs (Schevzov et al., 2011). This observation was also supported by earlier work in T84 epithelial cells demonstrating that Tpm1.8/9 are highly polarised, and mark an apical population of microfilaments that can regulate the insertion of the cystic fibrosis transmembrane conductance regulator (CFTR) (Dalby-Payne, O'Loughlin & Gunning, 2003). There has since been much debate in the literature over whether Tpm1.8/9 are present within the lamellipodium or confined only to other regions within the cell. Much of this debate stems from a lack of appropriate tools to study smaller subsets of tropomyosin isoforms. The initial purpose of this study was to characterise a newly generated monoclonal antibody which has specificity for Tpm1.8/9. Once characterised, this antibody was used to confirm the presence of Tpm1.8/9 in the lamellipodium. This finding not only served to provide a solution to the debate in the literature, but also paved the way for a series of experiments to investigate the role of these Tpm1.8/9 in regulating the actin network within the lamellipodium. The concept of cells utilising different isoforms of tropomyosin to provide discrete functions to their associated actin filament networks is not a new one. In fact, multiple studies in a variety of systems have demonstrated various roles for Tpm1.8/9 in building different actin filament populations within cells (Bryce, Schevzov, Ferguson, Percival, Lin, Matsumura, Bamburg, Jeffrey, Hardeman, & Gunning, 2003; Jalilian et al., 2015; Kee et al., 2015; Schevzov et al., 2015; Tojkander et al., 2011). It is therefore, at least with the benefit of hind-sight, not particularly surprising that a Tpm1.8/9-containing population of actin filaments should exist at the leading-edge of motile cells and that these Tpm1.8/9 isoforms should play a role in regulating Arp2/3-mediated leading edge protrusion.

The relationship between tropomyosin and the Arp2/3 complex

Once it was clear that Tpm1.8/9 did indeed localise to the lamellipodium as outlined in Chapter 3, the series of experiments that followed revealed a regulatory mechanism between Tpm1.8/9 and the Arp2/3 complex. This relationship appears to be one in which these two proteins compete for actin filaments at the leading edge. If Tpm1.8/9 is removed, then Arp2/3 appears to engage a greater portion of peripheral actin, occupying more of the cell edge and resulting in thicker lamellipodia. Conversely, if Arp2/3 is inhibited, Tpm1.8/9 protein levels are elevated, suggesting that, despite lacking a lamellipodium, the cell increases translation and/or stability of Tpm1.8/9, as if to compensate for the lack of Arp2/3-actin filaments. Whether this is an indication of a direct biological feedback loop remains unclear, but interestingly, when the source of preferred actin filaments is removed via the knockdown of coronin 1B and cofilin, Tpm1.8/9 mRNA levels remain constant, suggesting that protein degradation is the more likely reason for the subsequent reduction in Tpm1.8/9 protein levels. Perhaps even more interesting is the observation that, even in the presence of elevated levels of Tpm1.8/9, these isoforms do not appear to associate with stress fibres or other actin-based cellular structures. This provides further evidence to support the idea that specific isoforms or at least subsets thereof, have preferred associations with specific populations of actin filaments and are subsequently organised into discreet pockets within the cell, giving rise to the now well-established patterns of isoform sorting seen between Tpm's both at a tissue and cellular level in a wide variety of different cell and tissue types (Bryce, Schevzov, Ferguson, Percival, Lin, Matsumura, Bamburg, Jeffrey, Hardeman, & Gunning, 2003; Creed et al., 2008; Creed et al., 2011; Gunning, O'Neill & Hardeman, 2008; P. W. Gunning et al., 2005; Kee et al., 2015; Schevzov et al., 1997; Schevzov et al., 2005; Schevzov et al., 2011).

Another important question to be asked is how, under normal conditions, the architecture of the actin filament network at the leading edge is properly orchestrated to include both linear actin filaments and branched actin filaments, and does tropomyosin play a role in merely insulating one network from the other or also in mediating a transition between the two? Firstly, some of the ideas and concepts on this topic that have been put forward in the literature will be discussed.

Coupling the dynamics of two actin networks

Due to the biochemical incompatibility of Arp2/3 and most Tpms, early reports suggested that they were spatially segregated (Blanchoin, Pollard & Hitchcock-DeGregori, 2001; DesMarais et al., 2002). This model however does not explain how protrusion and contraction are mechanically coupled (Danuser, 2005). It has since been proposed that two molecularly distinct actin networks overlap at the leading edge, are weakly coupled, and whose transition may be defined by the initiation of substrate-cytoskeleton linkages and that persistent advancement of the cell relies on the underlying lamella (Lim et al., 2010; Ponti et al., 2004). This model is supported by the observations that cell migration is possible without a lamellipodium (Gupton et al., 2005) and that Arp2/3 is dispensable for chemotaxis (Wu et al., 2012). An important consideration here is an understanding of how Tpms allow multiple actin filament populations to co-exist in the same cellular region and be differentially regulated. It has recently been shown in vitro that severing of Arp2/3-generated networks by cofilin results in the generation of new pointed ends, to which the *Drosophila*-derived Tpm, Tm1A preferentially binds and that two sets of actin filaments, a Tpm-coated set and a Tpm-free set, that is competent to bind Arp2/3, can be stably maintained in vitro because they are insulated from one another (Hsiao et al., 2015b). These findings point

toward a potential mechanism of how branched actin filaments may in fact be remodelled in cells to include Tpm.

Tropomyosin allows the collaboration of distinct actin networks

Studies in a variety of systems have indicated that Tpm isoforms can be used to specify the functional and molecular properties of actin filaments to allow the collaboration of different filament populations within the cell (Gunning et al., 2015). Tpm isoforms display extensive intracellular sorting, resulting in spatially distinct actin-filament populations (Martin & Gunning, 2008). While the exact mechanisms which control isoform sorting in mammalian cells remain to be fully understood, the prevailing model is that Tpm's tend to be recruited on an ad-hoc basis (Schevzov et al., 2008; Schevzov et al., 1993) rather than via the presence of an autonomous targeting signal (Martin, Schevzov & Gunning, 2010). This model is supported by the results of this study whereby, upon removal of the source of their preferred actin filaments within the lamellipodium, Tpm1.8/9 do not appear to simply accumulate elsewhere (such as stress fibres), but are instead diminished at a protein level, suggesting that Tpm1.8/9, which cannot be incorporated into actin filaments in the lamellipodium, are degraded. Taken together, the data presented in this thesis allows a working model to be constructed which describes a novel mechanism whereby Tpm1.8/9 collaborates with various other lamellipodial proteins to achieve a persistent state of lamellipodial protrusion coupled to cell attachment.

Working model for the regulation of lamellipodial persistence by Tpm

The findings of this study provide a solution to the controversy found in the literature by offering a novel mechanism of how Tpm allows protrusive and adhesive actin networks to collaborate at the leading edge (illustrated in Figure 7.1). At the advancing cell edge,

cortactin and coronin 1B coordinate the transition between a network of non-Tpm containing Arp2/3-branched filaments and a second, Tpm-containing network of linear filaments that are derived from the first via cofilin which severs branch junctions, allowing the exposed pointed ends of filaments to become coated with Tpm1.8/9. This in turn provides the stability needed to enhance persistence through the subsequent promotion of substratum adhesions. In the absence of coronin 1B, SSH1L is not recruited, cofilin is not activated and fewer free pointed ends to which Tpm can bind are created. Tpm may be subsequently degraded and therefore depleted from the leading edge, an observation also seen following the knockdown of cofilin. As a result of reduced Tpm levels, the presence of more stable, unbranched filaments is diminished and lamellipodial persistence is impaired, along with whole-cell motility.

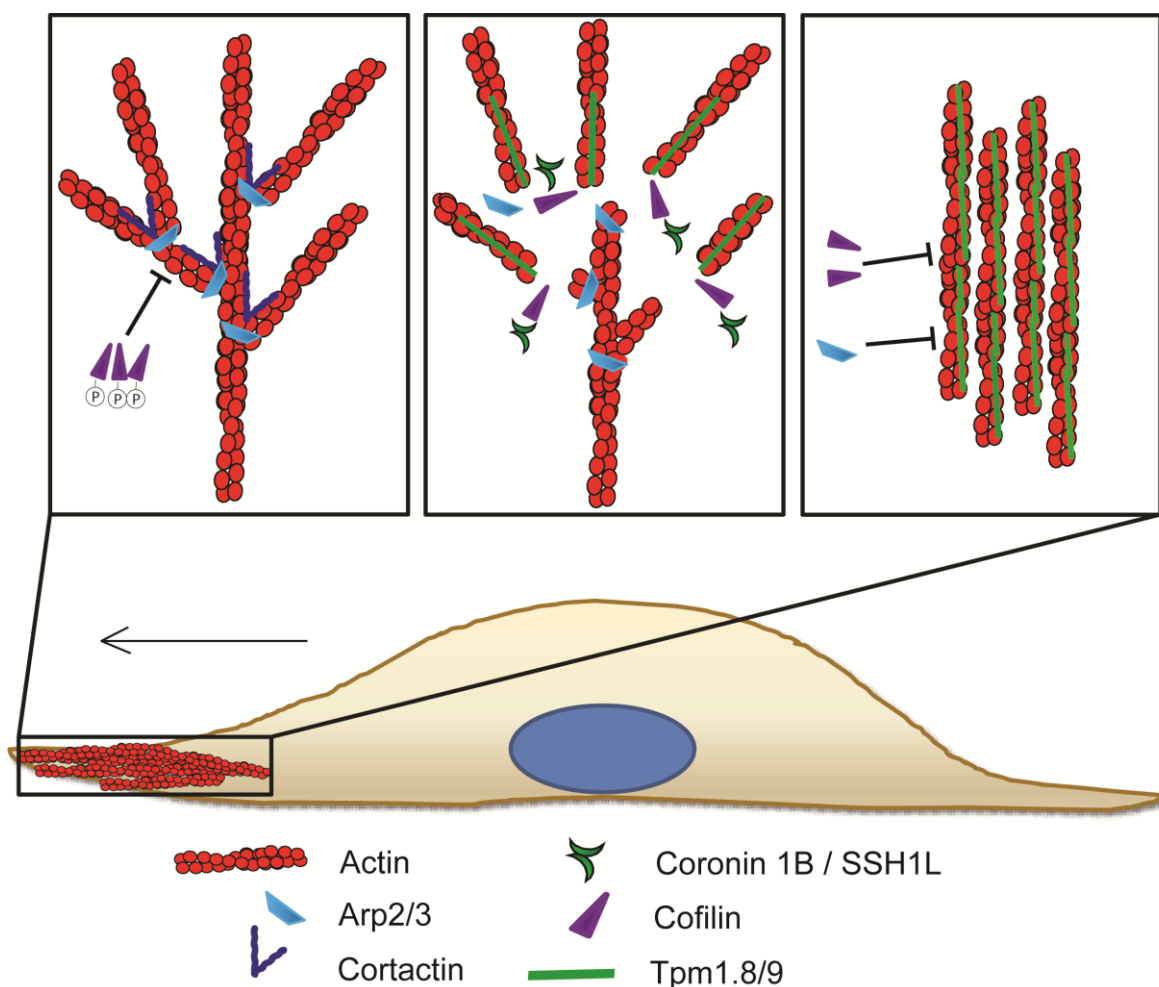


Figure 7.1. Working model for the regulation of lamellipodial persistence by tropomyosin.

Cortactin promotes and stabilises the Arp2/3-nucleated protrusive actin filament network. In order to translate protrusion into more stable filaments associated with adhesion, coronin 1B, along with SSH1L, activates cofilin via dephosphorylation which severs branched actin networks. This creates new free pointed ends to which tropomyosin preferentially binds, protecting filaments from further severing and branching and providing a more stable substrate for the recruitment of focal contact proteins, promoting the maturation of focal adhesions to drive lamellipodial based cell motility.

In the absence of Tpm1.8/9, there is no mechanism to stabilise the protrusion and the instability of the Arp2/3 network allows the membrane to retract. This explains why the front of the lamellipodium consists of adjacent Arp2/3-rich zones and Tpm1.8/9-rich zones.

Future Directions

If this study were to be extended or expanded upon, several possible directions and experiments are suggested by the author. Firstly, as discussed, Tpm1.8/9 are not degraded by the 26S proteasome. This raises the obvious question of how these isoforms are degraded. A fairly simple experiment would involve repetition of the one described for the generation of Figure 6.7 with substitution of MG132 for a cell penetrating protease inhibitor such as PepA-P (Zaidi et al., 2007). Secondly, it would be helpful to reinforce the proposed model proposed through further testing. This could involve *in vitro* studies using a pyrene actin assay with filaments grown on glass coverslips and comparing the extent of branching and severing of non-coated filaments to those coated with Tpm1.8 or Tpm1.9 in the presence of varying combinations of Arp2/3, coronin 1B and cofilin. Similar experiments to this have been successfully carried out previously (Hsiao et al., 2015a; Uruno et al., 2001; Weaver et al., 2001). Another important aspect of the model which could be further investigated is whether Tpm1.8/9-actin filaments in the lamellipodium increase their stability through their interaction with a bundling or cross-linking protein. This could be achieved by transfecting cells with fluorescently labelled α -actinin, performing live-imaging of lamellipodia in the presence or absence of Tpm1.8/9 siRNA, and quantifying the recruitment of α -actinin. Finally, the results presented in Chapter 5 could be further strengthened by examining the dynamics of focal adhesion assembly in live cells. Assembly of paxillin-based focal adhesions in control vs. Tpm1.8/9 knockdown cells could be measured by transfecting with GFP-paxillin and generating and analysing a time-series of fluorescent images. A very similar experiment to this is described by Bryce et al using HT1080 human fibrosarcoma cells (Bryce et al., 2005).

Concluding Remarks

The data presented in this thesis is most compatible with a model whereby rapid protrusion of the leading edge via the Arp2/3 branched network is followed by conversion of the braches to an unbranched, Tpm1.8/9 bound set of more stable filaments. In this way, the protrusion becomes more stable because the filaments within the protrusion become more stable and do not collapse. This also fits well with the observed lack of co-localisation of Tpm1.8/9 and Arp2/3 and so the lamellipodium becomes occupied by zones in which Arp2/3 branches convert to Tpm1.8/9 unbranched filaments in a cyclical fashion. The conversion to focal adhesions may be an indirect result or could be due to differential organisation occurring within nascent adhesions which could not be detected with the assays employed. Mechanistically, what this would mean is that the absence of Tpm1.8/9 leads to the total collapse of the Arp2/3 network and rapid membrane retraction. Conversely, in the presence of Tpm1.8/9, cofilin activity, directed by coronin 1B/SSH1L, replaces the Arp2/3 network with Tpm1.8/9 filaments which are stable and the membrane cannot retract. Tpm1.8/9 filaments are then replaced, via an as-yet unknown mechanism, by a newly formed Arp2/3 network. This cyclical actin remodelling, coupled to the generation of focal contacts would result in persistent lamellipodial protrusions. One might also suspect that there is a cross-linker or a bundling protein of some type which also holds the Tpm1.8/9 filaments in a more stable state so that focal adhesions may then mature following their formation. In conclusion, the tropomyosin isoforms Tpm1.8/9 are specifically recruited to the leading edge of migrating cells where they promote lamellipodial persistence by facilitating the transition from a branched actin network to a more stable actin network in order to achieve a persistent state of protrusion coupled to cellular attachment for effective lamellipodial based cell migration.

References

References

- Abercrombie, M., Heaysman, J. E., & Pegrum, S. M. (1970a). The locomotion of fibroblasts in culture. I. Movements of the leading edge. *Exp Cell Res*, 59(3), 393-398.
- Abercrombie, M., Heaysman, J. E., & Pegrum, S. M. (1970b). The locomotion of fibroblasts in culture. II. "Ruffling". *Exp Cell Res*, 60(3), 437-444.
- Agnew, B. J., Minamide, L. S., & Bamburg, J. R. (1995). Reactivation of phosphorylated actin depolymerizing factor and identification of the regulatory site. *J Biol Chem*, 270(29), 17582-17587.
- Alaiya, A. A., Franzen, B., Fujioka, K., Moberger, B., Schedvins, K., Silfversvard, C., Linder, S., & Auer, G. (1997). Phenotypic analysis of ovarian carcinoma: polypeptide expression in benign, borderline and malignant tumors. *Int J Cancer*, 73(5), 678-683.
- Alaiya, A. A., Oppermann, M., Langridge, J., Roblick, U., Egevad, L., Brindstedt, S., Hellstrom, M., Linder, S., Bergman, T., Jornvall, H., & Auer, G. (2001). Identification of proteins in human prostate tumor material by two-dimensional gel electrophoresis and mass spectrometry. *Cell Mol Life Sci*, 58(2), 307-311.
- Backert, S., Feller, S. M., & Wessler, S. (2008). Emerging roles of Abl family tyrosine kinases in microbial pathogenesis. *Trends Biochem Sci*, 33(2), 80-90.
- Bailly, M., Macaluso, F., Cammer, M., Chan, A., Segall, J. E., & Condeelis, J. S. (1999). Relationship between Arp2/3 complex and the barbed ends of actin filaments at the leading edge of carcinoma cells after epidermal growth factor stimulation. *J Cell Biol*, 145(2), 331-345.
- Balaban, N. Q., Schwarz, U. S., Riveline, D., Goichberg, P., Tzur, G., Sabanay, I., Mahalu, D., Safran, S., Bershadsky, A., Addadi, L., & Geiger, B. (2001). Force and focal adhesion assembly: a close relationship studied using elastic micropatterned substrates. *Nat Cell Biol*, 3(5), 466-472.

- Ballestrem, C., Hinz, B., Imhof, B. A., & Wehrle-Haller, B. (2001). Marching at the front and dragging behind: differential alphaVbeta3-integrin turnover regulates focal adhesion behavior. *J Cell Biol*, *155*(7), 1319-1332.
- Bamburg, J. R. (1999). Proteins of the ADF/cofilin family: essential regulators of actin dynamics. *Annu Rev Cell Dev Biol*, *15*, 185-230.
- Bamburg, J. R., McGough, A., & Ono, S. (1999). Putting a new twist on actin: ADF/cofilins modulate actin dynamics. *Trends Cell Biol*, *9*(9), 364-370.
- Bartles, J. R. (2000). Parallel actin bundles and their multiple actin-bundling proteins. *Curr Opin Cell Biol*, *12*(1), 72-78.
- Behrens, J., Mareel, M. M., Van Roy, F. M., & Birchmeier, W. (1989). Dissecting tumor cell invasion: epithelial cells acquire invasive properties after the loss of uvomorulin-mediated cell-cell adhesion. *J Cell Biol*, *108*(6), 2435-2447.
- Beningo, K. A., Dembo, M., Kaverina, I., Small, J. V., & Wang, Y. L. (2001). Nascent focal adhesions are responsible for the generation of strong propulsive forces in migrating fibroblasts. *J Cell Biol*, *153*(4), 881-888.
- Bershadsky, A., Kozlov, M., & Geiger, B. (2006). Adhesion-mediated mechanosensitivity: a time to experiment, and a time to theorize. *Curr Opin Cell Biol*, *18*(5), 472-481.
- Bharadwaj, S., Hitchcock-DeGregori, S., Thorburn, A., & Prasad, G. L. (2004). N terminus is essential for tropomyosin functions: N-terminal modification disrupts stress fiber organization and abolishes anti-oncogenic effects of tropomyosin-1. *J Biol Chem*, *279*(14), 14039-14048.
- Bhavsar, A. P., Guttman, J. A., & Finlay, B. B. (2007). Manipulation of host-cell pathways by bacterial pathogens. *Nature*, *449*(7164), 827-834.
- Blanchoin, L., Pollard, T. D., & Hitchcock-DeGregori, S. E. (2001). Inhibition of the Arp2/3 complex-nucleated actin polymerization and branch formation by tropomyosin. *Curr Biol*, *11*(16), 1300-1304.
- Block, J., Breitsprecher, D., Kuhn, S., Winterhoff, M., Kage, F., Geffers, R., Duwe, P., Rohn, J. L., Baum, B., Brakebusch, C., Geyer, M., Stradal, T. E., Faix, J., &

- Rottner, K. (2012). FMNL2 drives actin-based protrusion and migration downstream of Cdc42. *Curr Biol*, 22(11), 1005-1012.
- Bolte, S., & Cordelieres, F. P. (2006). A guided tour into subcellular colocalization analysis in light microscopy. *J Microsc*, 224(Pt 3), 213-232.
- Bonello, T. T., Stehn, J. R., & Gunning, P. W. (2009). New approaches to targeting the actin cytoskeleton for chemotherapy. *Future Med Chem*, 1(7), 1311-1331.
- Braverman, R. H., Cooper, H. L., Lee, H. S., & Prasad, G. L. (1996). Anti-oncogenic effects of tropomyosin: isoform specificity and importance of protein coding sequences. *Oncogene*, 13(3), 537-545.
- Bravo-Cordero, J. J., Magalhaes, M. A., Eddy, R. J., Hodgson, L., & Condeelis, J. (2013). Functions of cofilin in cell locomotion and invasion. *Nat Rev Mol Cell Biol*, 14(7), 405-415.
- Bresnick, A. R. (1999). Molecular mechanisms of nonmuscle myosin-II regulation. *Curr Opin Cell Biol*, 11(1), 26-33.
- Bryce, N. S., Clark, E. S., Leysath, J. L., Currie, J. D., Webb, D. J., & Weaver, A. M. (2005). Cortactin promotes cell motility by enhancing lamellipodial persistence. *Curr Biol*, 15(14), 1276-1285.
- Bryce, N. S., Schevzov, G., Ferguson, V., Percival, J. M., Lin, J. J., Matsumura, F., Bamburg, J. R., Jeffrey, P. L., Hardeman, E. C., & Gunning, P. (2003). Specification of actin filament function and molecular composition by tropomyosin isoforms. *Mol Biol Cell*, 14(3), 1002-1016.
- Bryce, N. S., Schevzov, G., Ferguson, V., Percival, J. M., Lin, J. J., Matsumura, F., Bamburg, J. R., Jeffrey, P. L., Hardeman, E. C., Gunning, P., & Weinberger, R. P. (2003). Specification of actin filament function and molecular composition by tropomyosin isoforms. *Mol Biol Cell*, 14(3), 1002-1016.
- Bryce, N. S., Schevzov, G., & Gunning, P. (2003). Specification of actin filament function and molecular composition by tropomyosin isoforms. *Mol Biol Cell*, 14(3), 1002-1016.

- Buccione, R., Caldieri, G., & Ayala, I. (2009). Invadopodia: specialized tumor cell structures for the focal degradation of the extracellular matrix. *Cancer Metastasis Rev*, 28(1-2), 137-149.
- Bugyi, B., Didry, D., & Carlier, M. F. (2010). How tropomyosin regulates lamellipodial actin-based motility: a combined biochemical and reconstituted motility approach. *EMBO J*, 29(1), 14-26.
- Cai, L., Holoweckyj, N., Schaller, M. D., & Bear, J. E. (2005). Phosphorylation of coronin 1B by protein kinase C regulates interaction with Arp2/3 and cell motility. *J Biol Chem*, 280(36), 31913-31923.
- Cai, L., Makhov, A. M., Schafer, D. A., & Bear, J. E. (2008). Coronin 1B antagonizes cortactin and remodels Arp2/3-containing actin branches in lamellipodia. *Cell*, 134(5), 828-842.
- Cai, L., Marshall, T. W., Uetrecht, A. C., Schafer, D. A., & Bear, J. E. (2007). Coronin 1B coordinates Arp2/3 complex and cofilin activities at the leading edge. *Cell*, 128(5), 915-929.
- Carlier, M. F., & Pantaloni, D. (1986). Direct evidence for ADP-Pi-F-actin as the major intermediate in ATP-actin polymerization. Rate of dissociation of Pi from actin filaments. *Biochemistry*, 25(24), 7789-7792.
- Carragher, N. O., Walker, S. M., Scott Carragher, L. A., Harris, F., Sawyer, T. K., Brunton, V. G., Ozanne, B. W., & Frame, M. C. (2006). Calpain 2 and Src dependence distinguishes mesenchymal and amoeboid modes of tumour cell invasion: a link to integrin function. *Oncogene*, 25(42), 5726-5740.
- Charras, G., & Paluch, E. (2008). Blebs lead the way: how to migrate without lamellipodia. *Nat Rev Mol Cell Biol*, 9(9), 730-736.
- Cheng, Y. (2009). Toward an atomic model of the 26S proteasome. *Curr Opin Struct Biol*, 19(2), 203-208.
- Chesarone, M. A., DuPage, A. G., & Goode, B. L. (2010). Unleashing formins to remodel the actin and microtubule cytoskeletons. *Nat Rev Mol Cell Biol*, 11(1), 62-74.

- Choi, C. K., Vicente-Manzanares, M., Zareno, J., Whitmore, L. A., Mogilner, A., & Horwitz, A. R. (2008). Actin and alpha-actinin orchestrate the assembly and maturation of nascent adhesions in a myosin II motor-independent manner. *Nat Cell Biol*, *10*(9), 1039-1050.
- Clayton, J. E., Sammons, M. R., Stark, B. C., Hodges, A. R., & Lord, M. (2010). Differential regulation of unconventional fission yeast myosins via the actin track. *Curr Biol*, *20*(16), 1423-1431.
- Coombes, J., Schevzov, G., Kan, C.-Y., Petti, C., Maritz, M. F., Whittaker, S., MacKenzie, K. L., & Gunning, P. W. (2015). Ras transformation overrides a proliferation defect induced by Tpm3.1 knockout. *Cell. Mol. Biol. Lett.*, *20*:4.
- Coulton, A. T., East, D. A., Galinska-Rakoczy, A., Lehman, W., & Mulvihill, D. P. (2010). The recruitment of acetylated and unacetylated tropomyosin to distinct actin polymers permits the discrete regulation of specific myosins in fission yeast. *J Cell Sci*, *123*(Pt 19), 3235-3243.
- Coussens, L. M., Fingleton, B., & Matrisian, L. M. (2002). Matrix metalloproteinase inhibitors and cancer: trials and tribulations. *Science*, *295*(5564), 2387-2392.
- Creed, S. J., Bryce, N., Naumanen, P., Weinberger, R., Lappalainen, P., Stehn, J., & Gunning, P. (2008). Tropomyosin isoforms define distinct microfilament populations with different drug susceptibility. *Eur J Cell Biol*, *87*(8-9), 709-720.
- Creed, S. J., Desouza, M., Bamburg, J. R., Gunning, P., & Stehn, J. (2011). Tropomyosin isoform 3 promotes the formation of filopodia by regulating the recruitment of actin-binding proteins to actin filaments. *Exp Cell Res*, *317*(3), 249-261.
- Critchley, D. R. (2000). Focal adhesions - the cytoskeletal connection. *Curr Opin Cell Biol*, *12*(1), 133-139.
- Dalby-Payne, J. R., O'Loughlin, E. V., & Gunning, P. (2003). Polarization of specific tropomyosin isoforms in gastrointestinal epithelial cells and their impact on CFTR at the apical surface. *Mol Biol Cell*, *14*(11), 4365-4375.

- Daly, R. J. (2004). Cortactin signalling and dynamic actin networks. *Biochem J*, 382(Pt 1), 13-25.
- Danuser, G. (2005). Coupling the dynamics of two actin networks--new views on the mechanics of cell protrusion. *Biochem Soc Trans*, 33(Pt 6), 1250-1253.
- Daubon, T., Rochelle, T., Bourmeyster, N., & Genot, E. (2012). Invadopodia and rolling-type motility are specific features of highly invasive p190(bcr-abl) leukemic cells. *Eur J Cell Biol*, 91(11-12), 978-987.
- Dawe, H. R., Minamide, L. S., Bamburg, J. R., & Cramer, L. P. (2003). ADF/cofilin controls cell polarity during fibroblast migration. *Curr Biol*, 13(3), 252-257.
- de Hostos, E. L., Rehfuess, C., Bradtke, B., Waddell, D. R., Albrecht, R., Murphy, J., & Gerisch, G. (1993). Dictyostelium mutants lacking the cytoskeletal protein coronin are defective in cytokinesis and cell motility. *J Cell Biol*, 120(1), 163-173.
- DesMarais, V., Ichetovkin, I., Condeelis, J., & Hitchcock-DeGregori, S. E. (2002). Spatial regulation of actin dynamics: a tropomyosin-free, actin-rich compartment at the leading edge. *J Cell Sci*, 115(Pt 23), 4649-4660.
- Diz-Munoz, A., Krieg, M., Bergert, M., Ibarlucea-Benitez, I., Muller, D. J., Paluch, E., & Heisenberg, C. P. (2010). Control of directed cell migration in vivo by membrane-to-cortex attachment. *PLoS Biol*, 8(11), e1000544.
- Dominguez, R. (2011). Tropomyosin: the gatekeeper's view of the actin filament revealed. *Biophys J*, 100(4), 797-798.
- Dominguez, R., & Holmes, K. C. (2011). Actin structure and function. *Annu Rev Biophys*, 40, 169-186.
- Donnelly, S. K., Weisswange, I., Zettl, M., & Way, M. (2013). WIP provides an essential link between Nck and N-WASP during Arp2/3-dependent actin polymerization. *Curr Biol*, 23(11), 999-1006.
- Drenckhahn, D., & Pollard, T. D. (1986). Elongation of actin filaments is a diffusion-limited reaction at the barbed end and is accelerated by inert macromolecules. *J Biol Chem*, 261(27), 12754-12758.

- Elbashir, S. M., Harborth, J., Lendeckel, W., Yalcin, A., Weber, K., & Tuschl, T. (2001). Duplexes of 21-nucleotide RNAs mediate RNA interference in cultured mammalian cells. *Nature*, *411*(6836), 494-498.
- Fanning, A. S., Wolenski, J. S., Mooseker, M. S., & Izant, J. G. (1994). Differential regulation of skeletal muscle myosin-II and brush border myosin-I enzymology and mechanochemistry by bacterially produced tropomyosin isoforms. *Cell Motil Cytoskeleton*, *29*(1), 29-45.
- Fidler, I. J. (2002). Critical determinants of metastasis. *Semin Cancer Biol*, *12*(2), 89-96.
- Fire, A., Xu, S., Montgomery, M. K., Kostas, S. A., Driver, S. E., & Mello, C. C. (1998). Potent and specific genetic interference by double-stranded RNA in *Caenorhabditis elegans*. *Nature*, *391*(6669), 806-811.
- Foger, N., Rangell, L., Danilenko, D. M., & Chan, A. C. (2006). Requirement for coronin 1 in T lymphocyte trafficking and cellular homeostasis. *Science*, *313*(5788), 839-842.
- Franzen, B., Linder, S., Uryu, K., Alaiya, A. A., Hirano, T., Kato, H., & Auer, G. (1996). Expression of tropomyosin isoforms in benign and malignant human breast lesions. *Br J Cancer*, *73*(7), 909-913.
- Friedl, P. (2004). Prespecification and plasticity: shifting mechanisms of cell migration. *Curr Opin Cell Biol*, *16*(1), 14-23.
- Friedl, P., & Gilmour, D. (2009). Collective cell migration in morphogenesis, regeneration and cancer. *Nat Rev Mol Cell Biol*, *10*(7), 445-457.
- Friedl, P., & Wolf, K. (2003). Tumour-cell invasion and migration: diversity and escape mechanisms. *Nat Rev Cancer*, *3*(5), 362-374.
- Friedl, P., & Wolf, K. (2010). Plasticity of cell migration: a multiscale tuning model. *J Cell Biol*, *188*(1), 11-19.
- Frischknecht, F., Moreau, V., Rottger, S., Gonfloni, S., Reckmann, I., Superti-Furga, G., & Way, M. (1999). Actin-based motility of vaccinia virus mimics receptor tyrosine kinase signalling. *Nature*, *401*(6756), 926-929.

- Frischknecht, F., & Way, M. (2001). Surfing pathogens and the lessons learned for actin polymerization. *Trends Cell Biol*, *11*(1), 30-38.
- Galbraith, C. G., Yamada, K. M., & Sheetz, M. P. (2002). The relationship between force and focal complex development. *J Cell Biol*, *159*(4), 695-705.
- Geeves, M. A., Hitchcock-DeGregori, S. E., & Gunning, P. W. (2014). A systematic nomenclature for mammalian tropomyosin isoforms. *J Muscle Res Cell Motil*.
- Geiger, B., & Bershadsky, A. (2001). Assembly and mechanosensory function of focal contacts. *Curr Opin Cell Biol*, *13*(5), 584-592.
- Geiger, B., Bershadsky, A., Pankov, R., & Yamada, K. M. (2001). Transmembrane crosstalk between the extracellular matrix--cytoskeleton crosstalk. *Nat Rev Mol Cell Biol*, *2*(11), 793-805.
- Geiger, B., Spatz, J. P., & Bershadsky, A. D. (2009). Environmental sensing through focal adhesions. *Nat Rev Mol Cell Biol*, *10*(1), 21-33.
- Giannone, G., Dubin-Thaler, B. J., Rossier, O., Cai, Y., Chaga, O., Jiang, G., Beaver, W., Dobereiner, H. G., Freund, Y., Borisy, G., & Sheetz, M. P. (2007). Lamellipodial actin mechanically links myosin activity with adhesion-site formation. *Cell*, *128*(3), 561-575.
- Gimona, M., Kazzaz, J. A., & Helfman, D. M. (1996). Forced expression of tropomyosin 2 or 3 in v-Ki-ras-transformed fibroblasts results in distinct phenotypic effects. *Proc Natl Acad Sci U S A*, *93*(18), 9618-9623.
- Gohla, A., Birkenfeld, J., & Bokoch, G. M. (2005). Chronophin, a novel HAD-type serine protein phosphatase, regulates cofilin-dependent actin dynamics. *Nat Cell Biol*, *7*(1), 21-29.
- Goley, E. D., & Welch, M. D. (2006). The ARP2/3 complex: an actin nucleator comes of age. *Nat Rev Mol Cell Biol*, *7*(10), 713-726.
- Gunning, Hardeman, E. C., Lappalainen, P., & Mulvihill, D. P. (2015). Tropomyosin - master regulator of actin filament function in the cytoskeleton. *J Cell Sci*, *128*(16), 2965-2974.

- Gunning, O'Neill, G., & Hardeman, E. (2008). Tropomyosin-based regulation of the actin cytoskeleton in time and space. *Physiol Rev*, 88(1), 1-35.
- Gunning, Schevzov, G., Kee, A. J., & Hardeman, E. C. (2005). Tropomyosin isoforms: divining rods for actin cytoskeleton function. *Trends Cell Biol*, 15(6), 333-341.
- Gunning, P. W., Schevzov, G., Kee, A. J., & Hardeman, E. C. (2005). Tropomyosin isoforms: divining rods for actin cytoskeleton function. *Trends Cell Biol*, 15(6), 333-341.
- Gupton, S. L., Anderson, K. L., Kole, T. P., Fischer, R. S., Ponti, A., Hitchcock-DeGregori, S. E., Danuser, G., Fowler, V. M., Wirtz, D., Hanein, D., & Waterman-Storer, C. M. (2005). Cell migration without a lamellipodium: translation of actin dynamics into cell movement mediated by tropomyosin. *J Cell Biol*, 168(4), 619-631.
- Gupton, S. L., & Waterman-Storer, C. M. (2006). Spatiotemporal feedback between actomyosin and focal-adhesion systems optimizes rapid cell migration. *Cell*, 125(7), 1361-1374.
- Hanahan, D., & Weinberg, R. A. (2011). Hallmarks of cancer: the next generation. *Cell*, 144(5), 646-674.
- Haynes, E. M., Asokan, S. B., King, S. J., Johnson, H. E., Haugh, J. M., & Bear, J. E. (2015). GMFBeta controls branched actin content and lamellipodial retraction in fibroblasts. *J Cell Biol*, 209(6), 803-812.
- Helfman, D. M., Flynn, P., Khan, P., & Saeed, A. (2008). Tropomyosin as a regulator of cancer cell transformation. *Adv Exp Med Biol*, 644, 124-131.
- Higgs, H. N., & Peterson, K. J. (2005). Phylogenetic analysis of the formin homology 2 domain. *Mol Biol Cell*, 16(1), 1-13.
- Hillberg, L., Zhao Rathje, L. S., Nyakern-Meazza, M., Helfand, B., Goldman, R. D., Schutt, C. E., & Lindberg, U. (2006). Tropomyosins are present in lamellipodia of motile cells. *Eur J Cell Biol*, 85(5), 399-409.
- Holmes, K. C., & Lehman, W. (2008). Gestalt-binding of tropomyosin to actin filaments. *J Muscle Res Cell Motil*, 29(6-8), 213-219.

- Horzum, U., Ozdil, B., & Pesen-Okvur, D. (2014). Step-by-step quantitative analysis of focal adhesions. *MethodsX*, 1, 56-59.
- Hotulainen, P., Paunola, E., Vartiainen, M. K., & Lappalainen, P. (2005). Actin-depolymerizing factor and cofilin-1 play overlapping roles in promoting rapid F-actin depolymerization in mammalian nonmuscle cells. *Mol Biol Cell*, 16(2), 649-664.
- Hsiao, J. Y., Goins, L. M., Petek, N. A., & Mullins, R. D. (2015a). Arp2/3 Complex and Cofilin Modulate Binding of Tropomyosin to Branched Actin Networks. *Curr Biol*, 25(12), 1573-1582.
- Hsiao, J. Y., Goins, L. M., Petek, N. A., & Mullins, R. D. (2015b). Arp2/3 Complex and Cofilin Modulate Binding of Tropomyosin to Branched Actin Networks. *Curr Biol*.
- Huang, T. Y., DerMardirossian, C., & Bokoch, G. M. (2006). Cofilin phosphatases and regulation of actin dynamics. *Curr Opin Cell Biol*, 18(1), 26-31.
- Huttenlocher, A., Ginsberg, M. H., & Horwitz, A. F. (1996). Modulation of cell migration by integrin-mediated cytoskeletal linkages and ligand-binding affinity. *J Cell Biol*, 134(6), 1551-1562.
- Iwasa, J. H., & Mullins, R. D. (2007). Spatial and temporal relationships between actin-filament nucleation, capping, and disassembly. *Curr Biol*, 17(5), 395-406.
- Jalilian, I., Heu, C., Cheng, H., Freittag, H., Desouza, M., Stehn, J. R., Bryce, N. S., Whan, R. M., Hardeman, E. C., Fath, T., Schevzov, G., & Gunning, P. W. (2015). Cell elasticity is regulated by the tropomyosin isoform composition of the actin cytoskeleton. *PLoS One*, 10(5), e0126214.
- Janssen, R. A., & Mier, J. W. (1997). Tropomyosin-2 cDNA lacking the 3' untranslated region riboregulator induces growth inhibition of v-Ki-ras-transformed fibroblasts. *Mol Biol Cell*, 8(5), 897-908.
- Johnson, M., East, D. A., & Mulvihill, D. P. (2014). Formins determine the functional properties of actin filaments in yeast. *Curr Biol*, 24(13), 1525-1530.

- Jung, M. H., Kim, S. C., Jeon, G. A., Kim, S. H., Kim, Y., Choi, K. S., Park, S. I., Joe, M. K., & Kimm, K. (2000). Identification of differentially expressed genes in normal and tumor human gastric tissue. *Genomics*, *69*(3), 281-286.
- Kee, A. J., Yang, L., Lucas, C. A., Greenberg, M. J., Martel, N., Leong, G. M., Hughes, W. E., Cooney, G. J., James, D. E., Ostap, E. M., Han, W., Gunning, P. W., & Hardeman, E. C. (2015). An actin filament population defined by the tropomyosin Tpm3.1 regulates glucose uptake. *Traffic*, *16*(7), 691-711.
- Kis-Bicskei, N., Vig, A., Nyitrai, M., Bugyi, B., & Talian, G. C. (2013a). Purification of tropomyosin Br-3 and 5NM1 and characterization of their interactions with actin. *Cytoskeleton (Hoboken)*.
- Kis-Bicskei, N., Vig, A., Nyitrai, M., Bugyi, B., & Talian, G. C. (2013b). Purification of tropomyosin Br-3 and 5NM1 and characterization of their interactions with actin. *Cytoskeleton (Hoboken)*, *70*(11), 755-765.
- Koestler, S. A., Steffen, A., Nemethova, M., Winterhoff, M., Luo, N., Holleboom, J. M., Krupp, J., Jacob, S., Vinzenz, M., Schur, F., Schluter, K., Gunning, P. W., Winkler, C., Schmeiser, C., Faix, J., Stradal, T. E., Small, J. V., & Rottner, K. (2013). Arp2/3 complex is essential for actin network treadmilling as well as for targeting of capping protein and cofilin. *Mol Biol Cell*, *24*(18), 2861-2875.
- Kruger, A., Soeltl, R., Sopov, I., Kopitz, C., Arlt, M., Magdolen, V., Harbeck, N., Gansbacher, B., & Schmitt, M. (2001). Hydroxamate-type matrix metalloproteinase inhibitor batimastat promotes liver metastasis. *Cancer Res*, *61*(4), 1272-1275.
- Lauffenburger, D. A., & Horwitz, A. F. (1996). Cell migration: a physically integrated molecular process. *Cell*, *84*(3), 359-369.
- Laukaitis, C. M., Webb, D. J., Donais, K., & Horwitz, A. F. (2001). Differential dynamics of alpha 5 integrin, paxillin, and alpha-actinin during formation and disassembly of adhesions in migrating cells. *J Cell Biol*, *153*(7), 1427-1440.
- Lazarides, E. (1976). Two general classes of cytoplasmic actin filaments in tissue culture cells: the role of tropomyosin. *J Supramol Struct*, *5*(4), 531(383)-563(415).

- Le Clainche, C., & Carlier, M. F. (2008). Regulation of actin assembly associated with protrusion and adhesion in cell migration. *Physiol Rev*, 88(2), 489-513.
- Li, X. E., Tobacman, L. S., Mun, J. Y., Craig, R., Fischer, S., & Lehman, W. (2011). Tropomyosin position on F-actin revealed by EM reconstruction and computational chemistry. *Biophys J*, 100(4), 1005-1013.
- Lim, J. I., Sabouri-Ghomi, M., Machacek, M., Waterman, C. M., & Danuser, G. (2010). Protrusion and actin assembly are coupled to the organization of lamellar contractile structures. *Exp Cell Res*, 316(13), 2027-2041.
- Lin, J. J., Hegmann, T. E., & Lin, J. L. (1988). Differential localization of tropomyosin isoforms in cultured nonmuscle cells. *J Cell Biol*, 107(2), 563-572.
- Liu, Z., Yang, X., Chen, C., Liu, B., Ren, B., Wang, L., Zhao, K., Yu, S., & Ming, H. (2013). Expression of the Arp2/3 complex in human gliomas and its role in the migration and invasion of glioma cells. *Oncol Rep*, 30(5), 2127-2136.
- Martin. (2010). *Intracellular localisation of tropomyosin isoforms : an investigation into the role of alternatively spliced exons and the N- and C-terminal regions in localisation of tropomyosin to actin filaments.* (Ph. D.), University of Sydney.
- Martin, & Gunning. (2008). Isoform sorting of tropomyosins. *Adv Exp Med Biol*, 644, 187-200.
- Martin, Schevzov, & Gunning. (2010). Alternatively spliced N-terminal exons in tropomyosin isoforms do not act as autonomous targeting signals. *J Struct Biol*, 170(2), 286-293.
- McDowell, J. M., Huang, S., McKinney, E. C., An, Y. Q., & Meagher, R. B. (1996). Structure and evolution of the actin gene family in *Arabidopsis thaliana*. *Genetics*, 142(2), 587-602.
- Millard, T. H., Sharp, S. J., & Machesky, L. M. (2004). Signalling to actin assembly via the WASP (Wiskott-Aldrich syndrome protein)-family proteins and the Arp2/3 complex. *Biochem J*, 380(Pt 1), 1-17.

- Mishima, M., & Nishida, E. (1999). Coronin localizes to leading edges and is involved in cell spreading and lamellipodium extension in vertebrate cells. *J Cell Sci*, *112* (Pt 17), 2833-2842.
- Moreau, V., Frischknecht, F., Reckmann, I., Vincentelli, R., Rabut, G., Stewart, D., & Way, M. (2000). A complex of N-WASP and WIP integrates signalling cascades that lead to actin polymerization. *Nat Cell Biol*, *2*(7), 441-448.
- Mullins, R. D., Heuser, J. A., & Pollard, T. D. (1998). The interaction of Arp2/3 complex with actin: nucleation, high affinity pointed end capping, and formation of branching networks of filaments. *Proc Natl Acad Sci U S A*, *95*(11), 6181-6186.
- Munter, S., Way, M., & Frischknecht, F. (2006). Signaling during pathogen infection. *Sci STKE*, *2006*(335), re5.
- Nishita, M., Tomizawa, C., Yamamoto, M., Horita, Y., Ohashi, K., & Mizuno, K. (2005). Spatial and temporal regulation of cofilin activity by LIM kinase and Slingshot is critical for directional cell migration. *J Cell Biol*, *171*(2), 349-359.
- Niwa, R., Nagata-Ohashi, K., Takeichi, M., Mizuno, K., & Uemura, T. (2002). Control of actin reorganization by Slingshot, a family of phosphatases that dephosphorylate ADF/cofilin. *Cell*, *108*(2), 233-246.
- Nobes, C. D., & Hall, A. (1995). Rho, rac, and cdc42 GTPases regulate the assembly of multimolecular focal complexes associated with actin stress fibers, lamellipodia, and filopodia. *Cell*, *81*(1), 53-62.
- Nolen, B. J., Tomasevic, N., Russell, A., Pierce, D. W., Jia, Z., McCormick, C. D., Hartman, J., Sakowicz, R., & Pollard, T. D. (2009). Characterization of two classes of small molecule inhibitors of Arp2/3 complex. *Nature*, *460*(7258), 1031-1034.
- O'Neill, G. M., Stehn, J., & Gunning, P. W. (2008). Tropomyosins as interpreters of the signalling environment to regulate the local cytoskeleton. *Semin Cancer Biol*, *18*(1), 35-44.

- Ohta, Y., Kousaka, K., Nagata-Ohashi, K., Ohashi, K., Muramoto, A., Shima, Y., Niwa, R., Uemura, T., & Mizuno, K. (2003). Differential activities, subcellular distribution and tissue expression patterns of three members of Slingshot family phosphatases that dephosphorylate cofilin. *Genes Cells*, 8(10), 811-824.
- Otomo, T., Tomchick, D. R., Otomo, C., Panchal, S. C., Machius, M., & Rosen, M. K. (2005). Structural basis of actin filament nucleation and processive capping by a formin homology 2 domain. *Nature*, 433(7025), 488-494.
- Pawson, T., & Warner, N. (2007). Oncogenic re-wiring of cellular signaling pathways. *Oncogene*, 26(9), 1268-1275.
- Petit, V., & Thiery, J. P. (2000). Focal adhesions: structure and dynamics. *Biol Cell*, 92(7), 477-494.
- Pollack, R., Osborn, M., & Weber, K. (1975). Patterns of organization of actin and myosin in normal and transformed cultured cells. *Proc Natl Acad Sci U S A*, 72(3), 994-998.
- Pollard, T. D. (1986). Rate constants for the reactions of ATP- and ADP-actin with the ends of actin filaments. *J Cell Biol*, 103(6 Pt 2), 2747-2754.
- Pollard, T. D., Blanchoin, L., & Mullins, R. D. (2000). Molecular mechanisms controlling actin filament dynamics in nonmuscle cells. *Annu Rev Biophys Biomol Struct*, 29, 545-576.
- Pollard, T. D., & Borisy, G. G. (2003). Cellular motility driven by assembly and disassembly of actin filaments. *Cell*, 112(4), 453-465.
- Pollitt, A. Y., & Insall, R. H. (2009). WASP and SCAR/WAVE proteins: the drivers of actin assembly. *J Cell Sci*, 122(Pt 15), 2575-2578.
- Ponti, A., Machacek, M., Gupton, S. L., Waterman-Storer, C. M., & Danuser, G. (2004). Two distinct actin networks drive the protrusion of migrating cells. *Science*, 305(5691), 1782-1786.
- Ponti, A., Matov, A., Adams, M., Gupton, S., Waterman-Storer, C. M., & Danuser, G. (2005). Periodic patterns of actin turnover in lamellipodia and lamellae of

- migrating epithelial cells analyzed by quantitative Fluorescent Speckle Microscopy. *Biophys J*, 89(5), 3456-3469.
- Poste, G., & Fidler, I. J. (1980). The pathogenesis of cancer metastasis. *Nature*, 283(5743), 139-146.
- Poukkula, M., Hakala, M., Penttimikko, N., Sweeney, M. O., Jansen, S., Mattila, J., Hietakangas, V., Goode, B. L., & Lappalainen, P. (2014). GMF promotes leading-edge dynamics and collective cell migration in vivo. *Curr Biol*, 24(21), 2533-2540.
- Prasad, G. L., Fuldner, R. A., & Cooper, H. L. (1993). Expression of transduced tropomyosin 1 cDNA suppresses neoplastic growth of cells transformed by the ras oncogene. *Proc Natl Acad Sci U S A*, 90(15), 7039-7043.
- Pruyne, D., Evangelista, M., Yang, C., Bi, E., Zigmond, S., Bretscher, A., & Boone, C. (2002). Role of formins in actin assembly: nucleation and barbed-end association. *Science*, 297(5581), 612-615.
- Riveline, D., Zamir, E., Balaban, N. Q., Schwarz, U. S., Ishizaki, T., Narumiya, S., Kam, Z., Geiger, B., & Bershadsky, A. D. (2001). Focal contacts as mechanosensors: externally applied local mechanical force induces growth of focal contacts by an mDia1-dependent and ROCK-independent mechanism. *J Cell Biol*, 153(6), 1175-1186.
- Rottner, K., Hall, A., & Small, J. V. (1999). Interplay between Rac and Rho in the control of substrate contact dynamics. *Curr Biol*, 9(12), 640-648.
- Sahai, E., & Marshall, C. J. (2003). Differing modes of tumour cell invasion have distinct requirements for Rho/ROCK signalling and extracellular proteolysis. *Nat Cell Biol*, 5(8), 711-719.
- Sanz-Moreno, V., Gadea, G., Ahn, J., Paterson, H., Marra, P., Pinner, S., Sahai, E., & Marshall, C. J. (2008). Rac activation and inactivation control plasticity of tumor cell movement. *Cell*, 135(3), 510-523.

- Scaplehorn, N., Holmstrom, A., Moreau, V., Frischknecht, F., Reckmann, I., & Way, M. (2002). Grb2 and Nck act cooperatively to promote actin-based motility of vaccinia virus. *Curr Biol*, 12(9), 740-745.
- Schäfer, C., Born, S., Mohl, C., Houben, S., Kirchgessner, N., Merkel, R., & Hoffmann, B. (2010). The key feature for early migratory processes: Dependence of adhesion, actin bundles, force generation and transmission on filopodia. *Cell Adh Migr*, 4(2), 215-225.
- Schevzov, G., Fath, T., Vrhovski, B., Vlahovich, N., Rajan, S., Hook, J., Joya, J. E., Lemckert, F., Puttur, F., Lin, J. J., Hardeman, E. C., Wieczorek, D. F., O'Neill, G. M., & Gunning, P. W. (2008). Divergent regulation of the sarcomere and the cytoskeleton. *J Biol Chem*, 283(1), 275-283.
- Schevzov, G., Gunning, P., Jeffrey, P. L., Temm-Grove, C., Helfman, D. M., Lin, J. J., & Weinberger, R. P. (1997). Tropomyosin localization reveals distinct populations of microfilaments in neurites and growth cones. *Mol Cell Neurosci*, 8(6), 439-454.
- Schevzov, G., Kee, A. J., Wang, B., Sequeira, V. B., Hook, J., Coombes, J. D., Lucas, C. A., Stehn, J. R., Musgrove, E. A., Cretu, A., Assoian, R., Fath, T., Hanoch, T., Seger, R., Pleines, I., Kile, B. T., Hardeman, E. C., & Gunning, P. W. (2015). Regulation of cell proliferation by ERK and signal-dependent nuclear translocation of ERK is dependent on Tm5NM1-containing actin filaments. *Mol Biol Cell*, 26(13), 2475-2490.
- Schevzov, G., Lloyd, C., Hailstones, D., & Gunning, P. (1993). Differential regulation of tropomyosin isoform organization and gene expression in response to altered actin gene expression. *J Cell Biol*, 121(4), 811-821.
- Schevzov, G., Vrhovski, B., Bryce, N. S., Elmir, S., Qiu, M. R., O'Neill G, M., Yang, N., Verrills, N. M., Kavallaris, M., & Gunning, P. W. (2005). Tissue-specific tropomyosin isoform composition. *J Histochem Cytochem*, 53(5), 557-570.
- Schevzov, G., Whittaker, S. P., Fath, T., Lin, J. J., & Gunning, P. W. (2011). Tropomyosin isoforms and reagents. *Bioarchitecture*, 1(4), 135-164.

- Seth, A., Otomo, C., & Rosen, M. K. (2006). Autoinhibition regulates cellular localization and actin assembly activity of the diaphanous-related formins FRLalpha and mDia1. *J Cell Biol*, 174(5), 701-713.
- Shin, S. I., Freedman, V. H., Risser, R., & Pollack, R. (1975). Tumorigenicity of virus-transformed cells in nude mice is correlated specifically with anchorage independent growth in vitro. *Proc Natl Acad Sci U S A*, 72(11), 4435-4439.
- Skau, C. T., & Kovar, D. R. (2010). Fimbrin and tropomyosin competition regulates endocytosis and cytokinesis kinetics in fission yeast. *Curr Biol*, 20(16), 1415-1422.
- Skau, C. T., Plotnikov, S. V., Doyle, A. D., & Waterman, C. M. (2015). Inverted formin 2 in focal adhesions promotes dorsal stress fiber and fibrillar adhesion formation to drive extracellular matrix assembly. *Proc Natl Acad Sci U S A*, 112(19), E2447-2456.
- Skoumpla, K., Coulton, A. T., Lehman, W., Geeves, M. A., & Mulvihill, D. P. (2007). Acetylation regulates tropomyosin function in the fission yeast *Schizosaccharomyces pombe*. *J Cell Sci*, 120(Pt 9), 1635-1645.
- Small, J. V. (2015). Pushing with actin: from cells to pathogens. *Biochem Soc Trans*, 43(1), 84-91.
- Snapper, S. B., Takeshima, F., Anton, I., Liu, C. H., Thomas, S. M., Nguyen, D., Dudley, D., Fraser, H., Purich, D., Lopez-Illasaca, M., Klein, C., Davidson, L., Bronson, R., Mulligan, R. C., Southwick, F., Geha, R., Goldberg, M. B., Rosen, F. S., Hartwig, J. H., & Alt, F. W. (2001). N-WASP deficiency reveals distinct pathways for cell surface projections and microbial actin-based motility. *Nat Cell Biol*, 3(10), 897-904.
- Sporn, M. B. (1996). The war on cancer. *Lancet*, 347(9012), 1377-1381.
- Stanyon, C. A., & Bernard, O. (1999). LIM-kinase1. *Int J Biochem Cell Biol*, 31(3-4), 389-394.
- Stehn, J. R., Haass, N. K., Bonello, T., Desouza, M., Kottyan, G., Treutlein, H., Zeng, J., Nascimento, P. R., Sequeira, V. B., Butler, T. L., Allanson, M., Fath, T., Hill,

- T. A., McCluskey, A., Schevzov, G., Palmer, S. J., Hardeman, E. C., Winlaw, D., Reeve, V. E., Dixon, I., Weninger, W., Cripe, T. P., & Gunning, P. W. (2013). A novel class of anticancer compounds targets the actin cytoskeleton in tumor cells. *Cancer Res*, 73(16), 5169-5182.
- Stehn, J. R., Schevzov, G., O'Neill, G. M., & Gunning, P. W. (2006). Specialisation of the tropomyosin composition of actin filaments provides new potential targets for chemotherapy. *Curr Cancer Drug Targets*, 6(3), 245-256.
- Stevenson, R. P., Veltman, D., & Machesky, L. M. (2012). Actin-bundling proteins in cancer progression at a glance. *J Cell Sci*, 125(Pt 5), 1073-1079.
- Sung, L. A., Gao, K. M., Yee, L. J., Temm-Grove, C. J., Helfman, D. M., Lin, J. J., & Mehrpouryan, M. (2000). Tropomyosin isoform 5b is expressed in human erythrocytes: implications of tropomodulin-TM5 or tropomodulin-TM5b complexes in the protofilament and hexagonal organization of membrane skeletons. *Blood*, 95(4), 1473-1480.
- Svitkina, T. M., & Borisy, G. G. (1999). Arp2/3 complex and actin depolymerizing factor/cofilin in dendritic organization and treadmilling of actin filament array in lamellipodia. *J Cell Biol*, 145(5), 1009-1026.
- Svitkina, T. M., Verkhovsky, A. B., McQuade, K. M., & Borisy, G. G. (1997). Analysis of the actin-myosin II system in fish epidermal keratocytes: mechanism of cell body translocation. *J Cell Biol*, 139(2), 397-415.
- Takenaga, K., & Masuda, A. (1994). Restoration of microfilament bundle organization in v-raf-transformed NRK cells after transduction with tropomyosin 2 cDNA. *Cancer Lett*, 87(1), 47-53.
- Takenaga, K., Nakamura, Y., & Sakiyama, S. (1988). Differential expression of a tropomyosin isoform in low- and high-metastatic Lewis lung carcinoma cells. *Mol Cell Biol*, 8(9), 3934-3937.
- Takenaga, K., Nakamura, Y., Tokunaga, K., Kageyama, H., & Sakiyama, S. (1988). Isolation and characterization of a cDNA that encodes mouse fibroblast tropomyosin isoform 2. *Mol Cell Biol*, 8(12), 5561-5565.

- Tanaka, K., Waxman, L., & Goldberg, A. L. (1983). ATP serves two distinct roles in protein degradation in reticulocytes, one requiring and one independent of ubiquitin. *J Cell Biol*, 96(6), 1580-1585.
- Temm-Grove, C. J., Guo, W., & Helfman, D. M. (1996). Low molecular weight rat fibroblast tropomyosin 5 (TM-5): cDNA cloning, actin-binding, localization, and coiled-coil interactions. *Cell Motil Cytoskeleton*, 33(3), 223-240.
- Temm-Grove, C. J., Jockusch, B. M., Weinberger, R. P., Schevzov, G., & Helfman, D. M. (1998). Distinct localizations of tropomyosin isoforms in LLC-PK1 epithelial cells suggests specialized function at cell-cell adhesions. *Cell Motil Cytoskeleton*, 40(4), 393-407.
- Tojkander, S., Gateva, G., Schevzov, G., Hotulainen, P., Naumanen, P., Martin, C., Gunning, P. W., & Lappalainen, P. (2011). A molecular pathway for myosin II recruitment to stress fibers. *Curr Biol*, 21(7), 539-550.
- Uetrecht, A. C., & Bear, J. E. (2006). Coronins: the return of the crown. *Trends Cell Biol*, 16(8), 421-426.
- Urban, E., Jacob, S., Nemethova, M., Resch, G. P., & Small, J. V. (2010). Electron tomography reveals unbranched networks of actin filaments in lamellipodia. *Nat Cell Biol*, 12(5), 429-435.
- Urano, T., Liu, J., Zhang, P., Fan, Y., Egile, C., Li, R., Mueller, S. C., & Zhan, X. (2001). Activation of Arp2/3 complex-mediated actin polymerization by cortactin. *Nat Cell Biol*, 3(3), 259-266.
- Vallotton, P., & Small, J. V. (2009). Shifting views on the leading role of the lamellipodium in cell migration: speckle tracking revisited. *J Cell Sci*, 122(Pt 12), 1955-1958.
- Vinzenz, M., Nemethova, M., Schur, F., Mueller, J., Narita, A., Urban, E., Winkler, C., Schmeiser, C., Koestler, S. A., Rottner, K., Resch, G. P., Maeda, Y., & Small, J. V. (2012). Actin branching in the initiation and maintenance of lamellipodia. *J Cell Sci*, 125(Pt 11), 2775-2785.

- Wang, F. L., Wang, Y., Wong, W. K., Liu, Y., Addivinola, F. J., Liang, P., Chen, L. B., Kantoff, P. W., & Pardee, A. B. (1996). Two differentially expressed genes in normal human prostate tissue and in carcinoma. *Cancer Res*, *56*(16), 3634-3637.
- Weaver, A. M., Heuser, J. E., Karginov, A. V., Lee, W. L., Parsons, J. T., & Cooper, J. A. (2002). Interaction of cortactin and N-WASp with Arp2/3 complex. *Curr Biol*, *12*(15), 1270-1278.
- Weaver, A. M., Karginov, A. V., Kinley, A. W., Weed, S. A., Li, Y., Parsons, J. T., & Cooper, J. A. (2001). Cortactin promotes and stabilizes Arp2/3-induced actin filament network formation. *Curr Biol*, *11*(5), 370-374.
- Webb, D. J., Donais, K., Whitmore, L. A., Thomas, S. M., Turner, C. E., Parsons, J. T., & Horwitz, A. F. (2004). FAK-Src signalling through paxillin, ERK and MLCK regulates adhesion disassembly. *Nat Cell Biol*, *6*(2), 154-161.
- Weed, S. A., Karginov, A. V., Schafer, D. A., Weaver, A. M., Kinley, A. W., Cooper, J. A., & Parsons, J. T. (2000). Cortactin localization to sites of actin assembly in lamellipodia requires interactions with F-actin and the Arp2/3 complex. *J Cell Biol*, *151*(1), 29-40.
- Weisswange, I., Newsome, T. P., Schleich, S., & Way, M. (2009). The rate of N-WASP exchange limits the extent of ARP2/3-complex-dependent actin-based motility. *Nature*, *458*(7234), 87-91.
- Winder, S. J., & Ayscough, K. R. (2005). Actin-binding proteins. *J Cell Sci*, *118*(Pt 4), 651-654.
- Wolf, K., Mazo, I., Leung, H., Engelke, K., von Andrian, U. H., Deryugina, E. I., Strongin, A. Y., Bocker, E. B., & Friedl, P. (2003). Compensation mechanism in tumor cell migration: mesenchymal-amoeboid transition after blocking of pericellular proteolysis. *J Cell Biol*, *160*(2), 267-277.
- Wu, C., Asokan, S. B., Berginski, M. E., Haynes, E. M., Sharpless, N. E., Griffith, J. D., Gomez, S. M., & Bear, J. E. (2012). Arp2/3 is critical for lamellipodia and response to extracellular matrix cues but is dispensable for chemotaxis. *Cell*, *148*(5), 973-987.

- Yager, M. L., Hughes, J. A., Lovicu, F. J., Gunning, P. W., Weinberger, R. P., & O'Neill, G. M. (2003). Functional analysis of the actin-binding protein, tropomyosin 1, in neuroblastoma. *Br J Cancer*, *89*(5), 860-863.
- Yamada, K. M., Spooner, B. S., & Wessells, N. K. (1971). Ultrastructure and function of growth cones and axons of cultured nerve cells. *J Cell Biol*, *49*(3), 614-635.
- Yamazaki, D., Kurisu, S., & Takenawa, T. (2009). Involvement of Rac and Rho signaling in cancer cell motility in 3D substrates. *Oncogene*, *28*(13), 1570-1583.
- Zaidel-Bar, R., Ballestrem, C., Kam, Z., & Geiger, B. (2003). Early molecular events in the assembly of matrix adhesions at the leading edge of migrating cells. *J Cell Sci*, *116*(Pt 22), 4605-4613.
- Zaidel-Bar, R., Itzkovitz, S., Ma'ayan, A., Iyengar, R., & Geiger, B. (2007). Functional atlas of the integrin adhesome. *Nat Cell Biol*, *9*(8), 858-867.
- Zaidi, N., Burster, T., Sommandas, V., Herrmann, T., Boehm, B. O., Driessen, C., Voelter, W., & Kalbacher, H. (2007). A novel cell penetrating aspartic protease inhibitor blocks processing and presentation of tetanus toxoid more efficiently than pepstatin A. *Biochem Biophys Res Commun*, *364*(2), 243-249.
- Zamir, E., & Geiger, B. (2001). Molecular complexity and dynamics of cell-matrix adhesions. *J Cell Sci*, *114*(Pt 20), 3583-3590.
- Zettl, M., & Way, M. (2001). New tricks for an old dog? *Nat Cell Biol*, *3*(3), E74-75.